



Journal of Naval Sciences and Engineering

Deniz Bilimleri ve Mühendisliği Dergisi

National Defence University

Milli Savunma Üniversitesi

Deniz Harp Okulu Dekanlığı

Turkish Naval Academy

Volume/Cilt: 19
Number/Sayı: 1
April/Nisan 2023

PRINTED BY / BASKI

National Defence University Turkish Naval Academy Printing House / Milli Savunma Üniversitesi Deniz Harp Okulu Matbaası

CORRESPONDENCE AND COMMUNICATION ADDRESS / YAZIŞMA VE HABERLEŞME ADRESİ

Milli Savunma Üniversitesi
Deniz Harp Okulu Dekanlığı 34940
Tuzla/İstanbul/Türkiye

Phone/Telefon : +90 216 395 26 30
E-mail/E-posta : jnse@dho.edu.tr
Web : <https://dergipark.org.tr/tr/pub/jnse>

**NATIONAL DEFENCE UNIVERSITY
TURKISH NAVAL ACADEMY
JOURNAL OF NAVAL SCIENCES AND ENGINEERING**

**MİLLİ SAVUNMA ÜNİVERSİTESİ
DENİZ HARP OKULU DEKANLIĞI
DENİZ BİLİMLERİ VE MÜHENDİSLİĞİ DERGİSİ**

Volume/Cilt: 19

Number/Sayı: 1

April/Nisan 2023

ISSN: 1304-2025

**Owner on Behalf of the Turkish Naval Academy
Deniz Harp Okulu Dekanlığı Adına Sahibi ve Sorumlusu
Prof.Dr. Cemalettin ŞAHİN**

Journal of Naval Sciences and Engineering (JNSE) is a peer reviewed, international, inter-disciplinary journal in science and technology, which is published semi-annually in April and November since 2003. It publishes full research articles, review articles, technical notes, short communications, book reviews, letters to the editor and extended versions of conference papers. Topics of interest include the technological and scientific aspects of the following areas: **Computer Science and Engineering, Electrical and Electronics Engineering, Naval/Mechanical Engineering, Naval Architecture and Marine Engineering, Industrial Engineering** and **Basic/Social Sciences**. The journal aims to provide a scientific contribution to the theory and applications of naval sciences and engineering, and share knowledge in relevant fields. The papers in the journal are published in English.

Following Open Access Model of Publishing, Journal of Naval Sciences and Engineering presents a variety of scientific viewpoints. The authors are responsible for the scientific, contextual and linguistic aspects of the articles published in the journal. The views expressed or implied in this publication, unless otherwise noted, should not be interpreted as official positions of the Turkish Naval Academy.

Our journal uses "double-blind review", which means that both the reviewer and author identities are concealed from the reviewers, and vice versa, throughout the review process. The articles submitted to JNSE to be published are free of article submission, processing and publication charges. The accepted articles are published free-of-charge as online from the journal website and printed.

DATABASES INDEXING OUR JOURNAL / TARANDIĞIMIZ VERİ TABANLARI

Open Academic Journals Index (OAJI) (13.03.2016)

Sobiad Citation Index (31.01.2018)

Scientific Indexing Services (SIS) (28.02.2018)

Arastirmax Scientific Publication Index (13.03.2018)

CiteFactor Academic Scientific Journals (14.05.2018)

Asian Digital Library (03.09.2018)

Idealonline (05.09.2018)

ULAKBİM TR Index (14.05.2020)

Deniz Bilimleri ve Mühendisliği Dergisi (DBMD); uluslararası düzeyde, hakemli, çok disiplinli, Nisan ve Kasım aylarında olmak üzere 2003 yılından bu yana yılda iki kez yayımlanan, bilim ve teknoloji dergisidir. Dergide; **Bilgisayar, Makine, Gemi İnşa, Elektrik/Elektronik, Endüstri Mühendisliği** ile **Temel/Sosyal Bilimler** alanlarında bilimsel nitelikli araştırma makaleleri, derlemeler, teknik notlar, kitap incelemeleri, editöre mektuplar ile konferans ve toplantıların genişletilmiş raporlarına yer verilmektedir. Dergi, deniz bilimleri ve mühendisliğinin teori ve uygulamalarına bilimsel katkı sağlamayı ve ilgili alanlarda bilgi paylaşımını amaçlamaktadır. Dergide yer alan makaleler İngilizce olarak yayımlanmaktadır.

Açık erişimli yayım politikası izleyen Deniz Bilimleri ve Mühendisliği Dergisi değişik bilimsel bakış açılarını okuyucularına sunmaktadır. Dergide yayınlanan makalelerin bilim, içerik ve dil bakımından sorumluluğu yazarlarına aittir. Doğrudan veya dolaylı olarak ifade edilen görüşler Deniz Harp Okulu'nun resmi görüşleri olarak görülmemelidir.

Dergimiz, makale değerlendirme sürecinde "çift-kör hakemlik" sistemini kullanmaktadır. DBMD'ye yayımlanmak üzere gönderilen makaleler; makale gönderim, işlem ve yayım ücretinden muafır. Kabul edilen makaleler, ücretsiz olarak basılı şekilde ve dergi web sayfasından çevrimiçi (on-line) olarak yayımlanmaktadır.

© 2023 Copyright by Turkish Naval Academy
Her hakkı saklıdır.

**NATIONAL DEFENCE UNIVERSITY
TURKISH NAVAL ACADEMY
JOURNAL OF NAVAL SCIENCES AND ENGINEERING**

**MİLLİ SAVUNMA ÜNİVERSİTESİ
DENİZ HARP OKULU DEKANLIĞI
DENİZ BİLİMLERİ VE MÜHENDİSLİĞİ DERGİSİ**

Volume/Cilt: 19

Number/Sayı: 1

April/Nisan 2023

ISSN: 1304-2025

EDITOR-IN-CHIEF / BAŞ EDITÖR

Associate Prof.Dr. Fatih ERDEN, National Defence University

ASSISTANT EDITOR / YARDIMCI EDITÖR

Assistant Prof.Dr. Onur USTA, National Defence University

EDITORIAL BOARD / YAYIN KURULU

Assoc.Prof.Dr. Adem ATMAZ, Purdue University
Assoc.Prof.Dr. Dođuş ÖZKAN, National Defence U.
Assoc.Prof.Dr. Erkan KAPLANOđLU, University of Tennessee
Assoc.Prof.Dr. Ertan YAKICI, National Defence U.
Assoc.Prof.Dr. H. Salih ERDEN, İstanbul Technical University
Assoc.Prof.Dr. Levent ERİŞKİN, National Defence U.
Assoc.Prof.Dr. Mariya S. ANTYUFYEVA, Newcastle University
Assoc.Prof.Dr. Muhammet DEVECİ, National Defence U.
Prof.Dr. Mustafa TÜRKMEN, Erciyes University
Assoc.Prof.Dr. Mümtaz KARATAŞ, National Defence U.
Assoc.Prof.Dr. Okan ERKAYMAZ, National Defence U.
Prof.Dr. Rumen KISHEV, Bulgarian Academy of Sciences

ADVISORY BOARD / DANIŞMA KURULU

Prof.Dr. Ahmet Arif ERGİN, Yeditepe University
Prof.Dr. Alexander NOSICH, Inst. of Radiophysics, Kharkiv
Prof.Dr. Alper ERTÜRK, Australian University - Kuwait
Prof.Dr. Atilla İNCECİK, University of Strathclyde
Prof.Dr. Bettar O. el MOCTAR, University of Duisburg
Prof.Dr. Cem ERSOY, Bogazici University
Prof.Dr. Cemal ZEHİR, Yıldız Technical University
Prof.Dr. Cengiz KAHRAMAN, İstanbul Technical University
Prof.Dr. Drazan KOZAK, University of Osijek
Prof.Dr. Ertuđrul KARAÇUHA, İstanbul Technical University
Prof.Dr. Gennady S. ZALEVSKY, Kharkiv National University
Prof.Dr. Hakan TEMELTAŞ, İstanbul Technical University
Prof. Mirza TIHIC, Syracuse University
Prof.Dr. Nafiz ARICA, Piri Reis University
Prof.Dr. Nurettin ACIR, National Defence U.
Prof.Dr. Osman TURAN, University of Strathclyde
Prof.Dr. Özlem ÖZKANLI, Ankara University
Prof.Dr. Serdar PİRTİNİ, Marmara University
Prof.Dr. Serdar SALMAN, National Defence U.
Prof.Dr. Sergej HLOCH, Technical University of Kosice
Prof.Dr. Süleyman ÖZKAYNAK, Piri Reis University
Prof.Dr. Yahya KARSLIGİL, Yıldız Technical University

TECHNICAL EDITOR / TEKNİK EDITÖR

Rıza KAYA, National Defence U.

LAYOUT EDITOR & SECRETARIAT / MİZANPAJ EDITÖRÜ & SEKRETERYA

Kürşat Alp ARPACI, National Defence U.

Özgür ÇOBAN, National Defence U.

NATIONAL DEFENCE UNIVERSITY
TURKISH NAVAL ACADEMY
JOURNAL OF NAVAL SCIENCES AND ENGINEERING

VOLUME: 19

NUMBER: 1

APRIL 2023

ISSN: 1304-2025

CONTENTS / İÇİNDEKİLER

EDITORIAL

Foreword from the Editor-In-Chief (Önsöz)

1-2

Fatih ERDEN

Materials Engineering / Malzeme Mühendisliği

RESEARCH ARTICLE

Production of Translucent Alumina Ceramics by Tape Casting

3-17

(Yarı Saydam Alümina Seramiklerin Şerit Döküm Yöntemi İle Üretimi)

Yasemin TABAK, Şeyda POLAT, Ayşen KILIÇ, Bayise KAVAKLI VATANSEVER

Physics / Fizik

RESEARCH ARTICLE

Spectroscopic Investigation of Argon DC Glow Discharge In Plasma Medium

19-33

(Plazma Ortamında Argon DC Glow Deşarjının Spektroskopik İncelenmesi)

Esra OKUMUŞ

Electrical-Electronics Engineering / Elektrik-Elektronik Mühendisliği

RESEARCH ARTICLE

**Thermal Analysis of XLPE Insulated Submarine Cables for
Different Loading Conditions**

35-51

(Farklı Yükleme Şartları İçin XLPE İzoleli Denizaltı Kablolarının Isıl Analizi)

Ahmet Yiğit ARABUL, Celal Fadıl KUMRU

Shipbuilding and Ocean Engineering / Gemi ve Deniz Teknolojisi Mühendisliği

RESEARCH ARTICLE

Scale Effects On The Linear Hydrodynamic Coefficients Of DARPA SUBOFF

53-76

(Lineer Hidrodinamik Katsayıların Hesabında Ölçek Etkisi)

Furkan KIYÇAK, Ömer Kemal KINACI

Naval Architecture Engineering / Gemi İnşaatı Mühendisliği

RESEARCH ARTICLE

**Numerical Investigation Of HVAC Systems of a Naval Ship Compartment:
Free Cooling And Air-Conditioning**

77-100

(Bir Savaş Gemisi Kompartımanında HVAC Sistemlerinin Sayısal İncelenmesi:
Doğal Havalandırma ve İklimlendirme)

Alpay ACAR, Murat URYAN, Ali DOĞRUL, Asım Sinan KARAKURT, Cenk ÇELİK

MİLLİ SAVUNMA ÜNİVERSİTESİ
DENİZ HARP OKULU DEKANLIĞI
DENİZ BİLİMLERİ VE MÜHENDİSLİĞİ DERGİSİ

CİLT: 19

SAYI: 1

NİSAN 2023

ISSN: 1304-2025

FOREWORD FROM THE EDITOR-IN-CHIEF

Welcome to the first issue for the year 2023, a significant milestone for us as we celebrate the centennial of the Republic of Türkiye, the quarter-millennial anniversary of the Turkish Naval Academy (TNA), and the vicennial celebration of the Journal of Naval Sciences and Engineering (JNSE). These historical connections symbolize the remarkable progress achieved by our country, academy, and journal.

In this issue, we are delighted to present five research papers that contribute to the advancement of naval sciences and engineering. These papers cover a wide range of topics, including the production of translucent alumina ceramics by tape casting, spectroscopic investigation of argon glow discharge in a plasma medium, thermal analysis of XLPE insulated submarine cables for different loading conditions, scale effects on the linear hydrodynamic coefficients of DARPA SUBOFF, and numerical investigation of HVAC systems in a naval ship compartment.

We would also like to remind you that starting from September 1, 2022, we have been providing Digital Object Identifiers (DOIs) for accepted papers, ensuring their persistent identification. Additionally, we have implemented a new publishing process where papers are made available online before the printed hardcopy format, allowing for broader accessibility and faster dissemination of research findings.


Our November 2023 issue is dedicated to highlighting cutting-edge advancements and research in naval technology and engineering. We have published a call for papers online, encouraging submissions on various topics, including 3D modeling, digital twin technology, IoT applications, 3D printing, virtual and augmented reality, high-performance computing, automation with robots, drones, and autonomous vehicles, shipyard construction and maintenance cost analysis, lean production methodologies, corrosion protection, wearable technologies for personnel monitoring, and big data analytics in preventive maintenance. We eagerly invite researchers and scholars to submit their work, contributing to this issue. The submitted

Fatih ERDEN

papers in these areas will be given special attention alongside the journal's regular coverage, offering a comprehensive exploration of the latest advancements in naval sciences and engineering.

We would like to extend our heartfelt gratitude to the authors for their valuable contributions to this issue, as well as our dedicated editorial and advisory board members for their expertise and guidance. We are also immensely grateful to the diligent reviewers who have generously contributed their time and expertise to ensure the quality and rigor of the papers published in this issue. Your insightful feedback and constructive criticism have played a vital role in shaping the content of this journal.





Additionally, we would like to express our appreciation to our readers for their continued support and trust in JNSE. Thank you all for your invaluable contributions.

Fatih ERDEN , Ph.D.
Editor-in-Chief
Journal of Naval Sciences and Engineering

RESEARCH ARTICLE

**An ethical committee approval and/or legal/special permission has not been required within the scope of this study.*

**PRODUCTION OF TRANSLUCENT ALUMINA CERAMICS
BY TAPE CASTING***

Yasemin TABAK^{1*} 
Şeyda POLAT² 
Ayşen KILIÇ³ 
Bayise KAVAKLI VATANSEVER⁴ 

¹ TÜBİTAK Marmara Research Center,
The Vice Presidency of Materials Technologies, Kocaeli, Türkiye,
yasemin.tabak@tubitak.gov.tr

² Kocaeli University, Faculty of Engineering,
Department of Metallurgical and Materials Engineering, Kocaeli, Türkiye,
sydpolat@gmail.com

³ TÜBİTAK Marmara Research Center,
The Vice Presidency of Materials Technologies, Kocaeli, Türkiye,
aysen.kilic@tubitak.gov.tr

⁴ TÜBİTAK Marmara Research Center,
The Vice Presidency of Materials Technologies, Kocaeli, Türkiye,
bayise.kavakli@tubitak.gov.tr

Received: 11.08.2022

Accepted: 14.10.2022

Yasemin TABAK, Şeyda POLAT, Ayşen KILIÇ,
Bayise KAVAKLI VATANSEVER

ABSTRACT

Alumina powders are utilized in many industries like electronics, metallurgy optoelectronics and fine ceramic composites. In this study, non-aqueous-based tape casting of alumina was carried out in a non-continuous single blade tape casting machine. A slurry of alumina powder in a solvent was cast on a stationary surface with additives like dispersants, binders and plasticizers. After the green tapes were dried, they were sintered to obtain the final desired shape. Hydraulic pressing method was used to increase the density of the alumina tapes. Layered alumina ceramics were produced at 5 different temperatures by pressureless sintering method (1450°C, 1500°C, 1550°C, 1600°C and 1650°C) for 5 h to observe the effect of sintering temperature. Results revealed the sintering conditions for obtaining translucent alumina, with the utilized slurry composition. Translucent alumina ceramics have gained importance as parts of semiconductor devices, substrates for electric parts, as heat/corrosion materials in reaction tubes and crucibles and are used in medical equipments.

Keywords: *Tape Casting, Alumina, Sintering, Layered Ceramics, Microstructure.*

YARI SAYDAM ALÜMİNA SERAMİKLERİN ŞERİT DÖKÜM YÖNTEMİ İLE ÜRETİMİ

ÖZ

Alümina tozları elektronik, metalurji, optoelektronik ve ince seramik kompozitler gibi birçok farklı endüstride kullanılmaktadır. Bu çalışmada, alüminanın su bazlı olmayan şerit dökümü, sürekli olmayan tek bıçaklı bir şerit döküm makinesinde gerçekleştirilmiştir. Dağıtıcılar, bağlayıcılar ve plastikleştiriciler gibi katkı maddeleri içeren bir çözücü içindeki alümina tozundan oluşan bir süspansiyon, sabit bir yüzey üzerine dökülmüştür. Ham şeritler daha sonra kurutulmuş ve son olarak istenen nihai şekli elde etmek için sinterlenmiştir. Alümina ham şeritlerin mikro yapısını optimize etmek ve yoğunluğunu artırmak için hidrolik presleme yöntemi ile preslenmiştir. Katmanlı alümina seramikler, sinterleme sıcaklığının mikroyapı üzerindeki etkisini gözlemlemek için 5 farklı sıcaklıkta (1450°C, 1500°C, 1550°C, 1600°C ve 1650°C) 5 saat süreyle basınçsız sinterleme yöntemiyle üretilmiştir. Sonuçlar, kullanılan süspansiyon bileşimi ile yarı saydam alümina elde etmek için sinterleme koşullarını ortaya çıkarmıştır. Yarı saydam alümina seramikler yarı iletken aygıtlarda, devre altlıklarında, ısı ve korozyona dayanıklı malzeme olarak reaksiyon tüpleri ve potalarda, medikal uygulamalarda kullanım alanı bulmaktadır.

Anahtar Kelimeler: *Şerit Dökümü, Alümina, Sinterleme, Tabakalı Seramikler, Mikroyapı.*

1. INTRODUCTION

Alumina is utilized in many applications due to its thermal and chemical stability, high wear and corrosion resistance, high hardness and strength and excellent electrical insulation properties (Fujiwara et al., 2007; Vuksic et al., 2021a; Yu et al., 2015; Vuksic et al., 2021b; Manotham et al., 2021). However, being a ceramic material, its inherent brittleness causes low mechanical stability and reliability and limits its use. Thus, many studies are being carried out to improve the toughness of alumina ceramics.

One of the methods to enhance reliability of such ceramics is production of laminated structures. Tape casting has been developed to produce ceramic tapes used in these laminated structures (Mortara, 2005). The process involves casting a specially formulated slurry onto a stationary or moving surface. The slurry involves ceramic powder in solvent having other additives like binders, dispersants, and plasticizers (Hou et al., 2019; Zhao et al., 2020). Resulting green body has better uniformity compared to traditional dry pressing since it is formed by in situ consolidation of polymers (Jurkow et al., 2011; Liu et al., 2012; Ba et al., 2013; Naebe & Shirvanimoghaddam, 2016; Vozdecky et al., 2010; Feng et al., 2020). Besides, large areas of thin sheets with controlled thickness, within the range of 10 µm to 1 mm, can be produced by this method with low cost (Mistler, 1995). Although pores and discontinuities between the layers present a problem, there are many ongoing studies to improve this production technique (Miao & Sun, 2010).

Ceramic tape technology provides means to create complex 3D structures, thus has a great potential for production of many devices (Roosen, 2006). It is also possible to produce functionally graded materials with tape casting, having dense outer layers and porous inner layers. The method is utilized for production of translucent polycrystalline alumina as well, which is the preferred material for arc tubes in high-pressure sodium (HPS) discharge lamps (Zhou et al., 2016, Pabst & Hříbalová, 2021; Wei et al., 2001; Willems, 1992).

Production of Translucent Alumina Ceramics by Tape Casting

The present study is carried out with the aim to determine the process parameters in tape casting for production of translucent alumina. A well-designed slurry composition is used for this purpose and the effect of sintering temperature on alumina ceramic thin layers is evaluated. Although translucent and transparent ceramics have six decades of history, extensive research is still being carried out on the development of these materials.

2. EXPERIMENTAL STUDIES

Alumina powder used as a raw material in this study, A-16 SG from Alcoa with 99,8 % purity, was characterized first in terms of particle size distribution and phases present. X-ray diffraction studies using Shimadzu XRD 6000 diffractometer revealed that alumina powder consisted of single phase of alumina (corundum). Average particle size of the powder was 300 nm as determined by laser particle size analyzer, Malvern Zetasizer NanoZS 3600. Microstructures of both alumina powder and sintered body were observed using JEOL 633F scanning electron microscope (SEM). Figure 1 shows the SEM image of α -alumina powder used in the study. In the suspension preparation process, MEK (Merck KGaA), EtOH (Merck KGaA) were used as solvent media, PVB (Chang Chun Petrochemical Co. Ltd.) was used as solvent-based binder, STPP (Eczacıbaşı) was used as dispersant, DBF (Plastifay Chemical Industry Co.) and PEG400 (Merck KGaA) were used as plasticizers.

The slurry composition was formulated to provide a good dispersion of ceramic and to obtain a stable suspension so that a homogeneous and compact green structure could be produced. The organic additives were selected to enhance the tape characteristics, without interacting. The binder system was chosen such that the mechanical characteristics of the tape would be improved without compromising the green density or inducing flocculation.

*Yasemin TABAK, Şeyda POLAT, Ayşen KILIÇ,
Bayise KAVAKLI VATANSEVER*

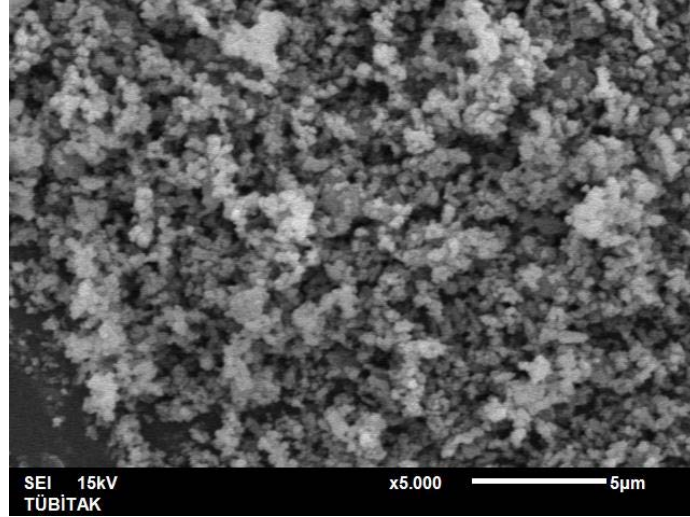


Figure 1. SEM image of the alumina powder.

The slurry was used in a non-continuous single blade tape casting machine to produce the green alumina tapes by non-aqueous alcohol based tape casting method. After drying the green tapes were sintered at temperatures 1450°C, 1500°C, 1550°C, 1600°C and 1650°C for 5 hours each. Preparation of the tapes and the layered structure is shown schematically in Figure 2, the slurry was spread by hand motion.

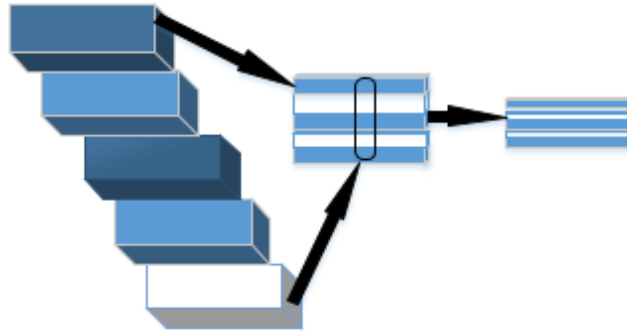


Figure 2. Preparation of the tapes and the layered structure.

Production of Translucent Alumina Ceramics by Tape Casting

Dispersion studies were carried out with ~ 50 wt % of solid content. Suspensions were prepared by dispersion of the alumina powder in MEK/EtOH based solvent system. First stage of the preparation was deagglomeration of alumina powder and its dispersion in the solvent. The solvent was an azeotropic mixture of 64 vol % MEK and 36 vol % EtOH. Second stage involved mixing of the solvent with the binder, dispersant and plasticizers. Ball milling was carried out by mixing 100 g slurry with 125 g zirconia balls for 24 h, for effective deagglomeration and dispersion. The viscosity was measured as 63 centipoise (cP) using Brookfield LVDV-II+P viscometer.

Tape casting was carried out using doctor blade technique on a clean glass bed using a laboratory tape caster (MSE Teknoloji Ltd., TR). The blade gap was kept at 250 µm. The cast tapes were dried at ambient conditions for 12 hours. After drying, tapes were released and inspected for potential defects.

Laminates were prepared by stacking 5 sheets manually, that were 2x1 cm in dimensions. They were then compressed by hydraulic press (PMK brand model) at 200 MPa. Sintering was carried out in a Protherm PLF160/63 furnace at air atmosphere at different temperatures (1450 °C, 1500 °C, 1550 °C, 1600 °C and 1600 °C) for 5 h each. A heating rate of 5 °C/min was used and furnace cooling was adopted. Thicknesses of the thin ceramics were measured and firing shrinkage values were calculated after sintering. Illustration of the whole tape casting process is given in the Figure 3.

*Yasemin TABAK, Şeyda POLAT, Ayşen KILIÇ,
Bayise KAVAKLI VATANSEVER*

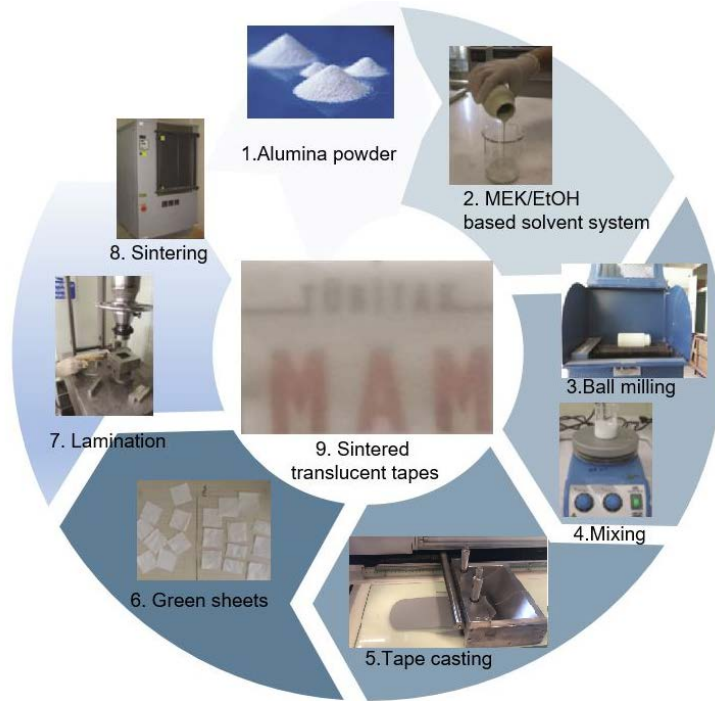


Figure 3. Illustration of the whole tape casting process.

3. RESULTS AND DISCUSSION

The microstructures of the sintered tape samples, examined using SEM at 2500X, are shown in Figure 4. Effect of sintering temperature on the grain shape and size can be clearly seen in these images. As the sintering temperature increases the grain size increases and porosity decreases indicating a denser structure. The SEM results are supported by the calculated theoretical density values of the samples which increased from 83,3 % (1450 °C) to 90 % (1650 °C). Theoretical densities were determined according to Archimedes principle and used in calculation of firing shrinkage values. For the samples sintered between 1450-1550 °C shrinkage was 16-17 %, whereas it was between 17-18 % for those sintered between 1600-1650 °C.

Production of Translucent Alumina Ceramics by Tape Casting

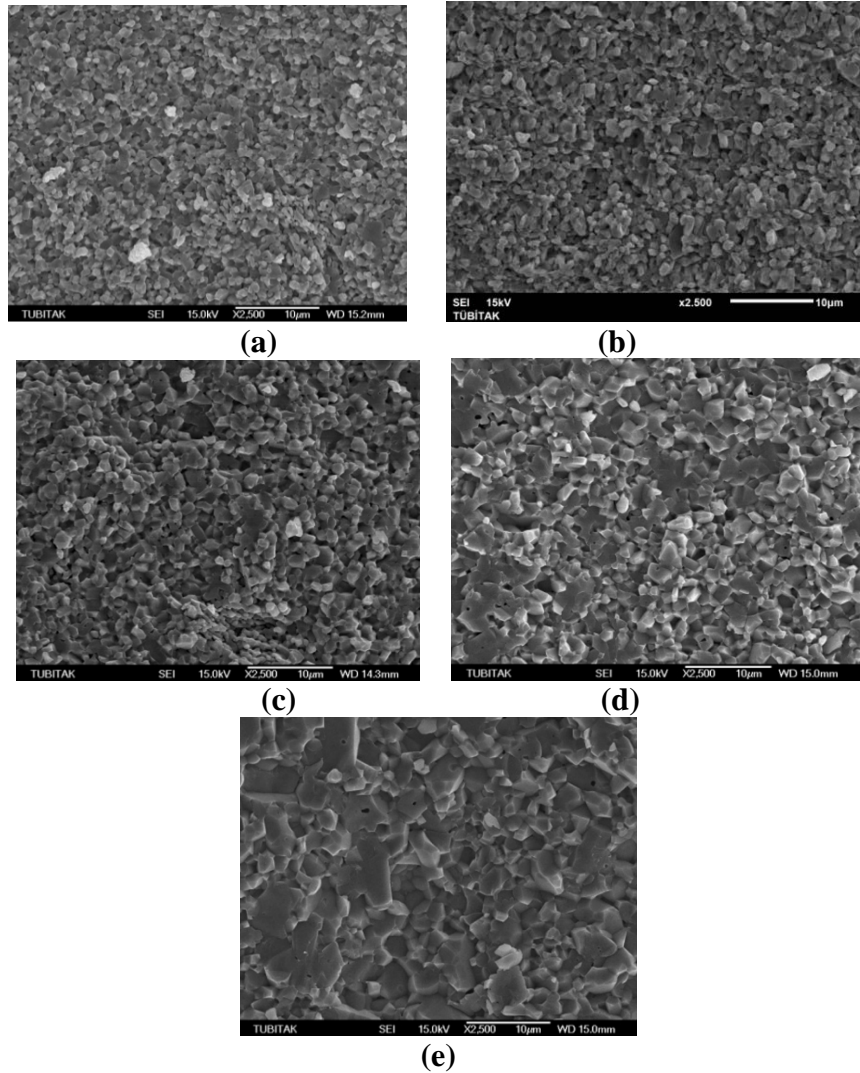


Figure 4. The microstructures of the sintered tape samples a) 1450 °C, b) 1500 °C, c) 1550 °C, d) 1600 °C, e) 1650 °C.

*Yasemin TABAK, Şeyda POLAT, Ayşen KILIÇ,
Bayise KAVAKLI VATANSEVER*

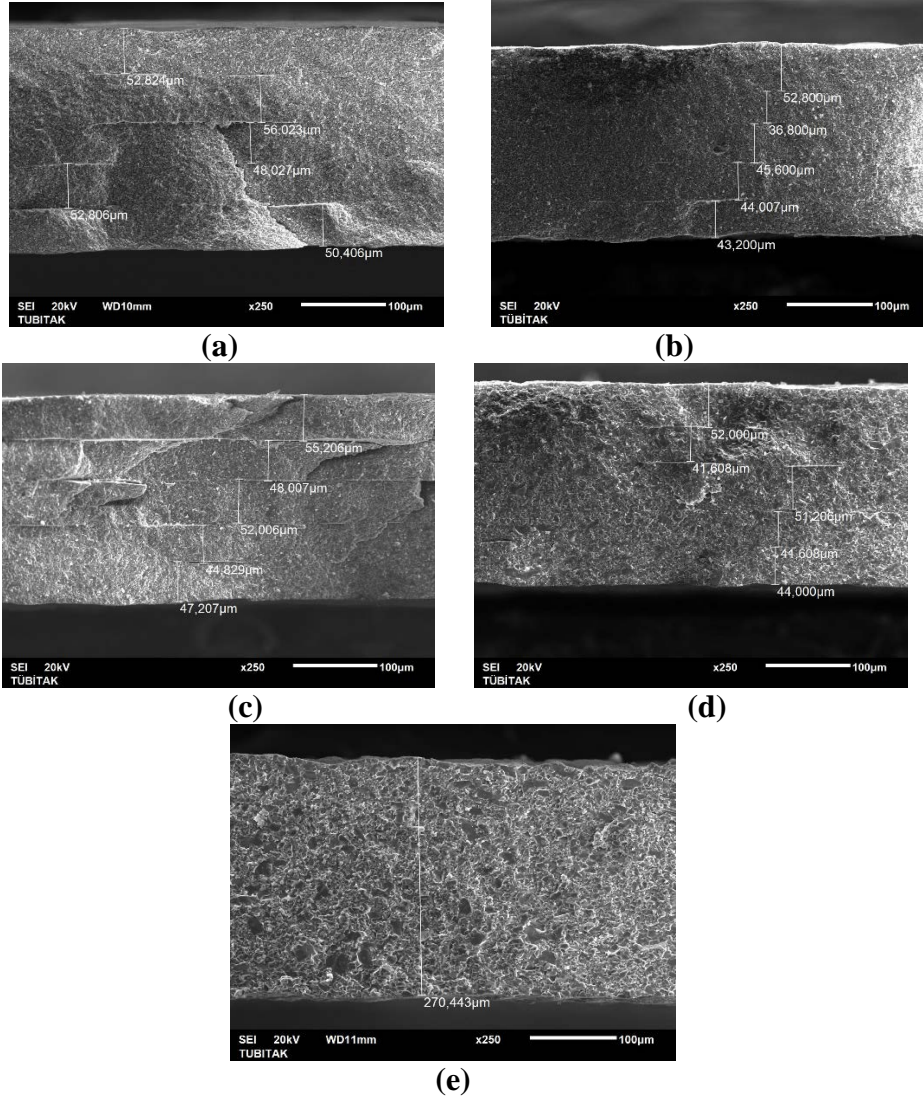


Figure 5. The cross sections of the alumina tapes sintered at different temperatures a) 1450 °C, b) 1500 °C, c) 1550 °C, d) 1600 °C, e) 1650 °C.

Production of Translucent Alumina Ceramics by Tape Casting

The cross sections of the alumina tapes sintered at different temperatures were also analyzed by SEM and layer thicknesses were determined (Figure 5).

As seen from the figures, sintering at temperatures between 1450-1600 °C revealed distinctly all five layers, with thicknesses varying between 36-52 μm (Figure 5a-d). However, at sintering temperature 1650 °C layers cannot be distinguished from one another resulting in the densest structure. A translucent alumina was actually produced by sintering at 1650 °C as shown in Figure 6.



Figure 6. Five layer tapes sintered at 1650 °C.

It is known that the sintering temperature for alumina densification usually increases with the increase in its purity and if high purity alumina powders are prepared by the traditional sintering method, the sintering temperature should be over 1700 °C to get a dense alumina sintered body (Verma & Kumar, 2016; Figiel et al., 2011). In this study, it is shown that with a well-designed slurry composition and high purity singlephase powder, it is possible to obtain a dense and translucent alumina at a lower sintering temperature than 1700 °C. Achieving a dense structure at lower temperatures helps also to avoid abnormal grain growth of alumina, which leads to loss in flexural strength, and wear resistance.

*Yasemin TABAK, Şeyda POLAT, Ayşen KILIÇ,
Bayise KAVAKLI VATANSEVER*

4. CONCLUSION

In this study alumina tapes were prepared by tape casting method and layered structures were obtained by pressureless sintering method using 5 different temperatures (1450°C, 1500°C, 1550°C, 1600°C and 1650°C) and 5 hours holding time, to observe the effect of sintering temperature on the microstructure. SEM studies revealed that as the sintering temperature increased the grain size increased and porosity decreased, indicating a denser structure. Theoretical density values increased from 83,3 to 90 % by increasing the sintering temperature from 1450 to 1650 °C, supporting the SEM studies. Theoretical densities were used in calculation of firing shrinkage values. For the samples sintered between 1450-1550 °C shrinkage was 16-17 % whereas it was between 17-18 % for those sintered between 1600-1650 °C. The cross sections of the layered structures were also studied by SEM and the sample sintered at the highest temperature revealed the most compact structure having translucent characteristics. This study has shown that it is possible to produce translucent alumina ceramics by tape casting without vacuum sintering process.

CONFLICT OF INTEREST STATEMENT

The authors declare no conflict of interest.

REFERENCES

Ba, X., Li, J., Pan, Y., Zeng, Y., Kou, H., Liu, W., Liu, J., Wu, L., & Guo, J. (2013). "Comparison of aqueous- and non-aqueous based tape casting for preparing YAG transparent ceramics". *Journal of Alloys and Compounds*, Vol. 577, pp. 228-231. doi:10.1016/j.jallcom.2013.04.209.

Feng, Z., Qi, J., & Lu, T. (2020). "Highly-transparent ALON ceramic fabricated by tape-casting and pressureless sintering method". *Journal of European Ceramic Society*, Vol. 40, Issue 4, pp. 1168-1173. doi:10.1016/j.jeurceramsoc.2019.11.065.

Figiel, P., Rozmus, M., & Smuk, B. (2011). "Properties of alumina ceramics obtained by conventional and non-conventional methods for sintering ceramics". *Journal of Achievements in Materials and Manufacturing Engineering*. Vol. 48, Issue 1, pp. 29-34.

Fujiwara, S., Tamura, Y., Maki, H., Azuma, N., & Takeuchi, Y. (2007). "Development of new high-purity alumina". *Sumitomo Kagaku*. Report No. 3.

Hou, Q., Luo, X., Xie, Z., An, D., Xiao, Z., & Ma, B. (2019). "Development of the environmental friendly non-aqueous tape casting process for high-quality Si₃N₄ ceramic substrates". *IOP Conference Series: Materials Science and Engineering*. Volume 678, 012042, pp. 1-9. doi:10.1088/1757-899X/678/1/012042.

Jurkow, D., Malecha, K., Stiernstedt, J., & Golonka, L. (2011). "Influence of tapes' properties on the laser cutting process". *Journal of the European Ceramic Society*. Volume 31, Issue 9, pp. 1589-1595. doi: 10.1016/j.jeurceramsoc.2011.02.034.

Liu, Z., Wang, Y., & Li, Y. (2012). "Combinatorial study of ceramic tape-casting slurries". *ACS Combinatorial Science*. Volume 14, Issue 3, pp. 205-210. doi: 10.1021/co200148q.

Manotham, S., Channasanon, S., Nanthananon, P., Tanodekaew, S., & Tesavibul, P. (2021). "Photosensitive binder jetting technique for the fabrication of alumina ceramic". *Journal of Manufacturing Processes*. Volume 62, pp. 313-322. doi:10.1016/j.jmapro.2020.12.011.

Miao, X., & Sun, D. (2010). "Graded/gradient porous biomaterials". *Materials*. Volume 3, Issue 1, pp. 26-47, 2010.

Mistler, R.E. (1995). "The principles of tape casting and tape casting applications". *Ceramic Processing*. R. A. Terpstra (Ed.), Chapman & Hall, London, pp. 147-173.

Mortara, L. (2005). *Analysis and development of an aqueous tape casting ceramic process* (Ph.D. Thesis). School of Industrial and Manufacturing Science, Cranfield University, United Kingdom.

Naebe, M., & Shirvanimoghaddam, K. (2016). "Functionally graded materials: A review of fabrication and properties". *Applied Materials Today*, Volume 5, pp. 223-245. doi:10.1016/j.apmt.2016.10.001.

Pabst, W., & Hříbalová, S. (2021). "Light scattering models for describing the transmittance of transparent and translucent alumina and zirconia ceramics". *Journal of European Ceramic Society*. Volume 41, pp. 2058-2075. doi:10.1016/j.jeurceramsoc.2020.10.025.

Roosen, A. (2006). "3-D structures via tape casting and lamination". *Advances in Science and Technology*, Volume 45, pp. 397-406, 2006.

Verma, V., & Kumar, B.V.M. (2017). "Processing of alumina-based composites via conventional sintering and their characterization". *Materials and Manufacturing Processes*. Volume 32, 1, 21-26. doi:10.1080/10426914.2016.1198023.

Vozdecky, P., Roosen, A., Knieke, C., & Peukert, W. (2010). "Direct tape casting of nanosized Al₂O₃ slurries derived from autogenous nanomilling". *Journal of the American Ceramic Society*. Volume 93, Issue 5, pp. 1313-1319. doi:10.1111/j.1551-2916.2009.03597.x.

Production of Translucent Alumina Ceramics by Tape Casting

Vuksic, M., Zmak, I., Curkovic, L., & Kocjan, A. (2021a). "Spark plasma sintering of dense alumina ceramics from industrial waste scraps". *Open Ceramics*. Volume 5, 100076, pp. 1-7. doi:10.1016/j.oceram.2021.100076.

Vuksic, M., Zmak, I., Curkovic, L., Coric, D., Jenus, P., & Kocjan, A. (2021b). "Evaluating recycling potential of waste alumina powder for ceramics production using response surface methodology". *Journal of Materials Research and Technology*. Volume 11, pp. 866-874. doi: 10.1016/j.jmrt.2021.01.064.

Yu, M., Zhang, J., Li, X., Liang H., Zhong, H., Li, Y., Duan, Y., Jiang D. L., Liu, X., & Huang, Z. (2015). "Optimization of the tape casting process for development of high-performance alumina ceramics". *Ceramics International*. Volume 41, Issue 10, pp. 14845-14853. doi:10.1016/j.ceramint.2015.08.010.

Wei, G. C., Hecker, A., & Goodman, D. A. (2001). "Translucent polycrystalline alumina with improved resistance to sodium attack". *Journal of the American Ceramic Society*. Volume 84, Issue 12, pp. 2853-2862. doi:10.1111/j.1151-2916.2001.tb01105.x.

Willems, H. X. (1992). *Preparation and properties of translucent gamma-aluminium oxynitride* (Ph.D. Dissertation). Technische Universiteit Eindhoven. doi:10.6100/IR382898.

Zhao, H., Tang, F., Xie, Y., Wen, Z., Tian, K., Nie, X., Cao, Y., & Tang, D. (2020). "Fabrication and rheological behavior of tape-casting slurry for ultra-thin multilayer transparent ceramics". *International Journal of Applied Ceramic Technology*. Volume 17, pp. 1255-1263. doi:10.1111/ijac.13421.

Zhou, C., Jiang, B., Fan, J., Mao, X., Pan, L., Jiang, Y., Zhang, L., & Fang, Y., (2016). "Translucent Al₂O₃ ceramics produced by an aqueous tape casting method". *Ceramics International*. Volume 42, Issue 1, pp. 1648-1652. doi:10.1016/j.ceramint.2015.09.117.

RESEARCH ARTICLE

**An ethical committee approval and/or legal/special permission has not been required within the scope of this study.*

**SPECTROSCOPIC INVESTIGATION OF ARGON DC GLOW
DISCHARGE IN PLASMA MEDIUM**

Esra OKUMUŞ 

*TÜBİTAK National Metrology Institute (UME),
Kocaeli, Türkiye, esraokumus_84@hotmail.com*

Received: 23.09.2022

Accepted: 31.01.2023

ABSTRACT

In this study, UV-VIS-NIR (Ultraviolet Visible Near-Infrared) spectra emitted from Argon Glow discharge plasma in a low vacuum were recorded with a high-resolution Czerny-Turner type spectrometer. Argon plasma was produced at a pressure of 5mTorr and with a voltage of 584 V. Argon plasma was produced between two parallel stainless steel plates anode and cathode with a diameter of 15 cm, a thickness of 0.8 cm, and a distance of 13 cm between them. The radiative and collisional processes of the Argon plasma medium were modeled by the PrismSPECT atomic physics software (Software). The distributions of ion densities were calculated using the Saha-Boltzmann equation. The intensity of the excited energy levels of Ar(I) and Ar (II) ions were calculated in the electron temperature range of (0.4-3.5eV) and the mass density of (10^{-4} - 10^{-1} gr/cm³). The UV-Visible-NIR spectra were simulated and compared with experimental spectra. The ratios of the intensities of the ArII/ArI ($1s^2 2s^2 2p^6 3s^2 3p^4 4f^1 / 1s^2 2s^2 2p^6 3s^2 3p^5 4p^1$) spectral lines were obtained for different plasma temperatures and densities. The temperature of the argon plasma was obtained from the spectral line intensity ratios.

Keywords: *Argon glow discharge plasma, Saha-Boltzmann equation, Prismspect atomic physics software.*

Esra OKUMUŞ

PLAZMA ORTAMINDA ARGON DC GLOW DEŞARJININ SPEKTROSKOPİK İNCELENMESİ

ÖZ

Bu çalışmada, düşük vakum ortamında Argon plazmasından yayılan UV-VIS-NIR (Morötesi-Görünür-Yakın Kızılaltı) spektrumları, yüksek çözünürlüklü bir Czerny-Turner tipi spektrometre ile kaydedilmiştir. Argon plazması, 5 mTorr basınç ve 584 V voltaj parametreleri kullanılarak elde edilmiştir. Argon plazması, 15 cm çapında, 0.8 cm kalınlığında ve aralarında 13 cm mesafe bulunan iki paralel paslanmaz çelik levha anot ve katot arasında üretilmiştir. Argon Glow discharge plazmasının ışınımsal ve çarpışma süreçleri, PrismSPECT atomic physics yazılımı ile modellendi. Ar(I) ve Ar(II) iyonlarının uyarılmış enerji seviyelerinin yoğunlukları, elektron sıcaklık aralığı (0.4-3.5eV) ve kütle yoğunluk aralıkları (10^{-4} - 10^{-1} gr/cm³) seçilerek Saha-Boltzmann denklemi aracılığıyla hesaplandı. UV-Visible-NIR spektrumları PrismSPECT atomic physics yazılımı ile modellendi ve deneysel spektrumlar ile karşılaştırıldı. ArII/ArI ($1s^22s^22p^63s^23p^44f^1/1s^22s^22p^63s^23p^54p^1$) spektral çizgi yoğunluk oranı farklı plazma sıcaklıkları ve yoğunlukları için elde edildi. Argon plazmasının sıcaklığı, PrismSPECT atomic physics yazılımı ile modellenen spektroskopik çizgi yoğunluk oranlarından yaklaşık olarak elde edildi.

Anahtar Kelimeler: Argon glow discharge plazma, Saha-Boltzmann denklemi, PrismSPECT atomic physics yazılımı.

Spectroscopic Investigation of Argon DC Glow Discharge in Plasma Medium

1. INTRODUCTION

The increase in the application of non-thermal plasma in various fields attracts the attention of researchers. The state of ionized plasma makes it different from normal gas. Laboratory plasmas are passed through a discharge tube where an electric current ionizes the gas (Braithwaite, 2000). The understanding of glowing discharge plasmas of pure or mixed gases is very important for industrial and medical applications (Stankov, Petković, Marković, Stamenković & Jovanović (2015)). Several applications include the use of chemical energy through active species in the surface treatment of thin film deposition (Rafatov, Akbar & Bilikmen, 2007), microelectronics (Jung, Chi, Hwang, Moon, Lee, 1999), sterilization (Park, Lee and Park, 2003), volumetric treatment of waste separation, pollution control (Amouroux, Morvan, Morel and Martin, 2004), and biomedical applications (Florian, Merbahi, Wattieaux and Yousf, 2015). Optical methods such as emission, absorption, and laser scattering are proven techniques and methods to probe plasma environments without degrading the state and composition of the plasma (Bouchikhi, Hamid, 2010). Among these techniques, optical emission spectroscopy is widely used (Sahu, Jin & Han, 2017). This technique is based on the measurement of optical radiation emitted from the plasma, as it gives information about the properties of the plasma in the immediate environment of atomic, molecular, and ionic radiators (Bings, Bogaerts & Broekaert, 2008).

In this paper, DC glow Discharge Argon plasma is generated under vacuum and emission from plasma is studied using high resolution UV-Visible-NIR spectrometer. Argon plasma media are widely used in thin film coatings. In this study, using the spectra emitted from the plasma medium occurring between the anode and cathode which are 15 cm diameter metal with a distance of 13 cm between them, the temperature of the plasma medium similar to the thin film coating conditions was obtained with the Collisional Radiative Model. The spectrum was simulated using a collisional radiative model and plasma temperature was determined from line intensity ratio (Goktas, Demir, Kacar, Hegazy, Turan, Oke & Seyhan, 2007).

2. EXPERIMENTAL AND MODELING DETAILS

The Figure1 shows the vacuum plasma system. The vacuum chamber is made of stainless steel (Nanovak, NVPR500-01) with a diameter and height of 50 cm. In the center of the chamber, there are two parallel stainless-steel plates of 15 cm in diameter and 0,8 cm in thickness, with a distance of 13 cm between them. The pressure of the vacuum chamber can be pumped down to a maximum of 10^{-7} Torr base pressure by 15 m³/h mechanical pumps and a 400 L/s turbo molecular pump (Nidec, EN-8T1). The gas is pumped into the vacuum chamber by a needle valve at a continuous dynamic gas flow in the range of 1 – 50 sccm. A DC- Glow discharge is set up and operated by applying an electric potential difference under vacuum between the electrodes that are, anode (high potential) and a cathode (low potential).

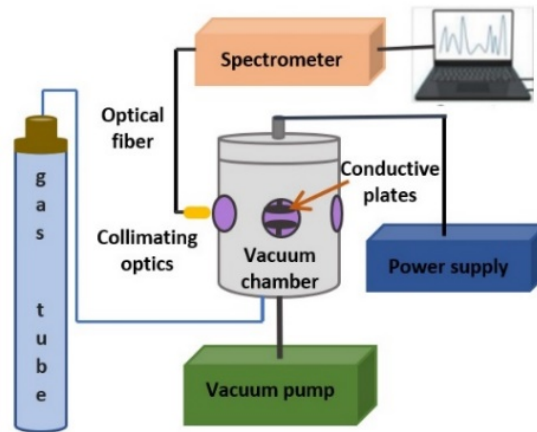


Figure1. Vacuum plasma system.

The free electrons are accelerated under applied potential within the neutral gas to the higher potential that ionizes the neutral gas particles along their path resulting in release of more electrons. The ions produced are accelerated towards the lower potential cathode, where they collide with the electrode acquiring an electron and colliding with the other electrons off the electrode into the plasma. Argon DC glow discharge plasma was produced in the vacuum chamber at 5 mTorr pressure, 24.6 – 24.9 sccm gas flow, and 584 V potential difference applied between parallel plates (see Figure 1).

Spectroscopic Investigation of Argon DC Glow Discharge in Plasma Medium

Radiation arises as a result of the interaction of electrons in the plasma with atoms or ions. In this case, three electron transitions can take place during these interactions: bonded-bonded transitions; unlimited passes; and free free passes. Light emitted from transitions creates line or continuous spectra. Atoms and ions of the gas and trace impurities emit radiation, which are in narrow spectral lines, when electron transitions occur between the various energy levels of the system (Garamoon, Samir, Elakshar, Nosair and Kotp, 2007).

According to the electron interaction process, McWhirter has suggested four plasma models, namely the local thermal equilibrium (LTE) model, the steady-state corona model, the time-dependent corona model, and the collision radiative model (P. McWhirter, 1965).

Whether the plasma is in Local Thermal Equilibrium or not is determined by the McWhirter criteria (Adrain, 1982). The Mc Whirter Criteria can be expressed as,

$$n_e \gg 10^{19} \left(\frac{T}{e}\right)^{\frac{1}{2}} \left(\frac{\Delta E}{e}\right)^3 \left(\frac{1}{m}\right)^3 \quad (1)$$

where n_e electron density, T electron temperature, e electron charge ΔE energy difference. Accordingly, the electron density has to be greater than the McWhirter equation. If the electron density satisfies this condition, the degree of ionization of the plasma and the total ion density is calculated by the Saha equation. Saha equation can be expressed as,

$$\frac{n_e n_{i+1}}{n_i} = \frac{g_{i+1}}{g_i} \left[2 \frac{m^3}{h^3} \left(\frac{2\pi T}{m}\right)^{3/2} e^{-\chi_i/kT} \right] \quad (2)$$

n_i ion density, h Planck constant, k Boltzmann constant; χ_i ionation energy. And the excited level densities of the ions are calculated by the Boltzmann equation. Boltzmann equation can be expressed as,

$$N_i = N_T g_i e^{-E_i/kT} \quad (3)$$

N_i excited level density, N_T total density, g_i statistical weight.

In the Collisional Radiative Model, ion densities and excited level densities are calculated by including the collisional and radiative processes between all levels. It can be calculated in two different ways, time-dependent and time-independent (Cowan, 1981). Ion density and excited level density change with respect to time can be expressed as,

$$\frac{dn_i}{dt} = n_e \{ n^{i-1} S^{i-1} + n^{i+1} [R_{rr}^{i+1} + n_e R_{cr}^{i+1} + R_{de}^{i+1}] - n^i [S^i + R_{rr}^i + n_e R_{cr}^i + R_{de}^i] \} \quad (4)$$

$$\frac{dn_m}{dt} = \sum_k \{ n_k [n_e C_{km} + A_{km} + B_{km} u(\lambda_{km})] - n_m n_e (C_{mk} + B_{mk} u(\lambda_{km})) + n_e \{ n^{i-1} S^{i-1} - n_i S^i + n^{i+1} [R_{rr} + n_e R_{cr} + R_{de}] \} \} \quad (5)$$

S ionation rate, R_{rr} radiative recombination rate, R_{cr} collisional radiative recombination rate, R_{de} dielectronic recombination, C collisional excitation rate, A spontaneous emission rate, B stimulated emission rate, u energy density, λ wave length. In this study, the densities of the energy levels were calculated according to the plasma temperature and density using the Collisional Radiative Model (equations 4-5) in PrismSPECT software.

Coronal Equilibrium Model is used in low-density plasma conditions. In this model, the radiation processes dominate because the collision processes are very weak due to the low density of the plasma (Hutchinson, 2002). In Coronal Equilibrium Model, it is assumed that changes in energy levels result from radiative processes. Coronal Equilibrium model is valid under low density and high-temperature plasma conditions. Electron density condition for Coronal Equilibrium can be expressed as,

$$n_e < 5,6 \times 10^{14} (Z + 1)^6 T_e^{\frac{1}{2}} \exp \left[\frac{1,62 \times 10^3 (Z + 1)^2}{T_e} \right] \quad (6)$$

where Z is atomic number.

Spectroscopic Investigation of Argon DC Glow Discharge in Plasma Medium

3. RESULTS AND DISCUSSION

The spectrum of the Argon glow discharge plasma produced in the vacuum is presented in Figure 2. This spectrum was recorded by a high-resolution Optical Emission Spectrometer. Baki spectrometer is a Czerny-Turner type emission spectrometer between 200 – 1100 nm, with integration time min. 10 μ s, resolution 0.5 nm, and trigger inputs and outputs. Since the plasma medium is continuous medium, measurements were made in 100 ms without any delay on the spectrometer. The rays emitted from the plasma were collected with a 1 – inch focal length parabolic mirror (Thorlabs) and propagated to the spectrometer with a fiber optic cable. The experimental spectra were simulated using a collisional radiative plasma code PrismSPECT software. The simulated spectrum of Argon plasma at $T_e = 2$ eV and $\rho_e = 1 \times 10^{-4}$ gr/cm³ is shown in Figure 3.

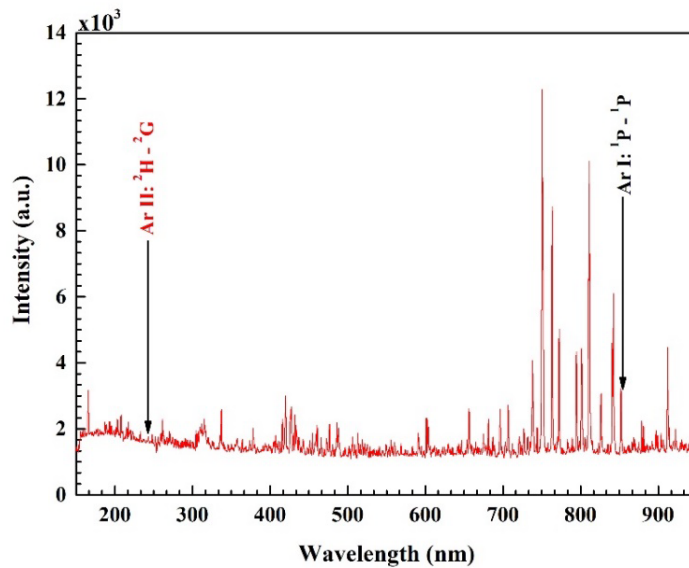


Figure 2. Optical Emission Spectrum of Argon glow discharge plasma produced in the laboratory.

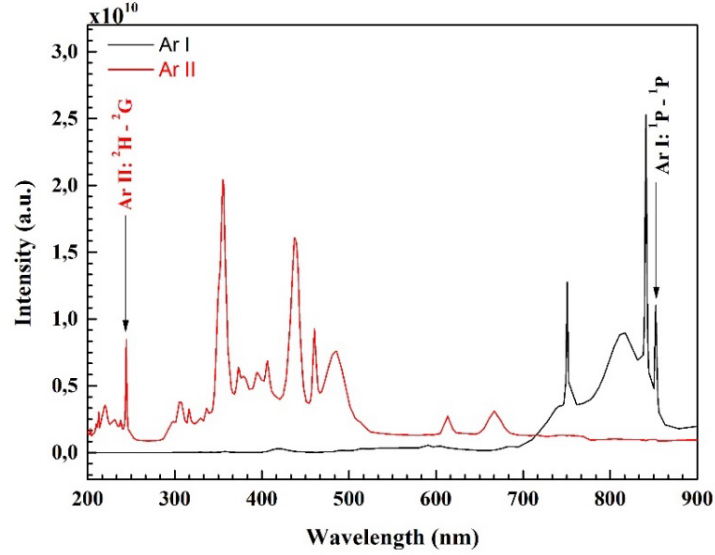


Figure 3. The simulated spectrum of Argon plasma at $T_e = 2 \text{ eV}$ and $\rho_e = 1 \times 10^{-4} \text{ gr/cm}^3$ with the PrismSPECT collisional radiative code.

It is presented in Figure 2 that the second ionization line is at 244.4 nm and its intensity is 1.76 a.u., the first ionization line is at 852.5 nm and its intensity is 3.16 a.u. Since the densities of the excited levels of two different ions are more sensitive to the electron temperature, the excited levels of ArI and Ar II ions were chosen for temperature measurement. In experimental measurements, the signal-to-noise (SNR) ratio ($SNR = P_{signal}/P_{noise}$) decreases due to the noise in the CCD of the spectrometer, and ArII ion densities seem low. Cooling the CCD detector can be beneficial to reduce noise. In the simulated spectrum of Argon plasma, it is only seen the spectral lines of the first ionization and the second ionization of argon. Therefore, as there are different ionizations of argon gas there are more ionization spectral lines in the experimental spectrum. The experimental intensity ratio of the spectral line of the second ionization of argon to the spectral line of the first ionization of argon is $Ar_{II}/Ar_I = 1.76/3.16 = 0.556$.

Spectroscopic Investigation of Argon DC Glow Discharge in Plasma Medium

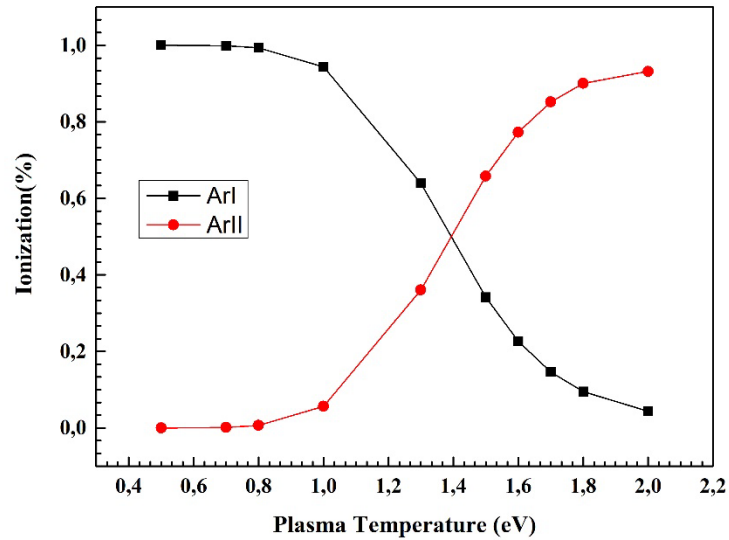


Figure 4. Graph of temperature versus percent ionization at a constant mass density of $\rho_e = 1 \times 10^{-4} \text{ gr/cm}^3$.

Figure 4 shows the temperature versus the ionization percentage at constant mass density of $\rho_e = 1 \times 10^{-4} \text{ gr/cm}^3$ with the PrismSPECT program. And Figure 5 shows simulated mass density versus the ionization percentage at the constant temperature of $T_e = 2 \text{ eV}$. As seen from Figure 4 while the temperature-dependent change of the first ionization percentage of argon decreases towards high temperature, temperature-dependent change in the second ionization percentage of it increases towards high temperatures. As illustrated in Figure 5, while in the mass density graph of the ionization percentage the mass density variation of the first ionization percentage of argon increases towards high mass density, the second ionization percentage of argon decreases towards high mass density.

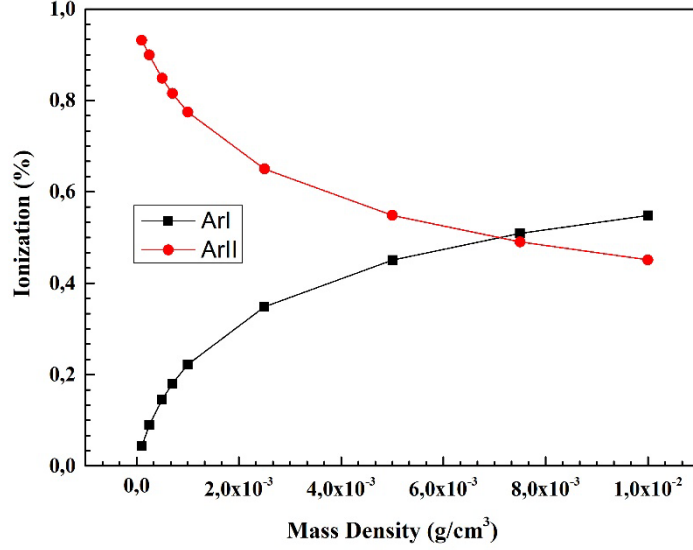


Figure 5. Graph of mass density versus percent ionization at a constant temperature of $T_e = 2 \text{ eV}$.

The Figure 6 shows that a graph of the change of the ratio of the second ionization to the first ionization of argon versus mass density at a constant temperature of $T_e = 2 \text{ eV}$ in the simulated with the PrismSPECT program. And also Figure 7 shows the intensity ratio of the second ionization to the spectral line of the first ionization of argon versus temperature at a constant mass density of $\rho_e = 1 \times 10^{-4} \text{ gr/cm}^3$. The atomic data taken from NIST (atomic-spectra-database) for the lines is shown in Table 1.

TABLE 1. Atomic data of Argon spectral lines.

Ion	Upper configuration	Term	Lower configuration	Term	wl(nm)	Osc. Str.
ArI	$1s^2 2s^2 2p^6 3s^2 3p^5 4p^1$	1P	$1s^2 2s^2 2p^6 3s^2 3p^5 4s^1$	1P	852.35	0.151
ArII	$1s^2 2s^2 2p^6 3s^2 3p^4 f^1$	2H	$1s^2 2s^2 2p^6 3s^2 3p^4 d^1$	2G	244.3	0.1979

Spectroscopic Investigation of Argon DC Glow Discharge in Plasma Medium

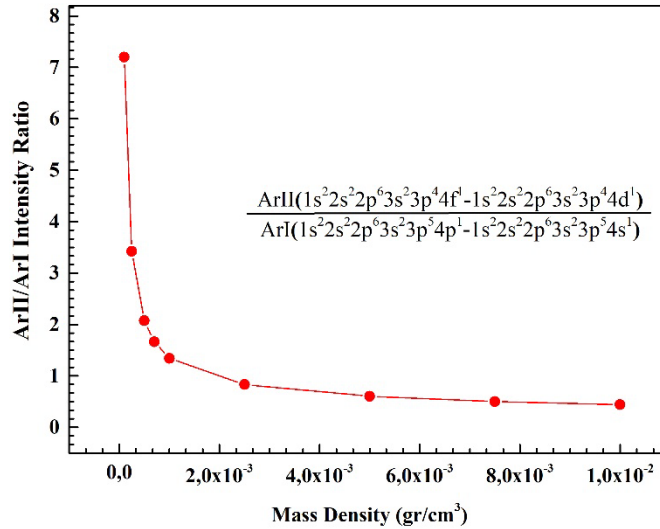


Figure 6. Graph of the change of the ratio of the second ionization to the first ionization of argon versus mass density at a constant temperature of $T_e = 2 \text{ eV}$.

As seen from Figure 6 and Figure 7, respectively, the intensity ratio of the spectral lines of argon decreases with respect to mass density, while the ratio of spectral lines of argon increases with respect to a higher temperature. The experimental intensity ratio of spectral lines ($\text{Ar}_{\text{II}}/\text{Ar}_{\text{I}} = 1.76/3.16 = 0.556$) obtained from Figure 2 is shown in the graph simulated by the PrismSPECT program in Figure 7. Accordingly, as seen from Figure 7 that the electron temperature of the Argon DC glow discharge plasma generated in a vacuum chamber is approximately **1.66 eV**

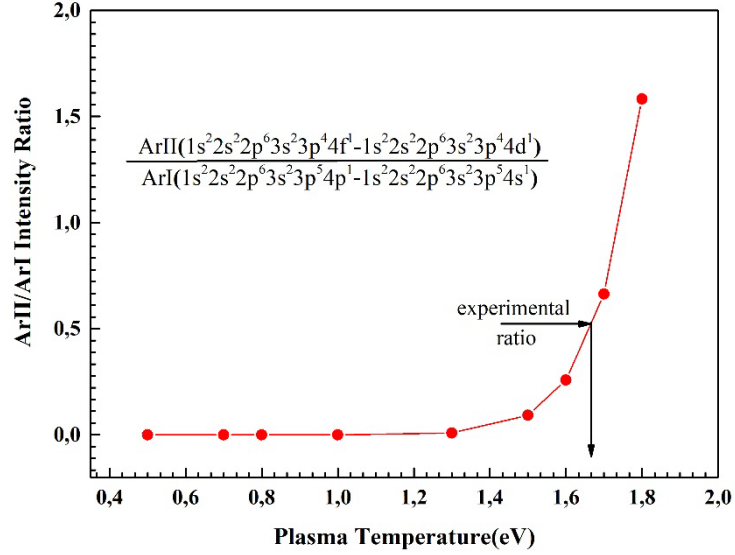


Figure 7. Graph of the change of the ratio of the second ionization to the first ionization of argon versus temperature at a constant mass density of $\rho_e = 1 \times 10^{-4} \text{ gr/cm}^3$.

5. CONCLUSION

DC glow discharge Ar plasma was created under vacuum, and the photons emitted from the plasma were analyzed by optical emission spectrometry. The emitted spectrum of the argon plasma was simulated by the PrismSPECT program. Plasma temperature was obtained from spectrum line ratios. By comparing the spectrum of Argon DC glow discharge plasma taken with an optical emission spectrometer with simulation graphics of ArII/ArI emission intensity ratio calculated with the PrismSPECT program, the temperature of the plasma created in the vacuum environment is approximately shown. In this study, Argon plasma conditions used in thin-film coating environments were examined spectroscopically and it contributed to the understanding and interpretation of similar plasma environments by simulation.

Spectroscopic Investigation of Argon DC Glow Discharge in Plasma
Medium

ACKNOWLEDGMENT

This research is founded by TÜBİTAK UME Project No: G2ED-E1-02-I.

CONFLICT OF INTEREST STATEMENT

The authors declare no conflict of interest.

REFERENCES

- Adrain, R. S. (1982). Some industrial uses of laser induced plasmas. In Koebner, H., *Industrial Applications of Lasers*, Wiley, New York.
- Bings, N. H., Bogaerts, A., Broekaert, J. A. C. (2008). "Atomic Spectroscopy", *Analytical Chemistry*, 80, 4317-4347.
- Bouchikhi, A., Hamid, A. (2010). "2D DC Subnormal Glow Discharge in Argon". *Plasma Science and Technology*, 12, 1.
- Cowan, R. D. (1981). *The Theory of Atomic Structure and Spectra*, Univ. of California Press, Berkeley.
- Florian, J., Merbahi, N., Wattieaux, G., Plewa, J. M., and Yousfi, M. (2004). "Comparative Studies of Double Dielectric Barrier Discharge and Microwave Argon Plasma Jets at Atmospheric Pressure for Biomedical Applications". *IEEE Transactions on Plasma Science*, 43,3332-3338.
- Goktas, H., Demir, A., Kacar, E., Hegazy, H., Turan, R., Oke, G., Seyhan, A. (2007). "Spectroscopic Measurements of Electron Temperature and Electron Density in Electron Beam Plasma Generator Based on Collisional Radiative Model". *Spectroscopy Letters*, 40, 183-192.
- Hutchinson, I. H., 2002. *Principles of Plasma Diagnostics*, 2nd Ed., Cambridge University Press.
- Jung, C. O., Chi, K. K., Hwang, B. G., Moon, J. T., Lee, M. Y., Lee, J. G. (1999). "Advanced plasma technology in microelectronics". *Thin Solid Films*, 341,112-119.
- McWhirter, R. W. P. (1965). *Plasma Diagnostics Techniques*, New York: Academic Press.
- N. St. J., Braithwaite. (2000). "Introduction to gas discharges". *J. Plasma Sources Sci. Technol*, 9, 517-527.

Spectroscopic Investigation of Argon DC Glow Discharge in Plasma Medium

NIST: Atomic Spectra Database. (September 2021).
<https://www.nist.gov/pml/atomic-spectra-database>.

Park, B. J., Lee, D. H., Park, J. C. (2003). "Sterilization using a microwave-induced argon plasma system at atmospheric pressure". *Physics of Plasmas*, 10, 4539-4544.

PrismSPECT software. (September 2021).
<https://www.prism-cs.com/Software/PrismSPECT/overview.html>.

Rafatov, I. R., Akbar, D. & Bilikmen, S. (2007). "Modelling of non-uniform DC driven glow discharge in argon gas". *Plasma Science and Technology*, A367, 114-119.

Sahu, B. B., Jin, S. B., Han, J. G. G. (2017). "Development and characterization of a multi-electrode cold atmospheric pressure DBD plasma jet aiming plasma application". *Journal of Analytical Atomic Spectrometry*, 32, 782-795.

Stankov M. N., Petković M. D., Marković V. Lj., Stamenković S. N., Jovanović A. P. (2015). "The Applicability of Fluid Model to Electrical Breakdown and Glow Discharge Modeling in Argon". *Chinese Physics Letters*, 32, 025101.

Journal of Naval Sciences and Engineering

2023, Vol. 19, No. 1, pp. 35-51

DOI: 10.56850/jnse.1252303

Electrical-Electronics Engineering/Elektrik-Elektronik Mühendisliği

RESEARCH ARTICLE

**An ethical committee approval and/or legal/special permission has not been required within the scope of this study.*

**THERMAL ANALYSIS OF XLPE INSULATED SUBMARINE
CABLES FOR DIFFERENT LOADING CONDITIONS**

Ahmet Yigit ARABUL^{1,3*} 

Celal Fadil KUMRU^{2,3} 

¹*Yildiz Technical University, Department of Electrical Engineering,
Istanbul, Türkiye, arabul@yildiz.edu.tr*

²*Suleyman Demirel University, Department of Electrical-Electronics
Engineering, Isparta, Türkiye, celalkumru@sdu.edu.tr*

³*University of Waterloo, Electrical and Computer Engineering, Waterloo,
ON, Canada*

Received: 17.02.2023

Accepted: 15.03.2023

ABSTRACT

Submarine cables are critical assets that play an indispensable role in interconnected power systems, particularly in cross-sea energy transmission and offshore wind turbines. Their importance is further accentuated in exigent situations such as natural disasters and war, which emphasize the need for secure, reliable and uninterrupted energy supply. Furthermore, the investment and operating costs of submarine cables are relatively higher than other power system equipment, making it essential to operate them under the rated operating conditions to prevent possible faults and ensure power system stability. As thermal stress can lead to damage of cable insulation, it is an essential parameter to consider. Overloading increases thermal stress, resulting in rapid aging of the cable insulation and a shorter cable lifetime. Therefore, it is imperative to determine the maximum conductor temperatures and current carrying capacities of submarine cables under varying loading rates and ambient conditions using thermal analysis. In this study, thermal analyses are carried out for a three-phase, 220 kV HVAC, XLPE insulated submarine cable under different loading conditions. The findings demonstrate that the maximum temperature, current carrying capacity, and total losses of the cable are significantly impacted by loading rate, phase imbalance, and seawater temperature.

Keywords: *Submarine cable, thermal analysis, loading rate, offshore wind turbine.*

FARKLI YÜKLEME ŞARTLARI İÇİN XLPE İZOLELİ DENİZALTI KABLOLARININ ISIL ANALİZİ

ÖZ

Denizaltı kabloları, enterkonnekte güç sistemlerinin en önemli ve kıymetli varlıklarından biri olup hem deniz aşırı enerji iletiminde hem de açık deniz rüzgar türbinlerinde yaygın biçimde kullanılmaktadır. Bu kablolar, özellikle doğal afet ve savaş gibi kritik ve stratejik durumlarda daha da önem kazanmaktadır. Ayrıca denizaltı kablolarının hem yatırım ve hem de işletme maliyetleri diğer güç sistem ekipmanlarına kıyasla ciddi derecede yüksektir. Bu sebeplerden ötürü, kablonun nominal işletme şartları içerisinde çalıştırılması ve böylelikle olası arızaların engellenmesi güç sistem kararlılığının sağlanması bakımından elzemdir. Kablo izolasyonunun zarar görmemesi için dikkat edilmesi gereken en önemli parametreler arasında ısıl zorlanma gelmektedir. Aşırı yüklenmeye bağlı artan ısıl zorlanmayla kablo yalıtkanı daha hızlı yaşlanmakta ve kablonun işletme ömrü azalmaktadır. Bu nedenle, denizaltı kablolarının farklı yüklenme oranları ve ortam şartları için maksimum iletken sıcaklıklarının ve akım taşıma kapasitelerinin ısıl analizler yardımıyla belirlenmesi önem arz etmektedir. Bu çalışmada, üç faz, 220 kV HVAC, XLPE izoleli bir denizaltı kablosunun farklı yüklenme koşulları altında ısıl analizleri gerçekleştirilmiştir. Sonuçlar, yüklenme oranının, faz dengesizliğinin ve deniz suyu sıcaklığının kablonun maksimum sıcaklığı, akım taşıma kapasitesi ve toplam kayıpları üzerinde önemli etkisi olduğunu göstermektedir.

Anahtar Kelimeler: *Denizaltı kablosu, ısıl analiz, yüklenme oranı, açık deniz rüzgar türbinleri.*

1. INTRODUCTION

Energy is a critical issue in modern society and its significance continues to grow with advancements in technology and increasing energy demands. Distributed generation facilities such as wind and solar power plants, as well as alternative energy sources, are being utilized to meet the rising energy demand in the most expedient and practical manner (Keskin Arabul et al., 2017). Offshore wind power plants have become increasingly popular in many countries due to their high energy production capacity. The literature and practice have seen numerous studies conducted to enhance the efficient use of energy resources. Despite these efforts, natural disasters and wars can lead to critical situations where the energy supply-demand balance cannot be maintained. While the occurrence probability of natural disasters such as earthquakes, floods, and hurricanes is low, their effects on the power system can be quite severe. In such scenarios, the existence of an interconnected network with submarine cables is vital in meeting energy needs.

Submarine cables are extensively used for energy transfer in interconnected networks, with approximately 1.3 million kilometers of such cables installed worldwide at different voltage levels (*Submarine Cable Almanac*, 2021). Guides and standards for the design, production, installation, and operation of submarine cables have been established and are presently in use (IEEE, 2004). However, the nominal operating ranges may vary based on factors such as cable type (AC or DC), voltage level, and ambient conditions in the installation region. In particular, it is critical to analyze parameters such as maximum operating temperature, ampacity, and critical loading rate in detail, depending on the cable type and the region. Another important aspect in submarine cable selection is determining whether energy transmission will be through AC or DC cable. Recent studies show that the topic of energy transmission through DC submarine cables has gained significant popularity (Hu et al., 2014; Lldstad, 1994; Mei et al., 2017; Zhang et al., 2021). Literature and practical examples reveal that optimal system design is performed based on the power to be transmitted, transmission distance, and investment cost (Takeshita et al., 2022). Submarine cables have a critical role in maintaining power system reliability, and their investment costs are quite high. Therefore, online monitoring of cable conditions is crucial to prevent unexpected faults (Ou et al., 2022). One of the primary reasons for submarine

Thermal Analysis of XLPE Insulated Submarine Cables for Different Loading Conditions

cable failure is thermal stress (Mei et al., 2017; Yu et al., 2022). In cases of excessive or unbalanced loading, thermal stress on cable insulation can increase, leading to a decrease in the cable's life. Consequently, there is a need for studies to determine cable operating limits for different loading conditions.

This study conducts thermal analyses of a three-phase, 220 kV, and 500 mm² submarine cable for various loading and environmental conditions, utilizing the COMSOL[®] Multiphysics 5.6 software. The study determines conductor, screen, and armor losses, as well as maximum and minimum operating temperatures under different loading rates, unbalanced loading conditions, and various seawater temperatures. Furthermore, cable's ampacity is calculated for various loading conditions, and the results obtained discussed.

2. METHODOLOGY AND MATERIAL

In this study, a numerical model of a lead-shielded, XLPE-insulated, three phase HVAC submarine cable with a nominal voltage of 220 kV is utilized for thermal analysis (COMSOL, 2023). The cable utilizes copper conductors with a phase conductor cross section of 500 mm² and a nominal current carrying capacity of 655 A. The design of the cable is modeled in 2D and is depicted in Figure 1.

The cable illustrated in Figure 1 has been installed 7 cm beneath the seabed on a bed of gravel. In this study, frequency domain analyses are conducted utilizing the “Magnetic Fields” and “Heat Transfer in Solids” interfaces. Conductor losses, shield losses, and armor losses due to phase currents are calculated by taking into account the inductive effects within the Magnetic Fields interface. These losses are defined as the heat source in the Heat Transfer in Solids interface, and temperature distributions within the cable are obtained. This approach enabled the establishment of a multiphysics coupling between electromagnetic fields and heat transfer by utilizing a frequency-stationary study type. Material properties and boundary conditions are defined with reference to the COMSOL[®] Multiphysics 5.6 library.

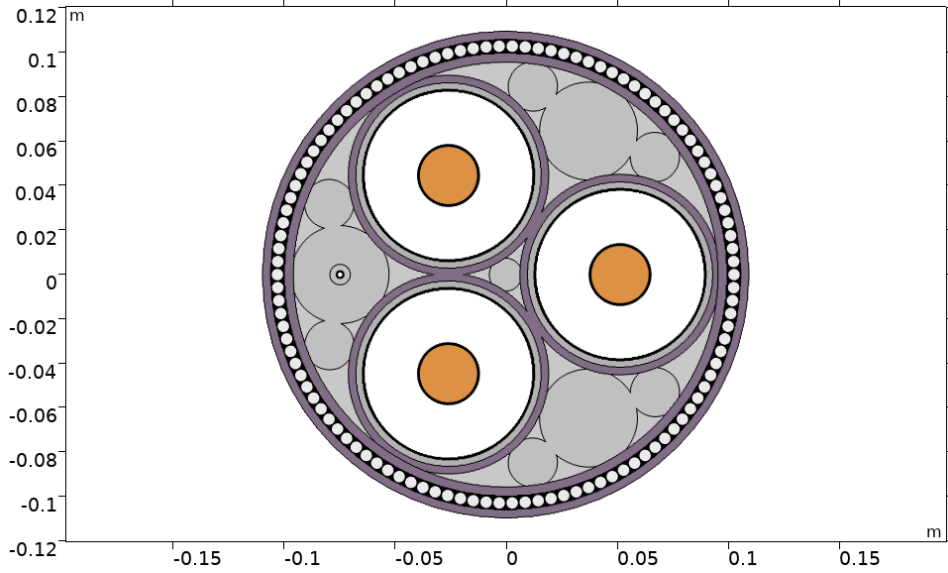


Figure 1. 2D geometry of three phase, 220 kV HVAC submarine cable used in the analyses.

The aim of this study is to investigate the effects of three different conditions on cable temperature, namely, loading ratio, unbalanced loading, and seawater temperature, on the cable's maximum temperature, ampacity, and total losses. Further details of the analyses are presented in Table 1.

Table 1. Description of analyses performed in the study.

Analysis	Description
Loading rate	Three phases are loaded from 50% to 120% with 10% steps
Unbalanced loading	2 phase is 50% loaded 1 phase is loaded from 50% to 120% with 10% steps
Seawater temperature	Seawater temperature is changed from 5°C to 30°C with 5°C steps.

3. RESULTS AND DISCUSSION

This section provides a presentation of the outcomes derived from simulation studies conducted on a submarine cable. The examination focuses on three distinct cases. Firstly, simulations are performed to investigate the thermal changes of the cable in both balanced and unbalanced loading conditions. Secondly, the studies are expanded to include simulations conducted under various sea water temperatures.

3.1. Effects of Varied Loading Rates

Simulation studies are conducted to explore various loading rates under conditions of balanced loading. In this scenario, the cable is subjected to operational loads ranging from 50% to 120% of its ampacity. The resulting maximum and minimum temperature values observed on the cable are presented in Figure 2.

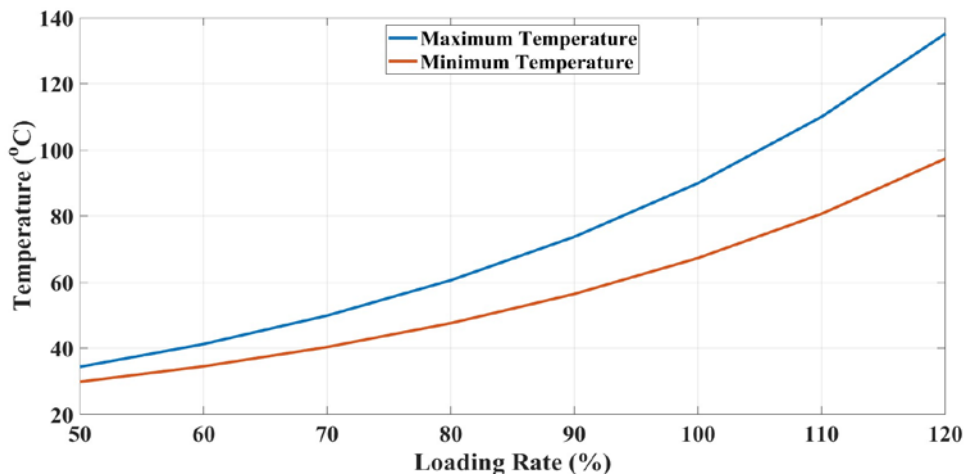


Figure 2. Temperature variations in a balanced loads under different loading conditions.

The aforementioned line chart illustrates the maximum and minimum temperatures of the submarine cable in response to various loading rates, ranging from 50% to 120%. It is evident that the temperature changes on the cable are non-linear with respect to changes in load, as the temperature rise is more pronounced at higher loading rates. Moreover, the difference between maximum and minimum temperatures increases from 4.54 °C to 37.77 °C, as

depicted by the diverging lines in the graph. Such temperature differences are undesirable, as they may lead to unfavorable deformation of the cable material. Losses, which are a crucial factor impacting temperature increases, are documented in Table 2 for distinct loading conditions under balanced loading.

Table 2. Submarine cable losses under different loading rates in a balanced loading.

Loading Rate (%)	Phase Losses (W/km)	Screen Losses (W/km)	Armor Losses (W/km)
50	10712	3254	1930
60	16111	4616	2745
70	23094	6166	3679
80	32040	7872	4713
90	43461	9691	5827
100	58058	11570	6989
110	76797	13447	8163
120	101050	15241	9303

The observations from Table 2 indicate that all losses increase in proportion to the loading ratio. Screen and armor losses exhibit a relatively lower rate of increase, while phase losses show a steep rise. The reason for this is the direct proportionality of phase losses to the square of the current. Upon examining the effect of these losses on the overall loss, it is evident that phase losses rise from 67% to 80%, while screen and armor losses drop from 20% to 12% and from 12% to 7%, respectively. The thermal distribution resulting from the operation of a 100% balanced loaded cable is depicted in Figure 3.

Thermal Analysis of XLPE Insulated Submarine Cables for Different Loading Conditions

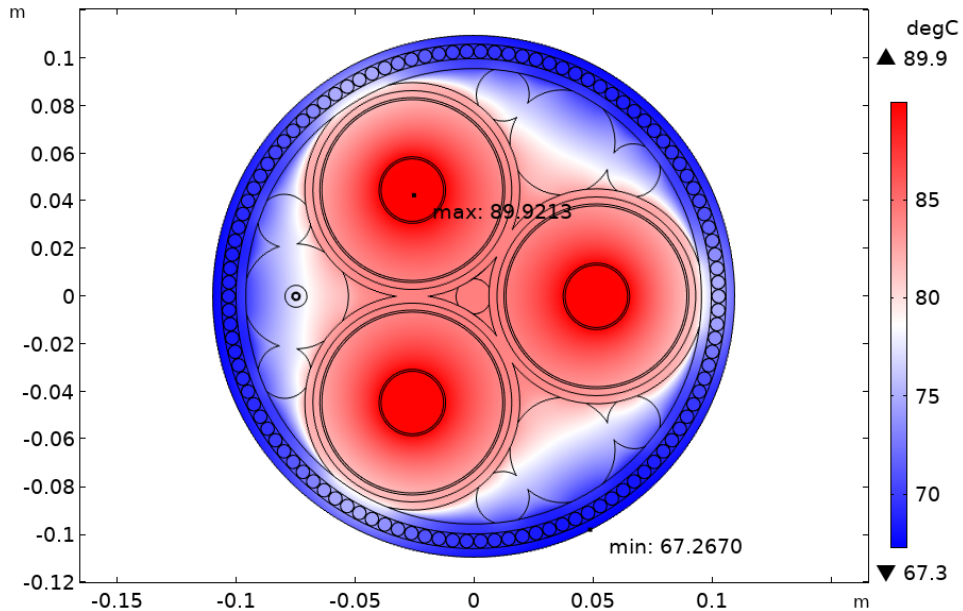


Figure 3. Temperature distribution across a cable under 100% balanced loading

3.2. Effects of Unbalanced Loading

In this stage of the simulation study, the three-conductor submarine cable is subjected to unbalanced loading by altering the current passing through a single phase. The loading rate of the unbalanced phase is varied between 50% and 120%, while the other two phases are held constant at 50% loading. The maximum and minimum temperatures recorded on the cable under these loading conditions are presented in Figure 4.

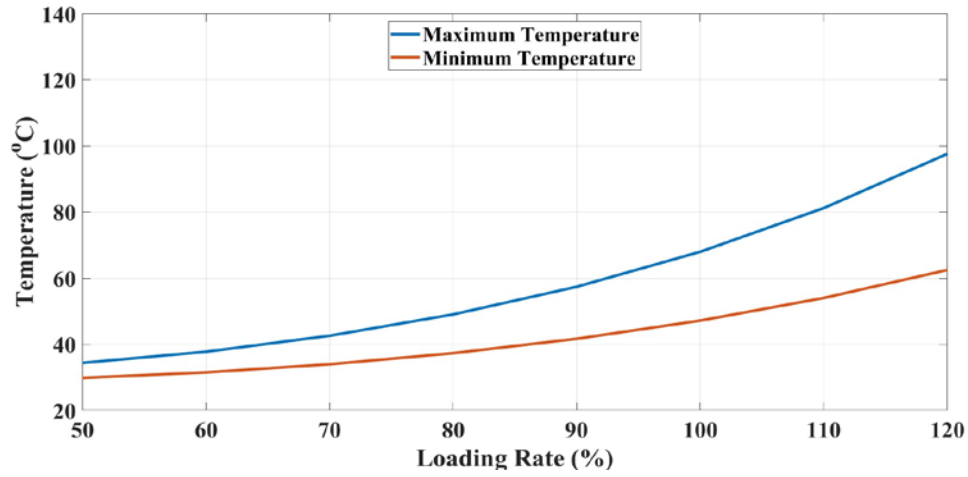


Figure 4. Temperature variations in an unbalanced loads under different loading conditions.

As can be observed from Figure 4, the maximum and minimum temperature changes on the cable exhibit a pattern similar to that of the balanced loading. In this figure, it is also noted that the temperature does not increase linearly, but rather increases more as the loading ratio increases. Since the loading rate of the two phases that are constantly loaded is 50% in the case of balanced loading, the temperature values are lower than those of the cable in which all three phases are balanced. In addition, it is observed that the difference between the maximum and minimum temperatures has increased from 4.54 °C to 35.12 °C. Although the maximum and minimum temperature values are lower than those of the balanced loading condition, the difference (Δt) between them is of similar magnitude. Under the conditions where one phase is altered, the cable has a current carrying capacity of up to 1067 A or 15% of its ampacity. Under unbalanced loading conditions, the submarine cable losses for different loading scenarios are presented in Table 3.

Thermal Analysis of XLPE Insulated Submarine Cables for Different Loading Conditions

Table 3. Submarine cable losses under different loading rates in an unbalanced loading.

Loading Rate (%)	Phase Losses (W/km)	Screen Losses (W/km)	Armor Losses (W/km)
50	10712	3254	1930
60	12690	3847	2271
70	15523	4788	2796
80	19325	6080	3509
90	24282	7729	4415
100	30638	9746	5523
110	38713	12145	6845
120	48910	14943	8396

Upon examination of Table 3, it is evident that phase losses display a considerably higher rate of increase compared to the screen and armor losses, owing to their direct proportionality with the square of current. Furthermore, when the effect ratios of these losses on the total loss are evaluated, it is seen that the loss ratios do not experience significant variations with the alteration of the loading ratio on one of the phases. The results of this study show that the average percentages of phase losses, screen losses, and armor losses are 67%, 21%, and 12%, respectively. The thermal distribution resulting from the operation of the unbalanced loaded cable, where one phase is loaded at 100% and the other two phases are loaded at 50%, is presented in Figure 5.

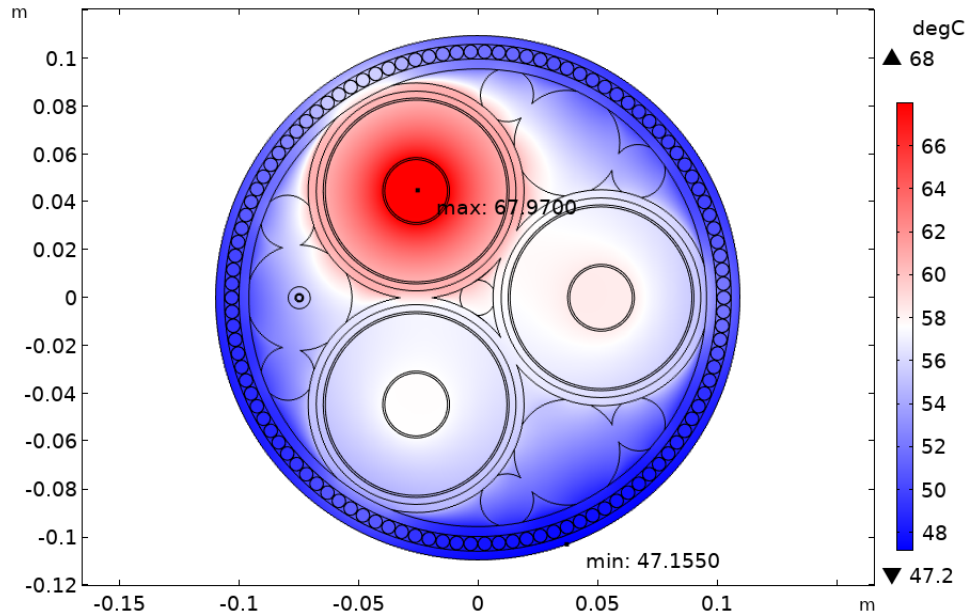


Figure 5. Temperature distribution under unbalanced loading: one phase loaded at 100%, other phases at 50%.

3.3. Effects of Sea Water Temperature

In this stage of the simulation study, an additional parameter affecting temperature, namely changes in seawater temperature, is investigated. Although seawater temperature is generally assumed to be 20 °C in the literature, fluctuations at this temperature can significantly affect the cable temperature and its ampacity. Therefore, simulations are conducted for seawater temperatures ranging from 5 °C to 30 °C, considering the minimum and maximum temperatures in oceans. The resulting maximum and minimum temperature variations on the cable for different seawater temperatures are depicted in Figure 6.

Thermal Analysis of XLPE Insulated Submarine Cables for Different Loading Conditions

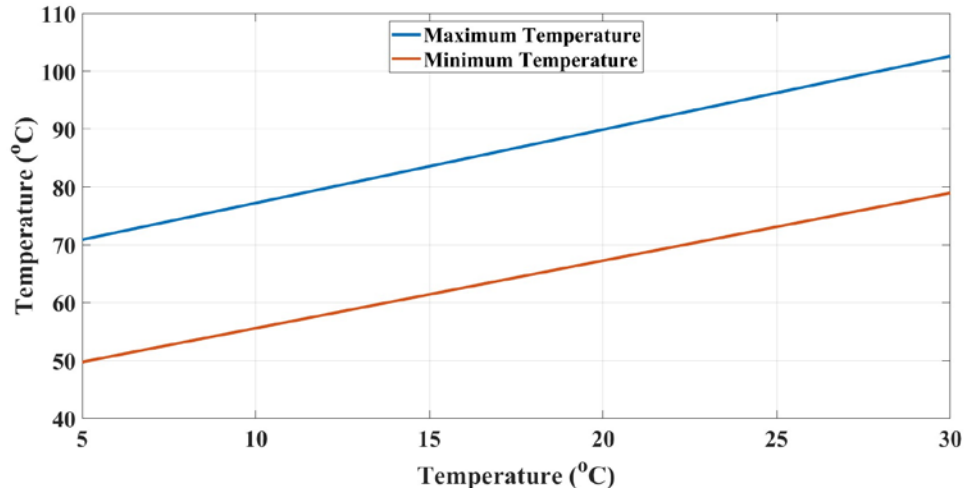


Figure 6. Temperature variations in a balanced loads under different seawater temperatures.

As opposed to the simulation results obtained in the previous subsections, it can be observed from Figure 6 that the maximum and minimum temperatures increase almost linearly with increasing seawater temperature. It is also noted that the difference between maximum and minimum temperatures (Δt) changes very slightly between 21.13 °C and 23.66 °C. This low variability in temperature difference is a positive factor for cable insulation. Specifically, it is observed that low seawater temperatures have a positive effect on the cable's current-carrying capacity. For instance, it can carry up to 10.1% more current (i.e., 1021.4 A instead of 927.72 A) under seawater temperature of 5 °C. Conversely, under seawater temperature of 30 °C, the current-carrying capacity decreases by 7.3% (i.e., from 927.72 A to 860 A). The submarine cable losses under these conditions are presented in Table 4.

Table 4. Submarine cable losses under different seawater temperatures.

Seawater Temperature (°C)	Phase Losses (W/km)	Screen Losses (W/km)	Armor Losses (W/km)
5	52782	12055	7308
10	54546	11891	7200
15	56304	11729	7093
20	58058	11570	6989
25	59806	11414	6886
30	61550	11261	6786

When considering the ratios of the losses in Table 4 with respect to the total loss, it can be seen that the ratios of phase losses vary between 73% and 77%, while screen losses vary between 16.71% and 14.15%, and armor losses vary between 10% and 8.5%. In the case of seawater temperature being 30 °C, the thermal distribution of the balanced loaded cable is shown in Figure 7.

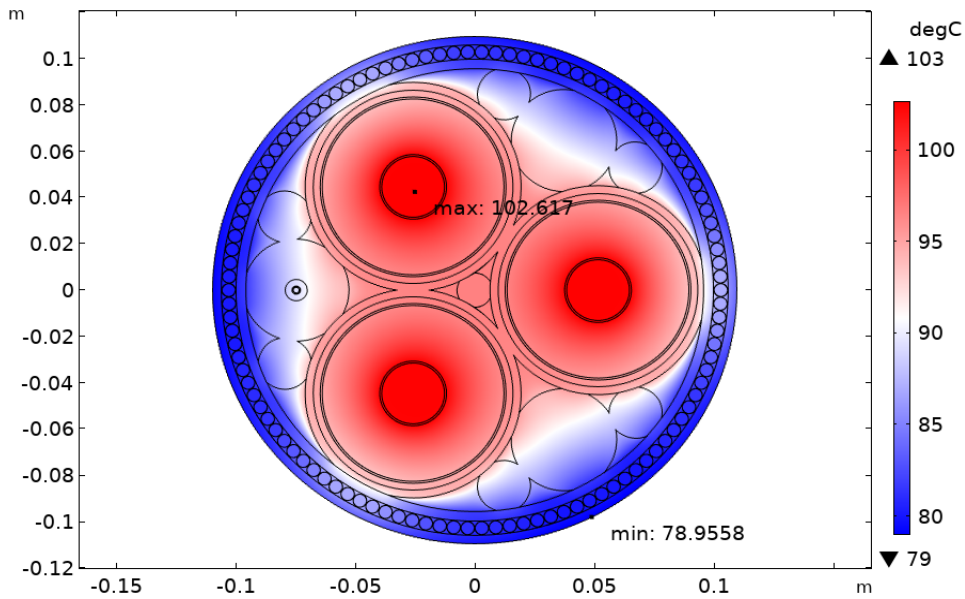


Figure 7. Thermal distribution across a 100% balanced loaded cable in 30 °C seawater.

Thermal Analysis of XLPE Insulated Submarine Cables for Different Loading Conditions

4. CONCLUSION

In this study, thermal analyses of a three-phase, 220 kV HVAC, XLPE insulated submarine cable used for offshore wind turbines under different loading conditions are carried out. In simulation studies, it is observed that as the cable's loading value increases at a constant sea temperature, its maximum temperature increases rapidly in a logarithmic manner. Similarly, when the phases are unbalanced, the maximum temperature also increases rapidly in a logarithmic manner. A similar rapid increase is also observed in the Phase Losses, which is related to the $I^2 \times R$ ratio. Additionally, the cable's thermal stress is investigated by analyzing the differences between its maximum and minimum points. The temperature difference (Δt) is found to be the same in the case of balanced operation, where all phases are loaded equally, as well as in the case where only one phase is loaded at high rates while two phases are loaded at 50%.

It is also observed that the current carrying capacity of the cable can increase by 10.1% if the sea water temperature is 15 °C lower than the nominal operating conditions, while it can decrease by 7.3% if the sea water temperature is 10 °C higher. Due to the significant effect of the sea water temperature on the cable's current carrying capacity, it may be considered as a criterion in the location preference during the installation of offshore wind turbines.

CONFLICT OF INTEREST STATEMENT

The authors declare no conflict of interest.

REFERENCES

COMSOL. (2023). *Modeling Cables in COMSOL®: An Electromagnetics Tutorial Series*. <https://www.comsol.com/model/cable-tutorial-series-43431>

Hu, M., Xie, S., Zhang, J., & Ma, Z. (2014). Design selection of DC & AC submarine power cable for offshore wind mill. *China International Conference on Electricity Distribution, CIGRE, 2014-December*, 1675–1679. <https://doi.org/10.1109/CIGRE.2014.6991991>

IEEE, 1120-2004. (2004). *1120-2004 IEEE Guide for the Planning, Design, Installation, and Repair of Submarine Power Cable Systems*.

Keskin Arabul, F., Arabul, A. Y., Kumru, C. F., & Boynuegri, A. R. (2017). Providing energy management of a fuel cell–battery–wind turbine–solar panel hybrid off grid smart home system. *International Journal of Hydrogen Energy*, 42(43). <https://doi.org/10.1016/j.ijhydene.2017.02.204>

Lldstad, E. (1994). World Record HVDC Submarine Cables. *IEEE Electrical Insulation Magazine*, 10(4), 64–67. <https://doi.org/10.1109/57.298131>

Mei, W., Pan, W., Chen, T., Song, G., & Di, J. (2017). Research and design of DC500kV optical fiber composite submarine cable. *4th IEEE International Conference on Engineering Technologies and Applied Sciences, ICETAS 2017, 2018-January*, 1–6. <https://doi.org/10.1109/ICETAS.2017.8277901>

Ou, X., Xu, W., Zang, Y., Wang, H., Wu, H., Lv, A., & Zhou, Z. (2022). Mechanical analysis of 500 kV oil-filled submarine power cable in anchor and blade damage based on Finite element method. *IEEE Advanced Information Technology, Electronic and Automation Control Conference (IAEAC)*, 2022-October, 1068–1072. <https://doi.org/10.1109/IAEAC54830.2022.9929551>

Submarine Cable Almanac. (2021). Global Submarine Cable Network. <https://www.submarinecablemap.com/>

Thermal Analysis of XLPE Insulated Submarine Cables for Different Loading Conditions

Takeshita, H., Nakamura, K., Matsuo, Y., Inoue, T., Masuda, D., Hiwatashi, T., Hosokawa, K., Inada, Y., & de Gabory, E. L. T. (2022). Demonstration of Uncoupled 4-Core Multicore Fiber in Submarine Cable Prototype with Integrated Multicore EDFA. *Journal of Lightwave Technology*. <https://doi.org/10.1109/JLT.2022.3195190>

Yu, X., Zhang, S., Peng, X., Feng, B., Yu, S., Zhu, W., & Deng, J. (2022). Simulation Study on Steady-State Ampacity of ± 400 kV J-tube DC Submarine Cable. *Proceedings - 2022 4th International Conference on Electrical Engineering and Control Technologies, CEECT 2022*, 546–551. <https://doi.org/10.1109/CEECT55960.2022.10030564>

Zhang, H., XIE, S., Hu, M., Zhang, X., Ling, Z., Zhan, H., & Jing, Y. (2021). *Development Prospects of High Economy XLPE Insulation HVDC Submarine Cable*. 1046–1055. <https://doi.org/10.1049/ICP.2021.2223>

Journal of Naval Sciences and Engineering

2023, Vol. 19, No. 1, pp. 53-76

DOI: 10.56850/jnse.1250094

Shipbuilding and Ocean Engineering/Gemi ve Deniz Teknolojisi Mühendisliđi

RESEARCH ARTICLE

**An ethical committee approval and/or legal/special permission has not been required within the scope of this study.*

**SCALE EFFECTS ON THE LINEAR HYDRODYNAMIC
COEFFICIENTS OF DARPA SUBOFF***

Furkan KIYÇAK¹ 
Ömer Kemal KINACI² 

¹*Istanbul Technical University, Department of Shipbuilding & Ocean
Engineering, Istanbul, Turkey,
kiycak15@itu.edu.tr*

²*Istanbul Technical University, Department of Shipbuilding & Ocean
Engineering, Istanbul, Turkey,
kinacio@itu.edu.tr*

Received: 11.02.2023

Accepted: 15.03.2023

ABSTRACT

It is well known that forces and moments acting on a ship are functions of Froude and Reynolds numbers. As a ship gets larger in size, these two numbers grow, which leads to different flow regimes around the hull. However, the state-of-the-art in maneuvering calculations is to consider the hydrodynamic coefficients as constants for model and full ship scales. For submerged bodies, the Froude number is insignificant due to the distant free water surface; therefore, these forces only depend on the Reynolds number. In this study, we consider the benchmark 'DARPA' Suboff form, which is extensively studied in the literature, and investigated the scale effects on the hydrodynamic coefficients with respect to the Reynolds number. Numerical studies are carried out on the bare hull form of the submarine. Captive motions of static drift and pure yaw motions are conducted utilizing the oblique towing and rotating arm tests via RANS-based CFD. Linear hydrodynamic coefficients are expressed with logarithmic equations as functions of the Reynolds number, explicitly showing the dependency on the ship's model scale.

Keywords: *CFD, DARPA, maneuvering derivatives, pure yaw, static drift.*

LİNEER HİDRODİNAMİK KATSAYILARIN HESABINDA ÖLÇEK ETKİSİ

ÖZ

Gemiye etki eden kuvvetlerin ve momentlerin Froude ve Reynolds sayılarının fonksiyonları oldukları iyi bilinmektedir. Geminin boyutu büyüdükçe, bu iki sayı da büyür ve bu da gövde etrafında farklı akış rejimlerine yol açar. Bununla birlikte, manevra hesaplamalarında, hidrodinamik katsayılar, model ve tam gemi ölçekleri için sabit olarak kabul edilmektedir. Suya batık cisimler için, uzaktaki serbest su yüzeyi nedeniyle Froude sayısı önemsizdir; bu nedenle, bu kuvvetler yalnızca Reynolds sayısına bağlıdır. Bu çalışmada, literatürde yoğun olarak çalışılan ve bir referans noktası niteliğindeki 'DARPA' Suboff formunu ele aldık ve ölçeğin hidrodinamik katsayılar üzerindeki etkilerini Reynolds sayısına göre inceledik. Denizaltının çıplak gövde formu üzerinde sayısal çalışmalar yapılmış, RANS tabanlı CFD aracılığıyla çekme tankı ve dönen kol testleri kullanılarak statik sürüklenme ve safi savrulma hareketleri gerçekleştirilmiştir. Lineer hidrodinamik katsayılar, Reynolds sayısının fonksiyonları olarak logaritmik denklemlerle ifade edilmiş ve geminin model ölçeğine bağımlılığı açıkça gösterilmiştir.

Anahtar Kelimeler: DARPA, HAD, manevra türevleri, safi savrulma, statik sürüklenme.

1. INTRODUCTION

As a result of developing technology and increasing computer capacities, the precision and importance of computational analysis are increasing day by day. In naval architecture, the ship hydrodynamics field has been positively affected by these developments due to the intense mathematical and physical computations involved.

Several different methods can be used in assessing the hydrodynamic performance of ships. These are empirical methods, model experiments, and computational fluid dynamics methods (Can, 2014). It is the navies that typically place submarines at the center of their attention, and, due to this reason, any research related to them is kept confidential. Although there are numerous empirical relations available for use, hydrodynamic analysis based on these formulas is not adequate and reliable. Model experiments are very useful but are both expensive and time-consuming (Budak & Beji, 2016). The last method, computational fluid dynamics, or CFD, has become very popular in recent years and its use is becoming widespread. With the advancement of modern CFD techniques, the method is believed to give pretty accurate estimates (He et al., 2016). Not only is it less expensive than conducting model experiments, CFD allows analyzing higher Reynolds number flows, making it a better alternative to empirical formulas.

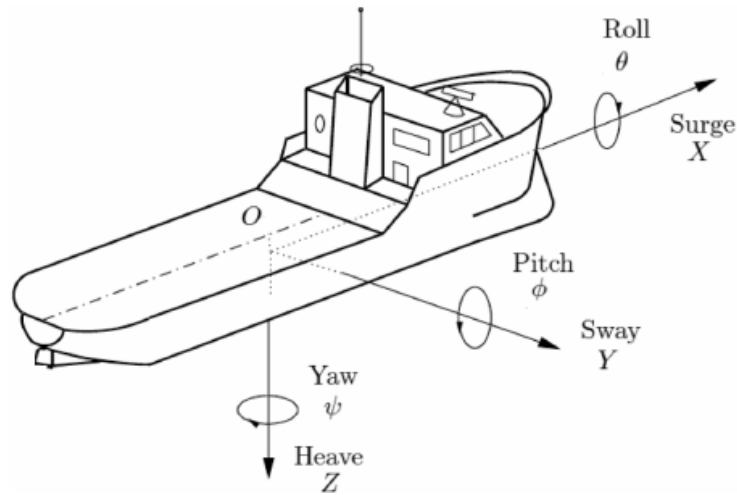


Figure 1. 6 DOF for ship motions (Krishna Kumar et al., 2018).

Ships, like any other mechanical body, possess six degrees-of-freedom (6DOF), as illustrated in Figure 1. Roll, pitch, and heave are defined in the vertical plane and mostly investigated in seakeeping. Surge, sway, and yaw are defined as horizontal plane motions and generally studied in maneuvering. Maneuverability is closely related to navigational safety and accurate calculation prior to the construction state is crucial. Briefly, maneuverability is the ability of a ship to change direction in a controlled manner in desired direction and continue without deviating from its route after this change (Sukas et al., 2017).

Today, navigation safety is a design parameter of greater significance in navy projects compared to commercial ones. When it comes to the design process, submarines vary significantly from surface ships in navy projects, with distinct design properties and concepts. Recent heavy investments in the defense industries from developed and developing countries increased the importance of studies based on submarines. Scientific studies on underwater hydrodynamics have gained momentum recently. For instance, the approaches used to evaluate the maneuvering capability of underwater vehicles are examined by Kirikbas et al. (2021). Linear and nonlinear hydrodynamic coefficients of underwater vehicles are evaluated using CFD by Ray et al. (2009). The scale effect on horizontal maneuvering derivatives of an underwater vehicle is investigated by Kahramanoglu (2023). Maneuvering of an underwater vehicle is simulated using CFD based method by Racine & Paterson (2005). Maneuvering forces on submarines using two viscous-flow solvers are calculated by Vaz et al. (2010). In addition, an experimental study was carried out in which linear hydrodynamic coefficients were calculated by Roddy (1990). That study provides the opportunity to compare the EFD results with the numerical studies of the DARPA form in deep water that has been studied in detail.

The governing Navier-Stokes equations for fluid flows implicate several non-dimensional parameters (namely Strouhal, Weber, Euler, Reynolds, and Froude numbers) to be acting on bodies in fluids. Not all of these parameters have significant effect on ships: the force and moment acting on a ship are functions of the Froude and Reynolds numbers and generally expressed in terms of these numbers. Hydrodynamic derivatives should be calculated to specify the maneuvering performance both on the water

surface or in deep water (Cavdar & Bal, 2022). Different from surface ships (because there are no waves far from the water surface), hydrodynamic forces will be independent from the Froude number for submarines. Therefore, in this paper, only the effects of the Reynolds number on maneuvering derivatives are investigated to assess the scale effect on a ship's maneuvering performance. The ship discussed in our study is the 'DARPA' submarine bare hull form, which is widely used in the literature.

In this paper, numerical analyses of static drift mentioned as oblique towing test, and pure yaw mentioned as rotating arm test in the literature are investigated with the help of CFD. Since the effect of the Reynolds number on the maneuvering derivatives of the DARPA Suboff is to be examined, the static drift and pure yaw analyses were completed at various sizes and speeds (which also changes the Reynolds numbers). From the CFD simulations, the forces and moments acting on the ship are obtained. These are graphed with respect to the ship's sway velocity v and yaw rate r . Then, equations are generated using a curve-fitting tool. These equations return Y_v , Y_r , N_v , and N_r for each studied case. Then, these linear hydrodynamic coefficients are graphed with respect to the Reynolds number. Results are generalized with logarithmic equations and a correlation was obtained between the maneuvering derivatives and the Reynolds number.

2. GEOMETRY AND MATHEMATICAL MODEL

2.1. Geometry

The properties of the bare hull form of the DARPA geometry named AFF-1 configuration at the scale that the model experiments done are shown in Table 1. The three-dimensional model of the form is shown in Figure 2.

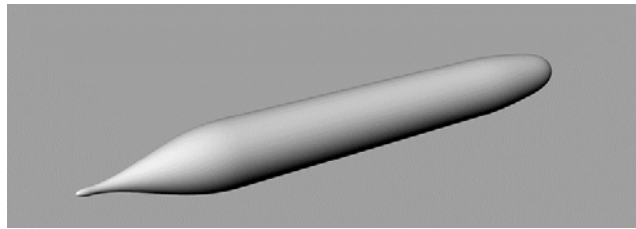


Figure 2. DARPA bare hull 3-D model.

Table 1. DARPA bare hull form properties.

Parameter	Value
Length Between Perpendiculars (m)	4.261
Length Overall (m)	4.356
Length of Forebody (m)	1.016
Length of Parallel Middlebody (m)	2.229
Length of Run (m)	1.111
Diameter (m)	0.508
LCB (m)	2.008
x_G (m)	0.0092

2.2. Equations of Motion

As mentioned in the introduction, when maneuverability is examined, usually a 3 DOF axis set is used (Sukas et al., 2019). These are surge representing translation in the x-axis, sway representing translation in the y-axis, and yaw representing rotation around the z-axis. The force calculated from the surge motion represents the resistance and is studied within the resistance problems. According to Newton's second law, Earth-fixed force and moment can be identified in the general form in equations 1, 2, and 3:

$$X_0 = m\ddot{x}_G \quad (1)$$

$$Y_0 = m\ddot{y}_G \quad (2)$$

$$N = I_z\dot{r} \quad (3)$$

In maneuvering, the sway and yaw effects are more dominant when compared with the surge. Therefore, it is possible to implement 2 DOF ship motion equations, which can be expressed as below:

$$(m + m_y)\dot{v} + (m + m_x)ur + x_G m\dot{r} = Y \quad (4)$$

$$(I_{zG} + x_G^2 m + J_z)\dot{r} + x_G m(\dot{v} + ur) = N \quad (5)$$

In equations 4 and 5, the right-hand side consists of the hull, the propeller, and the rudder for a conventional ship. We only focus on the linear hydrodynamic coefficients of the hull in this paper; therefore, linear terms can be identified as $Y_{\dot{v}}$, Y_v , $Y_{\dot{r}}$, Y_r , $N_{\dot{v}}$, N_v , $N_{\dot{r}}$, and N_r . Four of these terms are based on the added mass, which is extensively studied in the literature before. In this respect, we only paid attention to Y_v , Y_r , N_v , and N_r . After obtaining the forces and moments acting on the ship via CFD, they are nondimensionalized as in Table 2: (Feldman J, 1979)

Table 2. Nondimensionalization.

Parameter	Nondimensionalization	Notation
v	v/U	v'
X	$X/0.5*\rho*U^2*L_{pp}^2$	X'
Y	$Y/0.5*\rho*U^2*L_{pp}^2$	Y'
N	$N/0.5*\rho*U^2*L_{pp}^3$	N'

Since the studied geometry is bare hull form, hydrodynamic force and moment on the hull can be expressed with 2 DOF as in equations 6 and 7: (Yasukawa & Yoshimura, 2015)

$$Y'_H = Y'_v v' + (Y'_r - m' - m'_x) r' + Y'_{vvv} v'^3 + Y'_{vvr} v'^2 r' + Y'_{vrr} v' r'^2 + Y'_{rrr} r'^3 \quad (6)$$

$$N'_H = N'_v v' + (N'_r - m' x'_G) r' + N'_{vvv} v'^3 + N'_{vvr} v'^2 r' + N'_{vrr} v' r'^2 + N'_{rrr} r'^3 \quad (7)$$

In these equations, $Y'_v, Y'_{vvv}, N'_v,$ and N'_{vvv} maneuvering derivatives are obtained from the static drift analysis results, $Y'_r, Y'_{rrr}, N'_r,$ and N'_{rrr} maneuvering derivatives are obtained from the pure yaw analysis results with the multiple run method (Yoon, 2009). Other maneuvering derivatives are not investigated in this article.

3. NUMERICAL MODEL AND COMPUTATIONAL METHOD

Hydrodynamic forces and moments are solved with the commercial RANS solver program ANSYS Fluent by finite volume method (FVM) with the discretization of continuity and Navier-Stokes equations. The 'SIMPLE' algorithm is used in both static drift and pure yaw and a second-order

solution was made for pressure, momentum, and turbulence. SST k- ω was chosen as the turbulence model. While creating the boundary layer, $y^+=30$ is assumed. In all analyses, the density of seawater is taken at 997.51 kg/m^3 , and the kinematic viscosity of seawater is taken at $10^{-6} \text{ m}^2/\text{s}$.

3.1. Static Drift

In static drift, the object in the fluid is towed at different drift angles and the sway force and the yaw moment are measured. In the static drift study, the mesh was created with the Pointwise, which is the mesh generation program for CFD. In all cases, when creating the fluid domain, a distance of about 1.5L from the front of the object, about 2.5L from the back, and about 2L left in the other directions. Examples of mesh views of static drift are shown in Figure 3.

Table 3. Static drift cases.

Parameter	Case 1	Case 2	Case 3	Case 4	Case 5	Case 6
L_{pp} (m)	4.261	2.130	8.522	4.261	2.130	8.522
U_0 (m/s)	1.50	1.50	1.50	2.50	2.50	2.50
Re	6.36E+06	3.18E+06	1.27E+07	1.06E+07	5.30E+06	2.12E+07
Parameter	Case 7	Case 8	Case 9	Case 10	Case 11	Case 12
L_{pp} (m)	4.261	2.130	8.522	1.065	2.130	2.130
U_0 (m/s)	4.00	4.00	4.00	1.00	0.25	0.75
Re	1.70E+07	8.48E+06	3.39E+07	1.06E+06	5.30E+05	1.59E+06

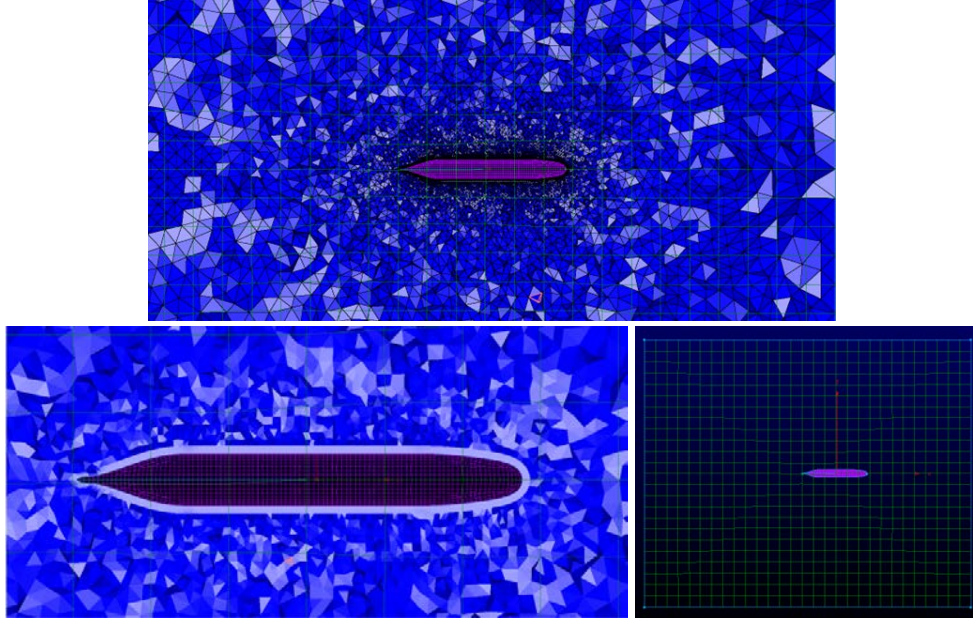


Figure 3. Example of static drift mesh views.

Static drift analysis was carried out at 12 different Reynolds numbers by scaling the length and service speed of the submarine. These 12 different cases are shown in Table 3.

In each of these 12 different situations, the flow was sent on the submarine at a drift angle of 0° , 3° , 6° , 9° , 12° , and 15° , and sway force Y and yaw moment N were taken as outputs. The values for Case 1 are given in Table 4.

Table 4. Forces and moments for Case 1.

β (deg)	β (rad)	v (m/s)	Y (N)	N (Nm)
0	0	0	0	0
3	0.0524	-0.0785	7.616	61.923
6	0.1047	-0.1568	18.567	119.504
9	0.1571	-0.2347	36.445	168.915
12	0.2094	-0.3119	64.011	208.230
15	0.2618	-0.3882	101.270	240.418

The lateral velocity is given in Table 4 and can be calculated with the help of the $v = U_0 * \sin\beta$ relation where β is drift angle, v is lateral velocity and U_0 is service speed.

Then, velocity, force and moment values are made nondimensional. Nondimensional values for Case 1 are shown in Table 5.

Table 5. Nondimensional forces and moments for Case 1.

v'	Y'	N'
0	0	0
-0.0523	0.00037	0.00071
-0.1045	0.00091	0.00138
-0.1564	0.00179	0.00195
-0.2079	0.00314	0.00240
-0.2588	0.00497	0.00277

Thereafter, with help of the mathematical models given in equations 8 and 9, fitted the optimal curve based on the models (Shenoi et al., 2013). With the help of the obtained force and moment values and mathematical model, linear hydrodynamic coefficients Y_v and N_v were obtained (Triantafyllou & Hover, 2003). Coefficients given in the Results part.

$$Y' = Y_v'v' + Y_{vvv}'v'^3 \quad (8)$$

$$N' = N_v'v' + N_{vvv}'v'^3 \quad (9)$$

Y_{vvv} and N_{vvv} are nonlinear derivatives of maneuvering and were not analyzed in this study.

3.2. Pure Yaw

In pure yaw, the submarine rotates around a fixed arm length of R with a constant speed of r . In the pure yaw study, the mesh was created within the commercial ANSYS program. Since the length of the arm of rotation changed in each of the 12 different situations, the distances left while creating the fluid domain could not be standardized, but care was taken to leave such a distance not to disturb the flow around the object. Examples of mesh views of pure yaw are shown in Figure 4.

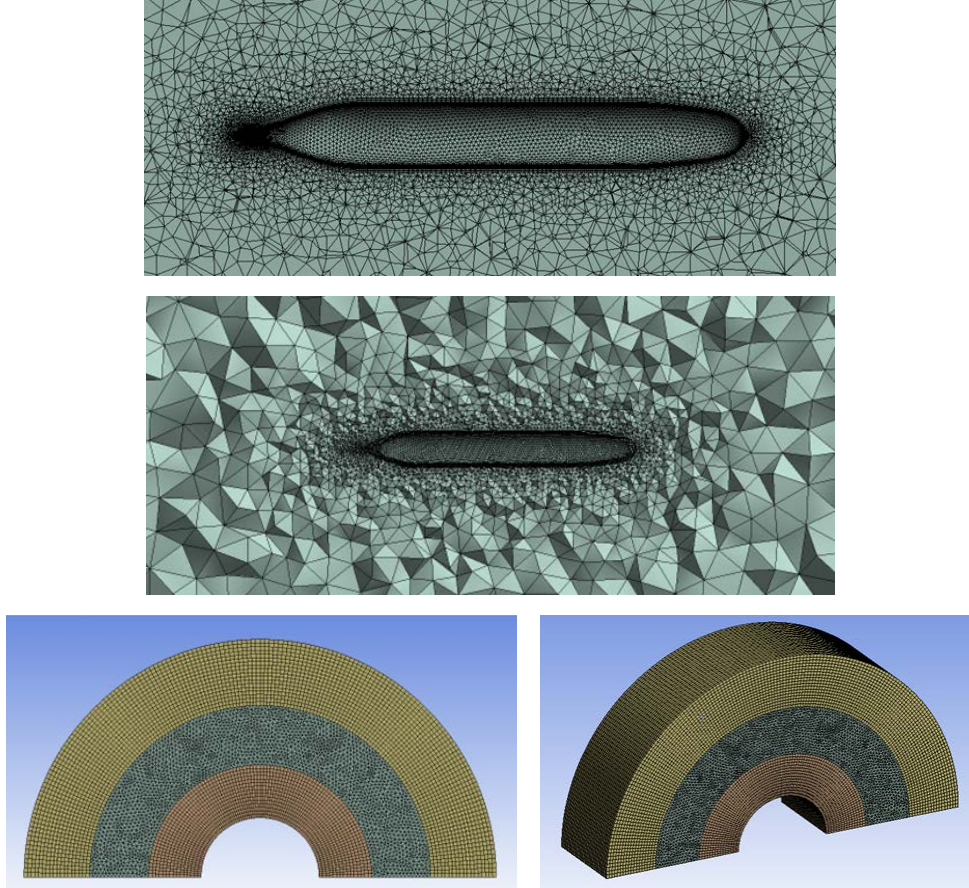


Figure 4. Example of pure yaw mesh views.

Pure yaw analysis was carried out at 12 different Reynolds numbers by scaling the length and service speed of the submarine. These 12 different cases are shown in Table 6.

In these 12 cases, the r'_{max} values were taken as 0.1, 0.2, 0.4, 0.6, and 0.8, the rotational speeds were calculated with $r'_{max} = rL/U_0$ relation, and the rotation arm length was found with the help of the $U_0 = rR$. As a result of the analyses, sway force Y and yaw moment N are taken as outputs. The values for Case 1 are given in Table 7. Then, velocity, force, and moment values are made nondimensional. Non dimensional values for Case 1 are shown in Table 8.

Scale Effect on The Linear Hydrodynamic Coefficients of DARPA Suboff

Table 6. Pure yaw cases.

Parameter	Case 1	Case 2	Case 3	Case 4	Case 5	Case 6
L_{pp} (m)	4.261	2.130	8.522	4.261	2.130	8.522
U_0 (m/s)	1.50	1.50	1.50	2.50	2.50	2.50
Re	6.36E+06	3.18E+06	1.27E+07	1.06E+07	5.30E+06	2.12E+07
Parameter	Case 7	Case 8	Case 9	Case 10	Case 11	Case 12
L_{pp} (m)	4.261	2.130	8.522	1.065	2.130	2.130
U_0 (m/s)	4.00	4.00	4.00	1.00	0.25	0.75
Re	1.70E+07	8.48E+06	3.39E+07	1.06E+06	5.30E+05	1.59E+06

Table 7. Forces and moments for Case 1.

r' (rad)	r (rad/s)	R (m)	Y (N)	N (Nm)
0.1	0.0352	42.609	1.584	-8.824
0.2	0.0704	21.305	3.448	-18.421
0.4	0.1408	10.652	9.017	-40.624
0.6	0.2112	7.102	15.734	-65.423
0.8	0.2816	5.326	24.895	-96.693

Table 8. Nondimensional forces and moments for Case 1.

r'	Y'	N'
0.1	0.00008	-0.00010
0.2	0.00017	-0.00021
0.4	0.00044	-0.00047
0.6	0.00077	-0.00075
0.8	0.00122	-0.00111

Thereafter, with help of the mathematical models given in equations 10 and 11, fitted the optimal curve based on the models (Rajita Shenoj et al., 2013). With the help of the obtained force and moment values and mathematical

model, linear hydrodynamic coefficients Y_r and N_r were obtained (Triantafyllou & Hover, 2003). Coefficients given in the Results part.

$$Y' = Y_r' r'_{\max} + Y_{rrr}' r'_{\max}^3 \quad (10)$$

$$N' = N_r' r'_{\max} + N_{rrr}' r'_{\max}^3 \quad (11)$$

Y_{rrr} and N_{rrr} are nonlinear derivatives of maneuvering and were not analyzed in this study.

4. GRID INDEPENDENCY

As a key factor in CFD, grid resolution is one of the most important elements for user decision making. Today, most scientific studies and simulations require grid-independent CFD solutions as a first and basic rule. A grid-independent CFD solution is achieved when the difference between numerical solutions at different grid numbers is negligible. The choice of grids to be tested and the determination of the grid-independent solution are at the discretion of the CFD user (Wang & Zhai, 2012).

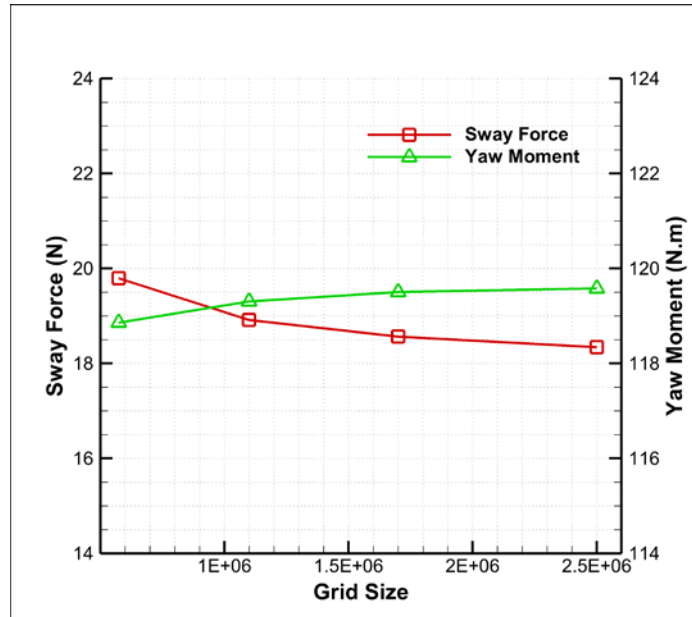


Figure 5. Grid convergence.

The grid convergence study was performed by developing four different meshes: with coarse, medium, medium-fine, and fine grids for 6 degrees static drift simulation in Case 1. The cell numbers varied from 5.75×10^5 to 2.50×10^6 for illustrating the sway force and yaw moment convergence as shown in Table 9 and Figure 5. It was found that there was no significant change in sway force (Y) and yaw moment (N) beyond the “medium-fine” grid density. Therefore, for the present paper, “medium-fine” grid density was used to perform all the simulations.

Table 9. Comparison of Y and N for different grid sizes.

Grid	Elements	Y (N)	N (N.m)
Coarse	575000	19.792	118.861
Medium	1100000	18.915	119.308
Medium-Fine	1700000	18.567	119.504
Fine	2500000	18.342	119.579

5. RESULTS

Static drift and pure yaw analyses were performed at 12 different Reynolds numbers. Static drift was completed at 0°, 3°, 6°, 9°, 12° ve 15° drift angles in each of these 12 cases, and pure yaw was completed for r'max values 0.1, 0.2, 0.4, 0.6, and 0.8 in each of the 12 cases.

Table 10. Linear hydrodynamic coefficients of static drift.

	L_{pp}	U₀	Re	Y_v'	N_v'
Case 1	4.261	1.50	6.36E+06	-0.006930	-0.013508
Case 2	2.130	1.50	3.18E+06	-0.008198	-0.013187
Case 3	8.522	1.50	1.27E+07	-0.006306	-0.013691
Case 4	4.261	2.50	1.06E+07	-0.006504	-0.013615
Case 5	2.130	2.50	5.30E+06	-0.007829	-0.013385
Case 6	8.522	2.50	2.12E+07	-0.005964	-0.013798
Case 7	4.261	4.00	1.70E+07	-0.006217	-0.013720

Case 8	2.130	4.00	8.48E+06	-0.007335	-0.013552
Case 9	8.522	4.00	3.39E+07	-0.005768	-0.013927
Case 10	1.065	1.00	1.06E+06	-0.011218	-0.012429
Case 11	2.130	0.25	5.30E+05	-0.011604	-0.012380
Case 12	2.130	0.75	1.59E+06	-0.009394	-0.012737
EFD	4.261	3.34	1.42E+07	-0.005948	-0.012795

5.1. Static Drift

After calculating Y_v' and N_v' in each Reynolds number, the distribution graph of hydrodynamic coefficients according to the Reynolds number was drawn and the most appropriate equation was selected. The calculated maneuvering derivatives and the experimental results published by DTRC (Roddy, 1990) are shown in Table 10, and the graphics are shown in Figure 6 and Figure 7.

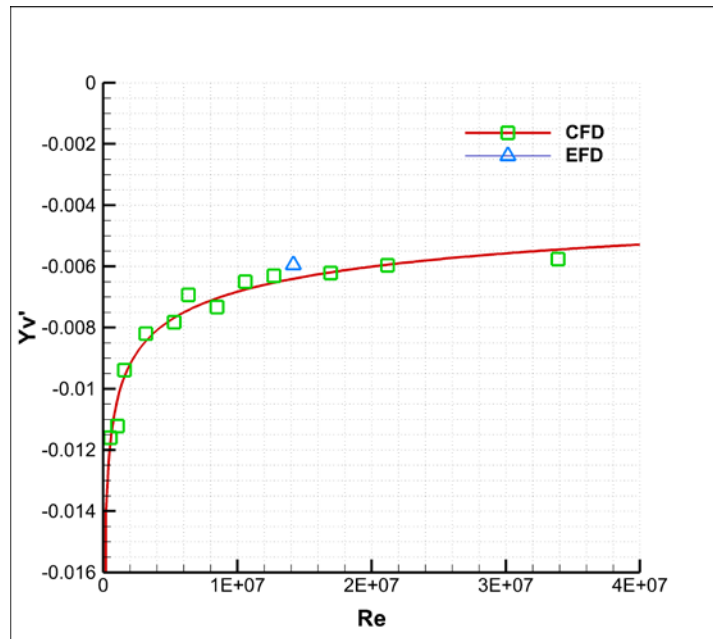


Figure 6. Re- Y_v' distribution of static drift.

Scale Effect on The Linear Hydrodynamic Coefficients of DARPA Suboff

Equation 12 and Equation 13 were obtained when the collected data as a result of CFD were fitted to the most appropriate equations. So, based on these two equations, if we have the Reynolds number of the bare hull form of the DARPA, we can calculate the Y_v' and N_v' .

$$Y_v' = 0.001527353 \ln(\text{Re}) - 0.03154784 \quad (12)$$

$$N_v' = -0.000410797 \ln(\text{Re}) - 0.006932722 \quad (13)$$

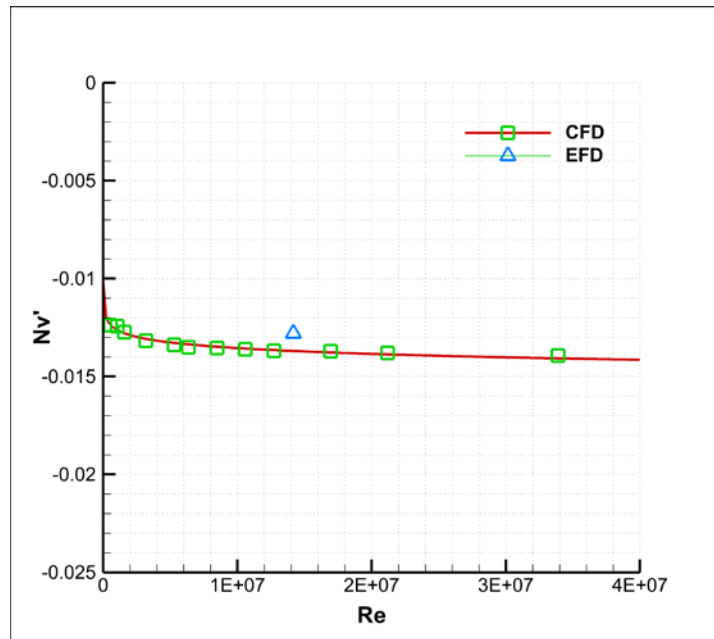


Figure 7. Re- N_v' distribution of static drift.

Table 11. Linear hydrodynamic coefficients of pure yaw.

	L_{pp}	U_0	Re	Y_r'	N_r'
Case 1	4.261	1.50	6.36E+06	0.001832	-0.001076
Case 2	2.130	1.50	3.18E+06	0.002116	-0.001225
Case 3	8.522	1.50	1.27E+07	0.001733	-0.001014
Case 4	4.261	2.50	1.06E+07	0.001749	-0.001021
Case 5	2.130	2.50	5.30E+06	0.001881	-0.001100
Case 6	8.522	2.50	2.12E+07	0.001691	-0.000980

Case 7	4.261	4.00	1.70E+07	0.001698	-0.000983
Case 8	2.130	4.00	8.48E+06	0.001780	-0.001027
Case 9	8.522	4.00	3.39E+07	0.001656	-0.000959
Case 10	1.065	1.00	1.06E+06	0.002467	-0.001469
Case 11	2.130	0.25	5.30E+05	0.002031	-0.001396
Case 12	2.130	0.75	1.59E+06	0.002486	-0.001435
EFD	4.261	3.34	1.42E+07	0.001811	-0.001597

5.2. Pure Yaw

After calculating Y_r' and N_r' in each Reynolds number, the distribution graph of hydrodynamic coefficients according to the Reynolds number was drawn and the most appropriate equation was selected. The calculated maneuvering derivatives and the experimental results published by DTRC (Roddy, 1990) are shown in Table 11, and the graphics are shown in Figure 8 and Figure 9.

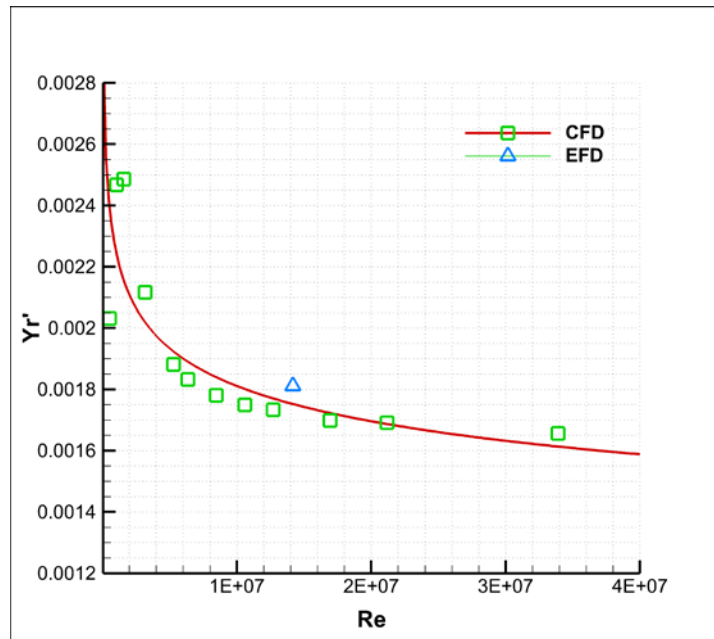


Figure 8. Re- Y_r' distribution of pure yaw.

Scale Effect on The Linear Hydrodynamic Coefficients of DARPA Suboff

Equation 14 and Equation 15 were obtained when the collected data as a result of CFD were fitted to the most appropriate equations. So, based on these two equations, if we have the Reynolds number of the bare hull form of the DARPA, we can calculate the Y_r' and N_r' .

$$Y_r' = -0.0001890118 \ln(\text{Re}) + 0.004868874 \quad (14)$$

$$N_r' = 0.0001419491 \ln(\text{Re}) - 0.003349958 \quad (15)$$

The length between perpendicular of DARPA $L_{pp} = 4.261$ m and the service speed of DARPA $U_0 = 3.34$ m/s in the experiment so the Reynolds number can be calculated as $\text{Re} = 1.42 \cdot 10^7$. Linear hydrodynamic coefficients can be obtained by placing this Reynolds number in equations 12, 13, 14, and 15, respectively. The comparison of the coefficients determined as a result of CFD and the experimental results published by DTRC (Roddy, 1990) are shown in Table 12.

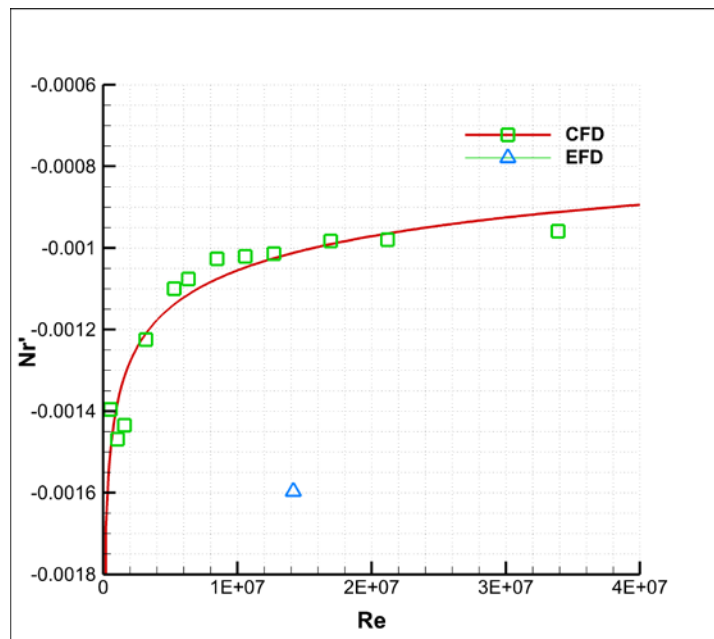


Figure 9. Re- N_r' distribution of pure yaw.

Table 12. Comparison of CFD and EFD results.

	Y_v'	N_v'	Y_r'	N_r'
EFD	-0.005948	-0.012795	0.001811	-0.001597
CFD	-0.006398	-0.013697	0.001756	-0.001013
Error	7.6%	7.1%	3.0%	36.6%

6. CONCLUSION

Maneuverability is one of the major design parameters especially for underwater vehicles to ensure proper handling and safety of the vessel. With recent advances in CFD capabilities and computational power, researchers have taken great interest in investigating issues with maneuverability using CFD. In this paper, the bare hull form of the DARPA geometry named AFF-1 configuration, which has plenty of previous results in the literature, has been studied. The study investigates the effects of scale on maneuver derivatives using various Reynolds numbers. By scaling the length and speed of this form, static drift and pure yaw simulations at 12 different Reynolds numbers were conducted with the help of CFD. From these simulations, linear hydrodynamic coefficients were calculated and used to establish logarithmic relationships between Reynolds number and maneuvering derivatives. Finally, the CFD-generated coefficients are compared to previously published experimental results.

Although the results in the Y_v' , N_v' , and Y_r' maneuvering derivatives are very close to the experimental results, there is a difference between the CFD and the test result in N_r' . It is known that N_r' is very sensitive to center of gravity of the vessel; any small change in this value might reflect as a big difference in this hydrodynamic coefficient. Despite this discrepancy, our study reveals the dependency of the hydrodynamic coefficients on the Reynolds number. Speed variation tests in some mathematical models try to compensate this deficiency of the state-of-the-art, but it is believed that the utilization of hydrodynamic coefficients as a function of the Reynolds number will increase the accuracy of maneuvering simulations.

APPENDIX

Abbreviation

CFD	:	Computational Fluid Dynamics
EFD	:	Experimental Fluid Dynamics
DOF	:	Degrees of Freedom
DTRC	:	David Taylor Research Center
FVM	:	Finite Volume Method
LCB	:	Longitudinal Center of Buoyancy
RANS	:	Reynolds Averaged Navier Stokes

Nomenclature

D	:	Diameter of Submarine
Fr	:	Froude Number
I _Z	:	Moment of Inertia of Yaw
L _{OA}	:	Length Overall of Submarine
L _{PP}	:	Length Between Perpendicular of Submarine
m	:	Mass of Submarine
m _x	:	Added Mass of x Axis Direction
N	:	Yaw Moment
N _H	:	Yaw Moment on the Hull Around The z Axis
N _r	:	1st Order Derivative Coeff. of N Moment Respect to r
N _r '	:	Non-Dimensionalized N _r
N _{rrr}	:	3rd Order Derivative Coeff. of N Moment Respect to r
N _v	:	1st Order Derivative Coeff. of N Moment Respect to v
N _v '	:	Non-Dimensionalized N _v
N _{vvv}	:	3rd Order Derivative Coeff. of N Moment Respect to v
N _{\dot{v}}	:	Added Mass Coefficient of N Moment Respect to \dot{v}
N _{\dot{r}}	:	Added Mass Coefficient of N Moment Respect to \dot{r}
r	:	Yaw Angular Velocity of Submarine
\dot{r}	:	Yaw Angular Acceleration of Submarine
Re	:	Reynolds Number
u	:	Longitudinal Velocity of Submarine
U ₀	:	Service Speed of Submarine
v	:	Lateral Velocity of Submarine
X	:	Surge Force

x_G	:	Longitudinal Center of Gravity
\ddot{x}_G	:	Acceleration at x Axis
X_H	:	Surge Force on the Hull in The x Axis
Y	:	Sway Force
Y_H	:	Sway Force on the Hull in The y Axis
Y_r	:	1st Order Derivative Coeff. of Y Force Respect to r
Y_r'	:	Non-Dimensionalized Y_r
Y_{rrr}	:	3rd Order Derivative Coeff. of Y Force Respect to r
Y_v	:	1st Order Derivative Coeff. of Y Force Respect to v
Y_v'	:	Non-Dimensionalized Y_v
Y_{vvv}	:	3rd Order Derivative Coeff. of Y Force Respect to v
\ddot{y}_G	:	Acceleration at y Axis
$Y_{\dot{v}}$:	Added Mass Coefficient of Y Force Respect to \dot{v}
$Y_{\dot{r}}$:	Added Mass Coefficient of Y Force Respect to \dot{r}
ρ	:	Water Density

CONFLICT OF INTEREST STATEMENT

The authors declare no conflict of interest.

REFERENCES

- Budak, G., & Beji, S. (2016). "Computational resistance analyses of a generic submarine hull form and its geometric variants." *The Journal of Ocean Technology*, 76-86.
- Can, M. (2014). *Numerical simulation of hydrodynamic planar motion mechanism test for underwater vehicles*. [M.Sc. Thesis]. Middle East Technical University.
- Çavdar, F. & Bal, Ş. (2022). "An investigation of hydrodynamic maneuvering derivatives and horizontal stability of DARPA suboff depending on depth." *Gemi ve Deniz Teknolojisi*, (221), 42-58. 10.54926/gdt.1084413
- Feldman, J. (1979). "DTNSRDC revised standard submarine equations of motion."
- He, S., Kellett, P., Yuan, Z., Incecik, A., Turan, O., & Boulougouris, E. (2016). "Manoeuvring prediction based on CFD generated derivatives." *Journal of Hydrodynamics*, 28, 284-292.
- Kahramanoglu, E. (2023). "Numerical investigation of the scale effect on the horizontal maneuvering derivatives of an underwater vehicle." <https://ssrn.com/abstract=4280314>
- Kırıkbaş, O., Kınacı, Ö. K. & Bal, Ş. (2021). "Sualtı araçlarının manevra karakteristiklerinin değerlendirilmesi-I: manevra analizlerinde kullanılan yaklaşımlar." *Gemi ve Deniz Teknolojisi*, (219), 6-58.
- Krishnakumar & Ramasamy, S., & Al-Mamun, A. (2018). "A study on dynamic positioning system robustness with wave loads predictions from deep belief network." 1520-1527. 10.1109/SSCI.2018.8628825.
- Racine, B., & Paterson, E. (2005). "CFD-based method for simulation of marine-vehicle maneuvering." 10.2514/6.2005-4904.
- Ray, A., & Singh, S., & Seshadri, V. (2009). "Evaluation of linear and nonlinear hydrodynamic coefficients of underwater vehicles using CFD." 10.1115/OMAE2009-79374.

Roddy, R.F. (1990). “Investigation of the stability and control characteristics of several configurations of the DARPA suboff model (DTRC Model 5470) from captive-model experiments.”

Shenoi, R., & Krishnankutty, P. & Selvam, Panneer. (2013). “Prediction of maneuvering coefficients of a container ship by numerically simulating HPMM using RANSE based solver.”

Sukas, O. F., Kinaci, Ö. K., & Bal, Ş. (2019). “System-based prediction of maneuvering performance of twin-propeller and twin-rudder ship using a modular mathematical model.” *Applied Ocean Research* , vol.84, 145-162.

Sukas, Ö. F., Kinaci, Ö. K., & Bal, Ş. (2017). “Gemilerin manevra performans tahminleri için genel bir değerlendirme 1.” *Gemi ve Deniz Teknolojisi* , vol.23, no.210, 37-75.

Triantafyllou S., & Hover S. (2003). *Manoeuvring and control of marine vehicles*, Department of Ocean Engineering, Massachusetts Institute of Technology, Cambridge, Massachusetts USA.

Vaz, G., & Toxopeus, S., & Holmes, S. (2010). “Calculation of manoeuvring forces on submarines using two viscous-flow solvers.” *Proceedings of the international conference on offshore mechanics and arctic engineering - OMAE*. 6. 10.1115/OMAE2010-20373.

Wang, H., & Zhai, Z. (2012). “Analyzing grid independency and numerical viscosity of computational fluid dynamics for indoor environment applications.” *Building and Environment*. 52. 107-118. 10.1016/j.buildenv.2011.12.019.

Yasukawa, H., & Yoshimura, Y. (2015). “Introduction of MMG standard method for ship maneuvering predictions.” *Journal of Marine Science and Technology*, 20, 37-52.

Yoon, H. (2009). “Phase-averaged stereo-PIV flow field and force/moment/motion measurements for surface combatant in PMM maneuvers.” [PhD Dissertation]. The University of Iowa.

RESEARCH ARTICLE

**An ethical committee approval and/or legal/special permission has not been required within the scope of this study.*

**NUMERICAL INVESTIGATION OF HVAC SYSTEMS OF A
NAVAL SHIP COMPARTMENT: FREE COOLING AND AIR-
CONDITIONING***

Alpay ACAR¹ 
Murat URYAN^{2*} 
Ali DOĞRUL³ 
Asım Sinan KARAKURT⁴ 
Cenk ÇELİK⁵ 

¹ *National Defence University, Turkish Naval Academy, Department of
Naval Architecture and Marine Engineering, Istanbul, Türkiye,
aacar@dho.edu.tr*

² *National Defence University, Turkish Naval Academy, Department of
Mechanical Engineering, Istanbul, Türkiye,
muryan@dho.edu.tr*

³ *National Defence University, Turkish Naval Academy, Department of
Naval Architecture and Marine Engineering, Istanbul, Türkiye,
adogrul@dho.edu.tr*

⁴ *Yildiz Technical University, Department of Naval Architecture and Marine
Engineering, Istanbul, Türkiye,
asinan@yildiz.edu.tr*

⁵ *Kocaeli University, Department of Mechanical Engineering, Kocaeli,
Türkiye,
cenkcelik@kocaeli.edu.tr*

Received: 31.03.2023

Accepted: 23.05.2023

*Alpay ACAR, Murat URYAN, Ali DOĞRUL,
Asım Sinan KARAKURT, Cenk ÇELİK*

ABSTRACT

HVAC system design and optimization of the ventilation and air-conditioning of indoor environments are crucial for human comfort. Especially in recent years, due to the COVID-19 pandemic, the importance of this hot topic is noticed. This study aims to focus on the HVAC performance of a dorm compartment onboard a naval surface ship since the ship environment is a good example of indoor air ventilation problem. The air circulation and thermal comfort were investigated using a RANS solver. The numerical analyses were conducted for different scenarios and the results were finally discussed in terms of HVAC system location, air temperature, air intake and outlet conditions. As a conclusion, the current HVAC system design was found insufficient and alternative solutions were proposed in order to improve air circulation and thermal comfort.

Keywords: *HVAC, Naval Ship, RANS, Thermal Comfort.*

*Numerical Investigation of HVAC Systems of A Naval Ship Compartment:
Free Cooling and Air-Conditioning*

**BİR SAVAŞ GEMİSİ KOMPARTIMANINDA HVAC
SİSTEMLERİNİN SAYISAL İNCELENMESİ: DOĞAL
HAVALANDIRMA VE İKLİMLENDİRME**

ÖZ

Kapalı mekanlarda HVAC sistem tasarımı ve havalandırma ile iklimlendirmenin optimizasyonu insan konforu için önemlidir. Özellikle geçtiğimiz birkaç yılda yaşanan COVID-19 pandemisi nedeniyle bu güncel konunun önemi fark edilmiştir. Bu çalışma bir savaş gemisi içerisinde bulunan ve yatakhane olarak kullanılan bir kompartımanın hava sirkülasyonu ve ısı konforu üzerine odaklanmaktadır. Savaş gemisi kompartımanı, kapalı mekan havalandırma problemi için iyi bir örnek teşkil etmektedir. HVAC performans analizi bir RANS çözücü kullanılarak yapılmıştır. Sayısal analizler farklı senaryolar için gerçekleştirilmiştir ve sonuçlar HVAC sisteminin yeri, hava sıcaklığı, hava giriş ve çıkış koşulları açısından tartışılmıştır. Sonuç olarak mevcut HVAC tasarımının yetersiz olduğu tespit edilmiş ve kapalı mekandaki hava sirkülasyonunu ve ısı konforu iyileştirmek amacıyla alternatif çözümler önerilmiştir.

Anahtar Kelimeler: Askeri Gemi, HVAC, Isı Konfor, RANS.

1. INTRODUCTION

The heating, ventilation and air-conditioning (HVAC) of indoor environments are significant in many aspects. The Covid-19 pandemic showed that the HVAC system design is crucial and the design should be optimized to gain maximum performance especially in pandemic conditions. The thermal comfort, air quality and particle distribution should be investigated by an appropriate method (experimental, numerical) and the system design should be finalized.

There are several studies focusing on air quality and thermal comfort of indoor environments. The studies involve experimental and/or numerical investigations. The study of Atthajariyakul and Leephakpreeda (2004) involves the experimental studies of a building having a 24-hour working HVAC system and the authors focused on the indoor air temperature, humidity, velocity and ventilation rate. A new methodology was proposed to determine the real-time optimum HVAC configuration instead of the conventional methods. Yang et al. (2014) showed the effect of an air-conditioner inside a bedroom on thermal comfort and air quality using the CFD method. It is concluded that the air-conditioner works effectively and provides good indoor thermal comfort. The authors mentioned that the CFD method can be used practically to design more human-friendly and healthy indoor environments. Shu et al. (2015) measured the air circulation ratios in 22 taxi cabs working in Los Angeles. The position of the windows and ventilation settings were investigated by testing 14 windows closed cabs and 8 windows closed and medium-ventilated cabs. Jin et al. (2016) conducted CFD simulations to investigate air ventilation by the wind for a multi-storey hospital located in a Chinese city. The openings in the balconies were analyzed for better free cooling in the rooms. It is concluded that CFD methods can be used for the free cooling performance of complex environments. In a review study by Kato (2018), the author mentioned the necessity of CFD methods to simulate air flow and heat transfer. It is concluded that the flow problems should be handled in 3-D instead of 1-D, however, this needs more computing capacity. In another study by Lau et al. (2019), the authors focused on the thermal comfort of the students on a university campus through three different ventilation strategies. These three strategies were air-conditioning, hybrid ventilation and free cooling. The

*Numerical Investigation of HVAC Systems of A Naval Ship Compartment:
Free Cooling and Air-Conditioning*

results showed that air-conditioning has more advantages than others in terms of temperature distribution and thermal comfort. Liu et al. (2020) investigated the aerodynamic nature of SARS CoV-2 virus at two Wuhan hospitals during the pandemic. The virus concentration on the aerosols was studied in isolation rooms, patient rooms and bathrooms. The isolation rooms were found cleaner than the others and some proposals were made for future studies. Chen et al. (2020) investigated the high temperature and particle distribution inside a kitchen using the CFD method. The effects of the particle behavior on air pollution were observed and it is emphasized that the current CFD model is a practical tool to model the air quality and thermal comfort in the kitchen. Tong et al. (2020) investigated the vertical temperature distribution in a large building having two indoor areas. The study was made to determine the effect of indoor heat sources and building heights on indoor thermal comfort air quality. In the study of Ullrich et al. (2020), they aimed to improve the development of the HVAC system, which is the largest secondary consumer in an electric vehicle. The goal was achieved by validating a numerical model that calculates the flow distributions in the air vents of the front seats in a full-scale car cabin. Velocity fields were examined by taking three different air flow rates. They found that the difference between the experimental and numerical results of the average airspeed was quite small. In the study of Wang et al. (2022), the efficiency of the air-conditioning system was investigated by simulating the air distribution inside a hotel lobby. The optimum lobby design depends on the thermal distribution and also air circulation for different summer working conditions. The study of Arpino et al. (2022) involves the CFD simulation of airflow inside a car cabin with passengers. One passenger was considered infected with the SARS-CoV-2 virus. The position of the infected passenger was analyzed in terms of HVAC system airflow velocity and HVAC mode. It is concluded that the infection emission into the air can be controlled with the appropriate design conditions. In the study of Natarajan et al. (2022), the authors tried to understand and analyze the air flow characteristics and temperature distribution changes in a shipping container factory with different inlet and outlet conditions. Two alternative designs for inlet and outlet conditions were expected to improve the uniformity of airflow and temperature distribution. Zhang et al. (Zhang et al., 2022) proposed a new design in an interior corridor configuration with double-sided classrooms to create a horizontal airflow channel throughout the

*Alpay ACAR, Murat URYAN, Ali DOĞRUL,
Asım Sinan KARAKURT, Cenk ÇELİK*

building to provide cross ventilation in classrooms on both sides to allow more outside air. They validated a computational fluid dynamics model using experimental data and used different sized ducts to predict the airflow velocity of the duct by examining wind directions, wind speeds and climate data. With this new design, they achieved an average of 215% increase in ventilation rate on an annual basis. Consequently, this study can be used to improve natural airflow rates in other buildings with interior corridors in their designs. Tai et al. (2022) performed a numerical study using computational fluid dynamics on cross ventilation for a building equipped with louvers. Shutter configurations without louver and with different angles were determined as variables. The highest air exchange efficiency was determined between 53.4% and 150 louver angles. The lowest air exchange efficiency was found at the louver angle of 20 to 100%. Based on these findings, they concluded that the opening position as well as the louver angle play an integral role in natural cross ventilation on internal air flow, pressure coefficient and air exchange efficiency. In a recent study by Chang et al. (2023), different modes of ventilation/circulation were simulated inside a vehicle cabin to observe the air quality. The validity of the CFD method was searched using the available experimental data in the literature. With the increase of passengers in the cabin, the temperature of the transition between different modes was determined.

This study mainly focuses on two different aspects. Firstly, the free cooling of the ship compartment was analyzed numerically for different cases in terms of air circulation. Secondly, the HVAC system was activated and the indoor thermal comfort was analyzed numerically with and without the free cooling. The numerical analyses were carried out employing a commercial CFD package. The governing equations are RANS equations. In addition to the continuity and momentum equations, the energy equation was solved in this study. The numerical results were then compared in terms of different scalar functions such as streamlines and velocity contours. The current HVAC system and the compartment layout were found insufficient and alternative solutions were proposed. The main highlight of the present study is that a real naval surface combatant ship was focused and HVAC problems inside a compartment were investigated numerically. Finally, some practical solutions were proposed to enhance HVAC performance.

2. COMPARTMENT GEOMETRY

The ship compartment investigated in the present study is a dorm located under the main deck of the ship. For this reason, indoor air quality and thermal comfort are of high importance. The 3-D compartment model is given in Figure 1 with a detailed arrangement. The total compartment volume is approximately 220 m³ and the number of people capacity is 60.

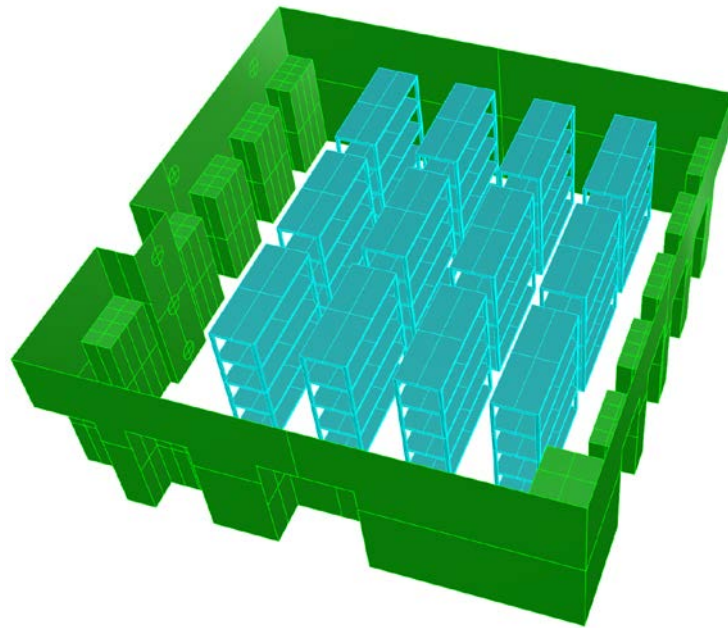


Figure 1. General arrangement of the ship compartment.

3. THEORETICAL BACKGROUND

The present study is a numerical investigation so the governing equations were solved using Siemens PLM Star CCM+ 16.02. The details of the conservation equations and the numerical approach are briefly explained in this chapter.

3.1. Governing Equations

The numerical analyses were conducted using commercial CFD software solving Reynolds-Averaged Navier-Stokes (RANS) equations. The governing equations are the continuity equation and the momentum equations considering the flow is incompressible and turbulent. The continuity equation can be given as:

$$\frac{\partial U_i}{\partial x_i} = 0 \quad (1)$$

The mean momentum equations can be written in tensor notation and Cartesian coordinates.

$$U_j \frac{\partial U_i}{\partial x_j} = -\frac{1}{\rho} \frac{\partial P}{\partial x_i} + \frac{\partial}{\partial x_j} \left[\nu \left(\frac{\partial U_i}{\partial x_j} + \frac{\partial U_j}{\partial x_i} \right) \right] - \frac{\partial \overline{u'_i u'_j}}{\partial x_j} \quad (2)$$

Here, ρ depicts the fluid density, kg/m^3 ; U_i is the velocity, m/s ; P represents the pressure, Pa ; ν is the kinematic viscosity, m^2/s . The last two terms belong to the viscous stress tensor and Reynolds stress tensor, respectively. The details about Reynolds stress tensor (i.e., $\overline{u'_i u'_j}$) and the turbulence model ($k - \omega SST$) can be found in Wilcox in detail (Wilcox, 2006, 2008). This turbulence model covers $k - \varepsilon$ turbulence model and it resolves the boundary layer using all wall y^+ approach. This turbulence model is widely used in aerodynamics, hydrodynamics and internal flow problems (Bilir et al., 2022; Sarı et al., 2021; Sezen et al., 2021). There are also recent studies using $k - \omega SST$ turbulence model (Bode et al., 2020; Croitoru et al., 2022; Fraña et al., 2014; Tien & Calautit, 2019). As stated in the papers (Bode et al., 2020; Croitoru et al., 2022), $k - \omega SST$ turbulence model models the flow separation and reattachments in complex flows better and it is suitable for indoor HVAC flow problems. In addition to these equations, in heat transfer analyses, the conservation of energy equation is also considered during the simulations (Bergman et al., 2011).

*Numerical Investigation of HVAC Systems of A Naval Ship Compartment:
Free Cooling and Air-Conditioning*

$$U_j \frac{\partial(T)}{\partial x_j} = \alpha \frac{\partial}{\partial x_i} \left[\frac{\partial T}{\partial x_j} \right] + \frac{v}{C_p} (\nabla U_j)^2 \quad (3)$$

Here, in the conservation of energy, T is the temperature while α is the thermal coefficient and C_p is the non-dimensional pressure coefficient. The left-hand side of the equation is the net rate of the thermal energy and the right-hand side of the equation comprises the thermal energy due to conduction and viscous dissipation, respectively. One may note that all three governing equations are given in steady form since the analyses were conducted steadily.

3.2. Numerical Setup

The numerical approach is based on commercial CFD software solving RANS equations and the energy equation for heat transfer cases. The computational domain consists of the dorm compartment in the naval ship and the fluid region was discretized with elements based on the finite volume method (FVM). Trimmer mesh algorithm was used and hexahedral finite volumes were created to represent the computational domain properly. The surface mesh structure on the walls was set to be denser than the whole volume considering a surface mesh refinement.

Table 1. The details of the numerical setup.

	Case 1	Case 2	Case 3	Case 4
Mesh number	3860862	3836762	3903274	3829604
Mesh type	Hexagonal			
Base size	750 mm			
Max. – Min. surface size	25% of base size			
Number of prism layer	4			
Surface growth rate	1.3			

*Alpay ACAR, Murat URYAN, Ali DOĞRUL,
Asım Sinan KARAKURT, Cenk ÇELİK*

The mesh structure on the walls were created keeping the wall y^+ value below 1 (Figure 3) that reduces the mesh dependency and makes the mesh structure more reliable for numerical analyses. Therefore, a mesh dependency/sensitivity study was not conducted in this study. In further studies, numerical uncertainty will be calculated for verification of the numerical method using Grid Convergence Index (GCI) (Celik et al., 2008; Roache, 1998) and Factors of Safety (FS) (Xing & Stern, 2010) methods in terms of grid size and time step size. The details of the mesh setup were given in Table 1. The boundary conditions on the domain surfaces were defined as velocity inlet for the air intakes and pressure outlet for the outlets. The mesh structure and the boundary conditions were given in Figure 2 and 4, respectively.

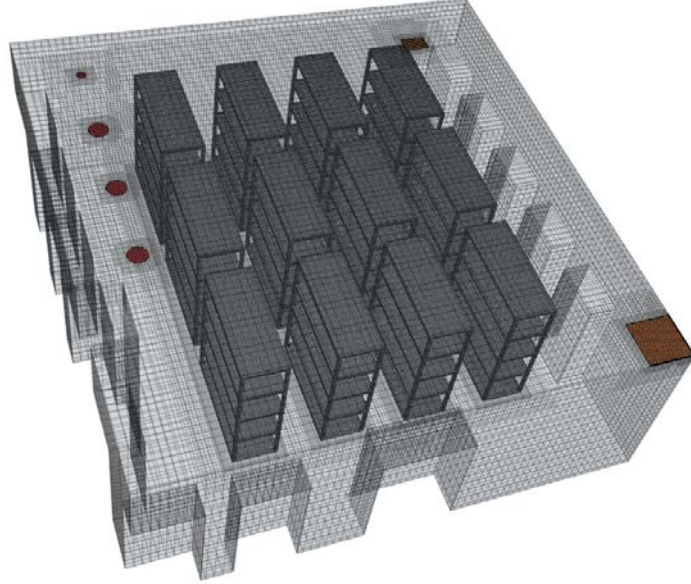


Figure 2. Mesh structure of the computational domain.

*Numerical Investigation of HVAC Systems of A Naval Ship Compartment:
Free Cooling and Air-Conditioning*

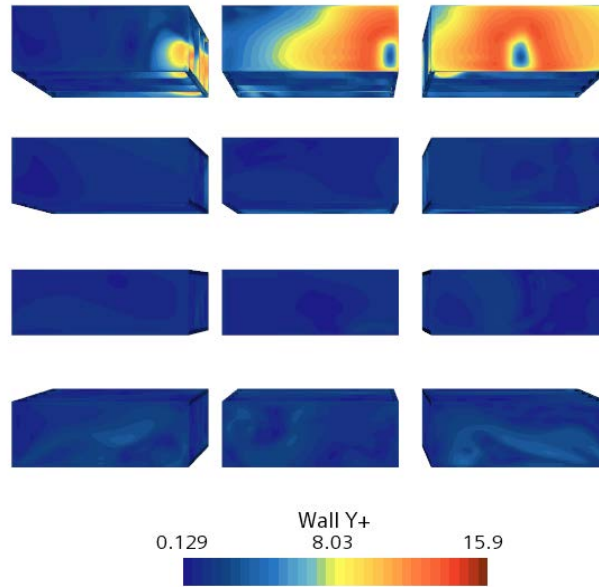


Figure 3. Wall y^+ distribution on the wall surfaces inside the compartment

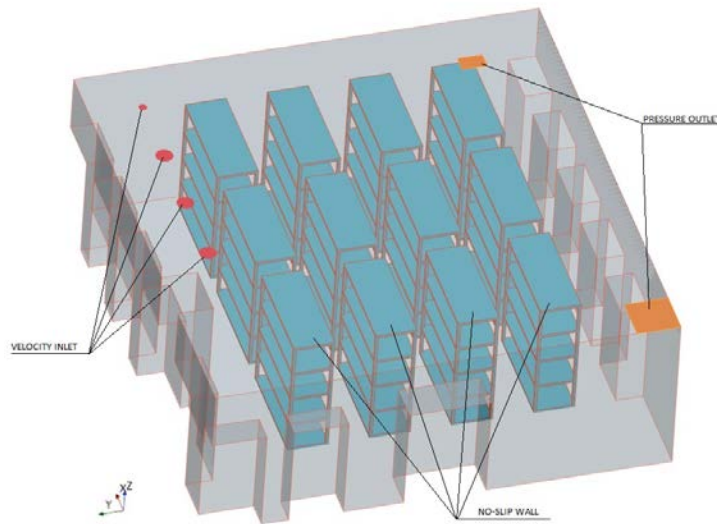


Figure 4. Boundary conditions applied on the surfaces: red (velocity inlet), orange (pressure outlet) and blue (no-slip wall)

4. NUMERICAL RESULTS

The present study focuses on the HVAC performance of a naval ship compartment using a numerical method. The numerical analyses were carried out in different aspects: free cooling to determine the air circulation and heat transfer to determine the indoor thermal comfort. The sub-chapters given below show the numerical results in these aspects and alternative HVAC solutions were proposed to improve the HVAC system performance in the compartment. Details of the boundary conditions were given in Table 2.

Table 2. The details of the boundary conditions.

	Case 1	Case 2	Case 3	Case 4
Compartment initial indoor temperature	26.85 °C	26.85 °C	26.85 °C	26.85 °C
Fan inlet temperature	28 °C	28 °C	28 °C	28 °C
Fan inlet velocity	4 m/s	4 m/s	4 m/s	4 m/s
Air-Conditioning inlet velocity	2 m/s	2 m/s	2 m/s	2 m/s
Pressure outlet (Gauge pressure)	0 Pa	0 Pa	0 Pa	0 Pa
Air-Conditioning inlet temperature	N/A	N/A	18 °C	18 °C

4.1. Case 1 (Free Cooling)

Case 1 is the free cooling scenario and the air-conditioning system was not taken into account. The streamlines and velocity distribution on particular plane sections were obtained to observe the air circulation inside the ship compartment.

*Numerical Investigation of HVAC Systems of A Naval Ship Compartment:
Free Cooling and Air-Conditioning*

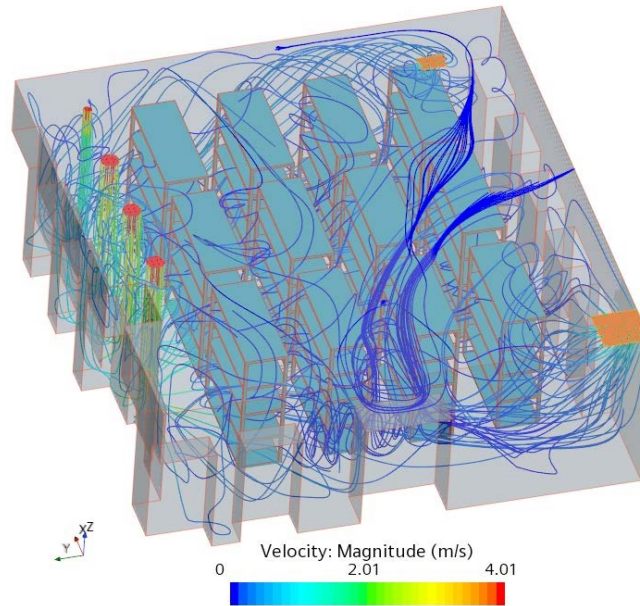


Figure 5. Streamlines inside the compartment for case 1.

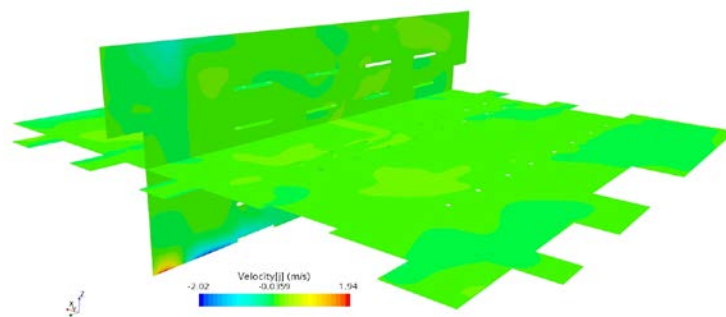


Figure 6. Velocity (y component) distribution inside the compartment for case 1.

The streamlines in Figure 5 show that the right side of the compartment and the upper part does not meet with the air because of the air inlet locations. Figure 6 gives the velocity-y distribution to show that the velocity-y

*Alpay ACAR, Murat URYAN, Ali DOĞRUL,
Asım Sinan KARAKURT, Cenk ÇELİK*

component is nearly zero in the whole compartment which means the airflow is poor in the y-direction.

4.2. Case 2 (Alternative Free Cooling)

Case 2 is similar to Case 1 while the air inlet locations were changed and additional outlets were added. An alternative fan arrangement was proposed for better air circulation.

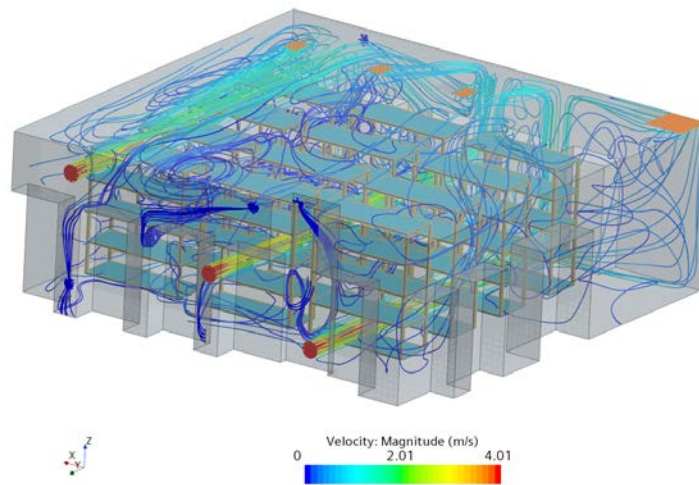


Figure 7. Streamlines inside the compartment for case 2.

One may see that the newly located air inlets feed the compartment in the y-direction in Figure 7. This leads to better air circulation and minimum stagnation inside the compartment.

*Numerical Investigation of HVAC Systems of A Naval Ship Compartment:
Free Cooling and Air-Conditioning*

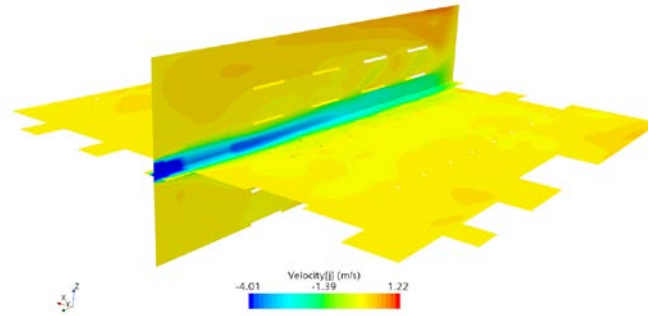


Figure 8. Velocity (y component) distribution inside the compartment for case 2.

Figure 8 shows the y-component of the velocity distribution. There are still stagnation zones however the airflow is maintained in the whole region around the bunk beds. It can be evaluated that there are fewer stagnation points when compared with the original fan arrangement. The newly added outlets help clean and circulate the air inside the compartment.

4.3. Case 3 (Free Cooling & Air-Conditioning)

Case 3 is the scenario in that free cooling and air-conditioning systems are both working. Since the air-conditioning was considered, indoor thermal comfort is of special interest. The indoor temperature was considered as 26.85 °C (300 °K). The ventilation fans blow the air taken from the atmosphere with a constant temperature of 28 °C while the air-conditioning air temperature is 18 °C.

*Alpay ACAR, Murat URYAN, Ali DOĞRUL,
Asım Sinan KARAKURT, Cenk ÇELİK*

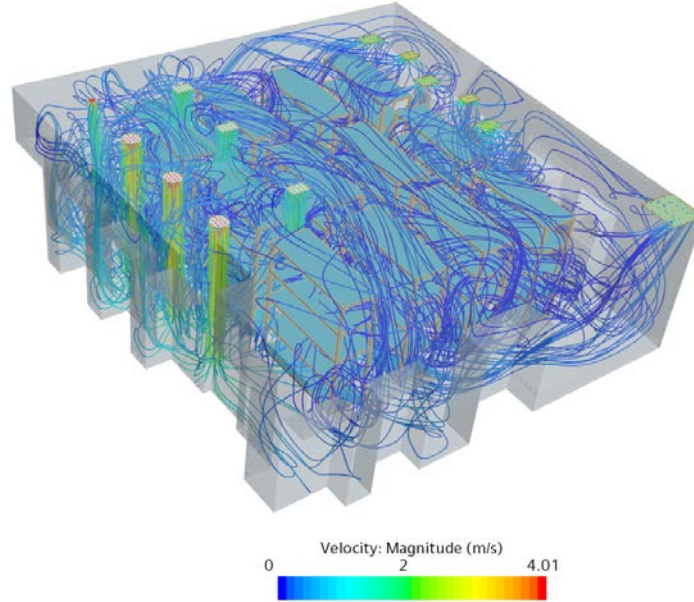


Figure 9. Streamlines inside the compartment for case 3.

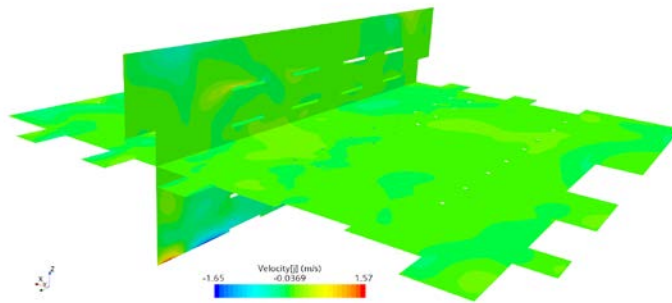


Figure 10. Velocity (y component) distribution inside the compartment for case 3.

Figure 9 shows the free cooling and air-conditioning systems working together. The air circulation is better than in Case 1, however, there are stagnation points inside the compartment. Figure 10 supports this situation as

*Numerical Investigation of HVAC Systems of A Naval Ship Compartment:
Free Cooling and Air-Conditioning*

well. The average temperature decreased to 24.89 °C. Thermal comfort is still poor because the air does not circulate inside the compartment effectively.

4.4. Case 4 (Alternative Free Cooling & Air-Conditioning)

Case 4 was investigated to show the effectiveness of the newly proposed free cooling arrangement working with the air-conditioning system. The boundary conditions and initial temperature values were kept the same as in Case 3.

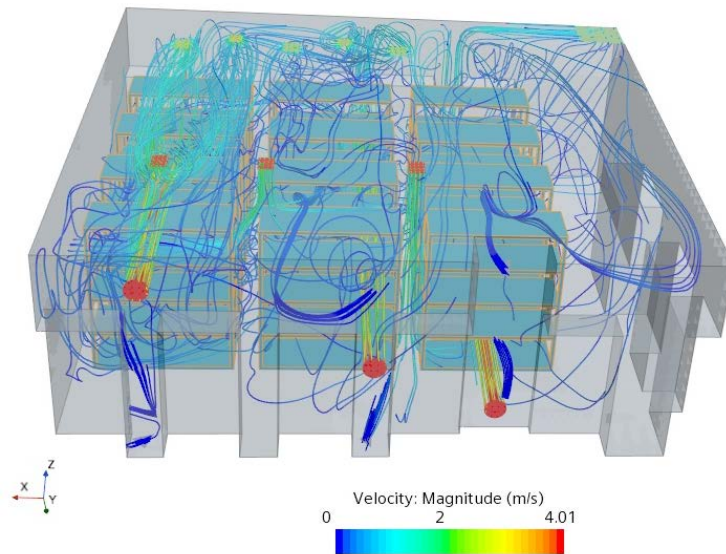


Figure 11. Streamlines inside the compartment for case 4.

Figure 11 shows the streamlines inside the compartment having new fan inlet locations and new outlets. Note that there are fewer stagnation spots in terms of the y-component of velocity as indicated in Figure 12. The free cooling feeds the compartment from the side while the air-conditioning system gives cold air from the top in the z-direction. This provides a mixing of hot and cold air and the thermal comfort is better than Case 3. The average temperature inside the compartment decreased to 24.57 °C.

*Alpay ACAR, Murat URYAN, Ali DOĞRUL,
Asım Sinan KARAKURT, Cenk ÇELİK*

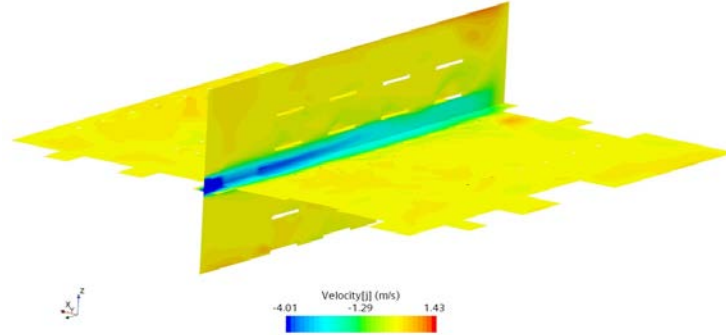


Figure 12. Velocity (y component) distribution inside the compartment for case 4.

Table 3 gives the final results of temperature and ACH rates for different cases. ACH is calculated using the equation below.

$$ACH = \frac{Q}{\nabla} \quad (4)$$

Here, Q is the volumetric flow rate of the total inlet surfaces and ∇ is the total compartment volume. One may see that ACH rate is much better for Case 3 than Case 4, however, the thermal comfort is better satisfied for Case 4.

Table 3. The results of temperature and ACH rates for different cases.

	Case 1	Case 2	Case 3	Case 4
Compartment final indoor temperature	N/A	N/A	24.89 °C	24.57 °C
Air changes per hour (ACH)	17.07	15.75	25.18	23.86

5. CONCLUSION

This study focuses on the numerical investigation of HVAC systems located inside a ship compartment. RANS equations were solved by discretizing the computational domain with finite volume elements. Air circulation and thermal comfort were examined for different cases.

The numerical results showed that the current HVAC system arrangement is insufficient. An alternative arrangement was proposed for the free cooling fan inlets and new fan outlets were added to the system. The newly proposed fan arrangement provides better air circulation however there are still some stagnation spots in the area. The air-conditioning (AC) system working with the newly proposed fan arrangement works better and decreases the inside average temperature more than the original case. This is because the new arrangement blows the air from the side while the AC system blows cold air from the top. This provides a mixing of hot and cold air and better cooling is obtained. From another point of view, the ACH rates showed that better ACH rate does not mean better thermal comfort. Thermal comfort can be maintained with proper air circulation and cooling, however, ACH is only related with the fan inlet velocity and flow rate. It is finally concluded that the numerical approach as used in the present study can help to determine the cause of the possible HVAC problems in indoor environments.

As a further study, it is planned to extend the present numerical approach for a verification study. The verification study will be made in terms spatial and temporal manners to verify the grid size and time step size of the numerical method. GCI and FS methods will be employed for this purpose. Within this, the numerical uncertainty will be calculated instead of mesh dependency/sensitivity approach.

*Alpay ACAR, Murat URYAN, Ali DOĐRUL,
Asım Sinan KARAKURT, Cenk ÇELİK*

ACKNOWLEDGEMENT

The authors declare no conflict of interest. The authors would like to thank Turkish Naval Academy Command and Training Commodore for giving advice and information for this study. The authors also thank to Prof. Halil İbrahim Saraç for his valuable comments on this study.

CONFLICT OF INTEREST STATEMENT

The authors declare no conflict of interest.

*Numerical Investigation of HVAC Systems of A Naval Ship Compartment:
Free Cooling and Air-Conditioning*

REFERENCES

Arpino, F., Grossi, G., Cortellessa, G., Mikszewski, A., Morawska, L., Buonanno, G., & Stabile, L. (2022). Risk of SARS-CoV-2 in a car cabin assessed through 3D CFD simulations. *Indoor Air*, 32(3), e13012. <https://doi.org/10.1111/ina.13012>

Atthajariyakul, S., & Leephakpreeda, T. (2004). Real-time determination of optimal indoor-air condition for thermal comfort, air quality and efficient energy usage. *Energy and Buildings*, 36(7), 720–733. <https://doi.org/10.1016/j.enbuild.2004.01.017>

Bergman, T. L., Lavine, A. S., Incropera, F. P., & DeWitt, D. P. (2011). *Fundamentals of Heat and Mass Transfer* (7th edition). John Wiley & Sons.

Bilir, A. Ç., Doğrul, A., & Vardar, N. (2022). An Extensive Investigation of Flow Conditioners Inside A Fi-Fi Monitor. *Brodogradnja : Teorija i Praksa Brodogradnje i Pomorske Tehnike*, 73(4), 161–177. <https://doi.org/10.21278/brod73408>

Bode, F., Meslem, A., Patrascu, C., & Nastase, I. (2020). Flow and wall shear rate analysis for a cruciform jet impacting on a plate at short distance. *Progress in Computational Fluid Dynamics, an International Journal*, 20(3), 169–185. <https://doi.org/10.1504/PCFD.2020.107276>

Celik, I. B., Ghia, U., Roache, P. J., Freitas, C. J., & Raad, P. E. (2008). Procedure for Estimation and Reporting of Uncertainty Due to Discretization in CFD Applications. *Journal of Fluids Engineering*, 130(7). <https://doi.org/10.1115/1.2960953>

Chang, T.-B., Lin, Y.-S., & Hsu, Y.-T. (2023). CFD simulations of effects of recirculation mode and fresh air mode on vehicle cabin indoor air quality. *Atmospheric Environment*, 293, 119473. <https://doi.org/10.1016/j.atmosenv.2022.119473>

Chen, Z., Xin, J., & Liu, P. (2020). Air quality and thermal comfort analysis of kitchen environment with CFD simulation and experimental calibration. *Building and Environment*, 172, 106691. <https://doi.org/10.1016/j.buildenv.2020.106691>

*Alpay ACAR, Murat URYAN, Ali DOĞRUL,
Asım Sinan KARAKURT, Cenk ÇELİK*

Croitoru, C., Nastase, I., Bode, F., & Sandu, M. (2022). Assessment of virtual thermal manikins for thermal comfort numerical studies. Verification and validation. *Science and Technology for the Built Environment*, 28(1), 21–41. <https://doi.org/10.1080/23744731.2021.1916379>

Fraña, K., Müller, M., & Zhang, J. S. (2014). *The effect of the window temperature on the thermal comfort in a room heated by a floor convector*. 13th International Conference on Indoor Air Quality and Climate, Indoor Air.

Jin, R., Hang, J., Liu, S., Wei, J., Liu, Y., Xie, J., & Sandberg, M. (2016). Numerical investigation of wind-driven natural ventilation performance in a multi-storey hospital by coupling indoor and outdoor airflow. *Indoor and Built Environment*, 25(8), 1226–1247. <https://doi.org/10.1177/1420326X15595689>

Kato, S. (2018). Review of airflow and transport analysis in building using CFD and network model. *JAPAN ARCHITECTURAL REVIEW*, 1(3), 299–309. <https://doi.org/10.1002/2475-8876.12051>

Lau, S. S. Y., Zhang, J., & Tao, Y. (2019). A comparative study of thermal comfort in learning spaces using three different ventilation strategies on a tropical university campus. *Building and Environment*, 148, 579–599. <https://doi.org/10.1016/j.buildenv.2018.11.032>

Liu, Y., Ning, Z., Chen, Y., Guo, M., Liu, Y., Gali, N. K., Sun, L., Duan, Y., Cai, J., Westerdahl, D., Liu, X., Xu, K., Ho, K., Kan, H., Fu, Q., & Lan, K. (2020). Aerodynamic analysis of SARS-CoV-2 in two Wuhan hospitals. *Nature*, 582(7813), Article 7813. <https://doi.org/10.1038/s41586-020-2271-3>

Natarajan, G., Zaid, M., Konka, H., Srinivasan, R., Ramanathan, S. S., Ahmed, T., & Chowdhury, H. (2022). Modeling of air distribution inside a shipping container plant factory using computational fluid dynamics (CFD). *AIP Conference Proceedings*, 2681(1), 020091. <https://doi.org/10.1063/5.0117095>

Roache, P. J. (1998). Verification of Codes and Calculations. *AIAA Journal*, 36(5), 696–702. <https://doi.org/10.2514/2.457>

*Numerical Investigation of HVAC Systems of A Naval Ship Compartment:
Free Cooling and Air-Conditioning*

Sarı, S., Doğrul, A., & Bayraktar, S. (2021). *On The Computational Aerodynamics of a Generic Frigate*. 397–403.

Sezen, S., Delen, C., Dogrul, A., & Atlar, M. (2021). An investigation of scale effects on the self-propulsion characteristics of a submarine. *Applied Ocean Research*, 113, 102728. <https://doi.org/10.1016/j.apor.2021.102728>

Shu, S., Yu, N., Wang, Y., & Zhu, Y. (2015). Measuring and modeling air exchange rates inside taxi cabs in Los Angeles, California. *Atmospheric Environment*, 122, 628–635. <https://doi.org/10.1016/j.atmosenv.2015.10.030>

Tai, V. C., Kai-Seun, J. W., Mathew, P. R., Moey, L. K., Cheng, X., & Baglee, D. (2022). Investigation of varying louver angles and positions on cross ventilation in a generic isolated building using CFD simulation. *Journal of Wind Engineering and Industrial Aerodynamics*, 229, 105172. <https://doi.org/10.1016/j.jweia.2022.105172>

Tien, P. W., & Calautit, J. K. (2019). Numerical analysis of the wind and thermal comfort in courtyards “skycourts” in high rise buildings. *Journal of Building Engineering*, 24, 100735. <https://doi.org/10.1016/j.jobbe.2019.100735>

Tong, Y., Lin, K., Hu, Q., Niu, X., Peng, J., Huo, D., & Yan, W. (2020). Field measurements on thermal stratification and cooling potential of natural ventilation for large space buildings. *International Journal of Ventilation*, 19(1), 49–62. <https://doi.org/10.1080/14733315.2018.1544730>

Ullrich, S., Buder, R., Boughanmi, N., Friebe, C., & Wagner, C. (2020). Numerical Study of the Airflow Distribution in a Passenger Car Cabin Validated with PIV. In A. Dillmann, G. Heller, E. Krämer, C. Wagner, C. Tropea, & S. Jakirlić (Eds.), *New Results in Numerical and Experimental Fluid Mechanics XII* (pp. 457–467). Springer International Publishing. https://doi.org/10.1007/978-3-030-25253-3_44

Wang, L., Kumar, P., Makhatha, M. E., & Jagota, V. (2022). Numerical simulation of air distribution for monitoring the central air conditioning in large atrium. *International Journal of System Assurance Engineering and Management*, 13(1), 340–352. <https://doi.org/10.1007/s13198-021-01420-4>

*Alpay ACAR, Murat URYAN, Ali DOĞRUL,
Asım Sinan KARAKURT, Cenk ÇELİK*

Wilcox, D. C. (2006). *Turbulence Modeling for CFD* (3rd edition). DCW Industries.

Wilcox, D. C. (2008). Formulation of the k-w Turbulence Model Revisited. *AIAA Journal*, 46(11), 2823–2838. <https://doi.org/10.2514/1.36541>

Xing, T., & Stern, F. (2010). Factors of Safety for Richardson Extrapolation. *Journal of Fluids Engineering*, 132(6). <https://doi.org/10.1115/1.4001771>

Yang, L., Ye, M., & he, B.-J. (2014). CFD simulation research on residential indoor air quality. *Science of The Total Environment*, 472, 1137–1144. <https://doi.org/10.1016/j.scitotenv.2013.11.118>

Zhang, Z.-Y., Yin, W., Wang, T.-W., & O'Donovan, A. (2022). Effect of cross-ventilation channel in classrooms with interior corridor estimated by computational fluid dynamics. *Indoor and Built Environment*, 31(4), 1047–1065. <https://doi.org/10.1177/1420326X211054341>

JOURNAL OF NAVAL SCIENCES AND ENGINEERING (JNSE) PUBLISHING RULES

Submission of Papers: Manuscripts which are submitted to the journal should not be published elsewhere or sent to be published. Authors are (preferably) requested to submit an electronic copy of their original works to the given "System Address" or one hard copy to the address and a soft copy to the "e-mail address" which have been given below. It is necessary for the authors to submit their manuscripts together with the "Copyright Release Form". "Copyright Release Form" can be downloaded from the "Copyright Page" of JNSE's Web Page. Authors are requested to obtain the relevant documents for their studies that require "Ethics Committee Approval and/or Legal/Special Permission" and submit these approval documents to the system together with their study. The author(s) of the manuscript must declare that there are no conflicts of personal and/or financial interest within the scope of the study.

System Address:

<https://dergipark.org.tr/tr/pub/jnse>

Address:

Assoc.Prof.Dr. Fatih ERDEN
National Defence University (Milli Savunma Üniversitesi)
Turkish Naval Academy (Deniz Harp Okulu Dekanlığı)
34942 Tuzla/İstanbul/Türkiye

E-mail: jnse@dho.edu.tr

Types of Contributions: The journal publishes original papers, review articles, technical notes, book reviews, letters to the editor, extended reports of conferences and meetings.

Manuscript Evaluation Process: The Peer Review Step:

- The content and layout format of manuscript are examined, and the originality of study is checked by iThenticate Software Programme.
- The language and correlation of the English abstract with Turkish abstract are checked.
- Manuscript which has a similarity index above 40% is rejected. The author is informed about the manuscript which has a similarity index between 20% and 40% (must not contain more than 4% from a single source), which is not appropriate for the writing rules of JNSE or needs correction in English and Turkish abstracts and the author is requested to revise the manuscript within "two weeks". Otherwise, the article is considered as a retracted manuscript. The similarity percentage criteria may differ for review articles, letters to the editor, book reviews, and invited articles. Special care is taken to ensure that more than 50% of the articles in an issue are original research articles.

Our journal uses **double-blind** review, which means that both the reviewer and author identities are concealed from the reviewers, and vice versa, throughout the review process. So, the uploaded manuscript does not contain the name, address, and affiliation of author(s). The manuscript evaluation steps are as follows:

- Editor is assigned by the Editor-in-Chief.
- The relevant reviewers are assigned by the Editors.
- As a result of the reviewer's evaluation, the manuscript may be rejected, accepted or a correction for the manuscript may be requested.
- If the negative feedback is given by major number of the reviewers, the process is terminated, and the article is rejected.
- If major/minor revisions are required for the manuscript, the author has to do this revision according to the reviewers' comments in "three weeks".
- If the revision is accepted by the reviewers, the article is accepted.

The Workflow Diagram for the evaluation process can be accessed from the web page of the journal.

The articles submitted to JNSE to be published are free of article submission, processing and publication charges.

The accepted articles are published **free-of-charge** as online from the journal website and printed.

DENİZ BİLİMLERİ VE MÜHENDİSLİĞİ DERGİSİ (DBMD) YAYIN KURALLARI

Yazların Gönderilmesi: Dergiye gönderilen makaleler başka bir yerde yayımlanmamış ya da yayımlanmak üzere gönderilmemiş olmalıdır. Yayımlanması istenilen yazılar (tercihen) aşağıda verilen “Sistem Adresi”nden yüklenmeli veya aşağıdaki adrese bir kopya kâğıda basılı olarak ve aynı zamanda “E-mail Adresi”ne dijital olarak gönderilmelidir. Dergimize makale gönderen yazarların makaleleriyle birlikte “Yayın Hakkı Devir Formu”nu da göndermeleri gerekmektedir. “Yayın Hakkı Devir Formu”na DBMD Web Sayfasındaki “Telif Hakkı” sayfasından erişilebilmektedir. Yazarların “Etik Kurul İzni ve/veya Yasal/Özel İzin” gerektiren çalışmaları için ilgili izin belgelerini temin etmesi ve bu izin belgelerini çalışmalarıyla birlikte sisteme yüklemeleri gerekmektedir. Yazarlar çalışmalarını gönderirken çalışma kapsamında herhangi bir kişisel ve/veya finansal çıkar çatışması olmadığını bildirmek zorundadır.

Sistem Adresi:

<https://dergipark.org.tr/tr/pub/jnse>

Adres:

Doç.Dr. Fatih ERDEN
Deniz Harp Okulu Dekanlığı
34942 Tuzla/ İstanbul/Türkiye

E-mail: jnse@dho.edu.tr

Yazı Türleri: Dergide; orijinal yazılar, derlemeler, teknik notlar, kitap incelemeleri, editöre mektuplar ile konferans ve toplantıların genişletilmiş raporları yayımlanır.

Yazların Değerlendirilme Süreci: Makalenin Ön Kontrol Süreci:

- Makalenin içeriği ve yazım formatı incelenir ve iThenticate Programı ile benzerlik taraması yapılır.
- Makalenin İngilizce özetinin, Türkçe öz ile uygunluğu ve yazım dili kontrol edilir.
- Benzerlik oranı %40’ın üzerinde olan makale reddedilir. Benzerlik oranı %20 ile %40 arasında olan (tek bir kaynakla benzerlik %5’ten fazla olmamalıdır), yazım formatına uymayan ya da İngilizce ve Türkçe özetinde düzeltme gereken makale yazara bildirilir ve “iki hafta” içerisinde makalenin düzeltilmesi istenir. Aksi takdirde makale geri çekilmiş kabul edilir. Derleme makaleler, editöre mektuplar, kitap incelemeleri ve davetli makaleler için benzerlik yüzdesi kriterleri farklılık gösterebilir. Bir sayıdaki makalelerin %50’den fazlasının özgün araştırma makalesi olmasına özen gösterilmektedir.

Dergimiz, makale değerlendirme sürecinde **çift-kör** hakemlik sistemini kullanmaktadır. Buna göre değerlendirme sürecinde hakem ve yazarlar birbirlerinin bilgilerini görememektedir. Bu nedenle, yüklenen ön yükleme formatında yazar(lar)ın isim, adres ve bağlı olduğu kuruluş(lar) yer almamaktadır. Makale değerlendirme sürecindeki adımlar ise aşağıdaki gibidir;

- Baş editör tarafından makaleye Editör atanır.
- Editörler makale için hakemleri atar.
- Hakem değerlendirmesi sonucunda makale reddedilebilir, kabul edilebilir veya makalenin düzeltilmesi istenebilir.
- Hakem görüşlerinin çoğunluğu doğrultusunda makale reddedilmiş ise süreç sonlandırılır ve makale reddedilir.
- Makale için majör / minör düzeltme istenirse hakem görüşleri doğrultusunda yazarın gerekli düzeltmeleri en geç “üç hafta” içerisinde yapması istenir.
- Revize edilmiş makale kabul alırsa düzenleme aşamasına geçilir.

Değerlendirme sürecine ilişkin Akış Şemasına, derginin web sayfasından erişilebilir.

DBMD’ye yayımlanmak üzere gönderilen makaleler; makale gönderim, işlem ve yayın ücretinden muafır.

Kabul edilen makaleler, **ücretsiz** olarak basılı şekilde ve dergi web sayfasından çevrimiçi (online) olarak yayımlanmaktadır.

JOURNAL OF NAVAL SCIENCES AND ENGINEERING (JNSE) WRITING RULES

General: Manuscripts must be prepared in MS Word, single-spaced with justify. Font: Times New Roman, 12 points. Margins: left 4,5 cm- right 3,5 cm, top 5 cm- bottom 7 cm, header 3,25 cm- footer 6 cm, gutter 0. Paper type: A4. Page numbers should be on the middle of bottom of page with -1-, -2-, -3- etc. format. Using footnotes is not allowed.

Ethics Committee Approval and/or Legal/Special Permission: The articles must state whether an ethical committee approval and/or legal/special permission is required or not. If these approvals are required, then it should be clearly presented from which institution, on what date and with which decision or number these approvals are obtained.

Body of Text: Follow this order when typing manuscripts: Title, Authors, Abstract, Keywords, Title (Turkish), Abstract (Turkish), Keywords (Turkish), Main Text, Appendix (if any), References.

Title: Title should reflect objectives of the paper clearly, be easily understandable and not exceed 15 words.

Abstracts: Each paper should have an abstract with 100-200 words and have a structured form, i.e. standard structure of an article (background, purpose, material and methods used, results, conclusion).

Paper Length: The manuscript should be minimum 2000 words or 5 pages, maximum 7000 words or 25 pages including references.

Keywords: Author must provide some keywords (between 3 and 5) that will be used to classify the paper.

Unit: International System of Unit (Système Internationale d'Unités; SI) (<https://www.britannica.com/science/International-System-of-Units>) should be used for all scientific and laboratory data.

References: References should be given according to the APA standard as effective from November, 2020 issue.

Abbreviations and Acronyms: Standard abbreviations and acronyms should be used for each related discipline. Acronyms should be identified at the first occurrence in the text. Abbreviations and acronyms may also be attached to main text as an appendix.

Equations and Formulas: Equations and formulas should be numbered consecutively. These numbers must be shown within parentheses being aligned to the right. In the text, equations and formulas should be referred with their numbers given in parentheses. Comprehensive formulas, not appropriate to be written in the texts, should be prepared in figures.

Figures and Tables: Figures and tables should be numbered consecutively. In the text referring to figures and tables should be made by typing "Figure 1." or "Table 1." etc. A suitable title should be assigned to each of them.

DENİZ BİLİMLERİ VE MÜHENDİSLİĞİ DERGİSİ (DBMD) YAZIM KURALLARI

Genel Bilgiler: Yazılar; Microsoft Word'de tek satır aralığı ve iki yana yaslanarak hazırlanmalıdır. Yazı tipi: Times New Roman, 12 punto. Kenar boşlukları: sol 4,5 cm- sağ 3,5 cm- üst 5 cm- alt 7 cm- üst bilgi 3,25 cm- alt bilgi 6 cm, oluk 0. Kâğıt ölçüsü: A4. Sayfa numaraları sayfanın alt ortasında -1-, -2-, -3- vb. şeklinde yer almalıdır. Dipnot kullanılmamalıdır.

Etik Kurul İzni ve/veya Yasal/Özel İzin: Makalelerde etik kurul izni ve/veya yasal/özel izin alınmasının gerekip gerekmediği belirtilmiş olmalıdır. Eğer bu izinlerin alınması gerekli ise, izinlerin hangi kurumdan, hangi tarihte ve hangi karar veya sayı numarası ile alındığı açıkça sunulmalıdır.

Yazı Yapısı: Yazı şu sırada hazırlanmalıdır: Başlık, Yazarlar, Özet, Anahtar Kelimeler, Başlık (Türkçe), Özet (Türkçe), Anahtar Kelimeler (Türkçe), Ana Metin, Ek (varsa), Referanslar.

Başlık: Başlık; açık, net, anlaşılır olmalı ve 15 kelimeyi geçmemelidir.

Öz (Abstract): Yazı, 100-200 kelimelik, arka plan, amaç, yöntem, bulgular ve sonuçtan oluşan yapılandırılmış bir özeti içermelidir.

Sayfa Sayısı: Dergiye gönderilecek yazıların boyutu, kaynakça dâhil asgari 2000 kelime veya 5 sayfa, azami 7000 kelime veya 25 sayfa arasında olmalıdır.

Anahtar Kelimeler: Yazıyı sınıflandırmaya yarayacak, anahtar görevi yapan 3-5 kelime yer almalıdır.

Birimler: Yazının uluslararası alanlarda da kolay izlenebilir ve anlaşılabilir olması için Uluslararası Birim Sistemine (<https://www.britannica.com/science/International-System-of-Units>) uygun olarak hazırlanması gerekir.

Referans: Referanslar Kasım, 2020 sayısından itibaren geçerli olmak üzere APA standardına göre verilmelidir.

Notasyon ve Kısaltmalar: İlgili bilim alanının standart notasyon ve kısaltmaları kullanılmalı, yeni notasyonlar ise metin içinde ilk geçtiği yerde tanımlanmalıdır. Gerekli durumlarda, notasyon ve kısaltmalar ek olarak konulabilir.

Denklem ve Formüller: Denklem ve formüller ardışık olarak numaralandırılmalı ve bu numaralar sağa dayalı parantez içinde yazılmalıdır. Metin içinde denklem ve formüllere parantez içinde yazılan numaraları ile atıfta bulunulmalıdır. Metin arasında verilmesi uygun olmayan kapsamlı formüller şekil olarak hazırlanmalıdır.

Şekiller ve Tablolar: Şekiller ve tablolar, ardışık olarak numaralandırılmalıdır. Bunlara metin içinde "Şekil 1." veya "Tablo 1." şeklinde atıfta bulunulmalıdır. Her bir şekil ve tablo için uygun bir başlık kullanılmalıdır.

Ethical Principles and Publication Policy

Journal of Naval Sciences and Engineering (hereafter JNSE) is a peer reviewed, international, inter-disciplinary journal in science and technology, which is published semi-annually in November and April since 2003. JNSE is committed to provide a platform where highest standards of publication ethics are the key aspect of the editorial and peer-review processes.

The editorial process for a manuscript to the JNSE consists of a double-blind review, which means that both the reviewer and author identities are concealed from the reviewers, and vice versa, throughout the review process. If the manuscript is accepted in the review stage of the Editorial Process then, the submission goes through the editing stage, which consists of the processes of copyediting, language control, reference control, layout and proofreading. Reviewed articles are treated confidentially in JNSE.

Papers submitted to JNSE are screened for plagiarism regarding the criteria specified on the [Publishing Rules](#) page with plagiarism detection tool. In case that the editors become aware of proven scientific misconduct, they can take the necessary steps. The editors have the right to retract an article whether submitted to JNSE or published in JNSE.

Following the completion of the editing stage, the manuscript is then scheduled for publication in an issue of the JNSE. The articles which are submitted to JNSE to be published are free of article submission, processing and publication charges. The accepted articles are published free-of-charge as online from the journal website and printed. The articles that are accepted to appear in the journal are made freely available to the public via the journal's website. The journal is also being printed by National Defence University Turkish Naval Academy Printing House on demand.

JNSE has editors and an editorial board which consists of academic members from at least five different universities. JNSE has an open access policy which means that all contents are freely available without charge to the user or his/her institution. Users are allowed to read, download, copy, distribute, print, search, or link to the full texts of the articles, or use them for any other lawful research purposes.

Publication ethics of the JNSE are mainly based on the guidelines and recommendations which are published by the Committee on Publication Ethics (COPE), World Federation of Engineering Organizations (WFEO), Council of Science Editors (CSE) and Elsevier's Publishing Ethics for Editors statements.

The duties and responsibilities of all parties in the publishing process including editors, authors and others are defined below.

The Responsibilities of the Authors:

- Authors are responsible for the scientific, contextual, and linguistic aspects of the articles which are published in the journal. The views expressed or implied in this publication, unless otherwise noted, should not be interpreted as official positions of the Institution.
- Authors should follow the "Author Guidelines" in JNSE's web page on DergiPark.
- Authors should conduct their researches in an ethical and responsible manner and follow all relevant legislation.
- Authors should take collective responsibility for their work and for the content of their publications.
- Authors should check their publications carefully at all stages to ensure that methods and findings are reported accurately.
- Authors must represent the work of others accurately in citations, quotations and references.
- Authors should carefully check calculations, data presentations, typescripts/submissions and proofs.
- Authors should present their conclusions and results honestly and without fabrication, falsification or inappropriate data manipulation. Research images should not be modified in a misleading way.
- Authors should describe their methods to present their findings clearly and unambiguously.
- Authors accept that the publisher of JNSE holds and retains the copyright of the published articles.
- Authors are responsible to obtain permission to include images, figures, etc. to appear in the article.

- In multi-authored publications -unless otherwise stated- author rankings are made according to their contributions.
- Authors should alert the editor promptly if they discover an error in any submitted.
- Authors should follow the publication requirements regarding that the submitted work is original and has not been published elsewhere in any language.
- Authors should work with the editor or publisher to correct their work promptly if errors are discovered after publication.
- If the work involves chemicals, procedures or equipment that have any unusual hazards inherent in their use, the authors must clearly identify these in the manuscript.
- If the work involves the use of animals or human participants, the authors should ensure that all procedures were performed in compliance with relevant laws and institutional guidelines and that the appropriate institutional committee(s) has approved them; the manuscript should contain a statement to this effect.
- Authors should also include a statement in the manuscript that informed consent was obtained for experimentation with human participants. Because the privacy rights of human participants must always be preserved. It is important that authors have an explicit statement explaining that informed consent has been obtained from human participants and the participants' rights have been observed.
- Authors have the responsibility of responding to the reviewers' comments promptly and cooperatively, in a point-by-point manner.

The Responsibilities of the Reviewers:

- Peer review process has two fundamental purposes as follow: The first purpose is to decide whether the relevant article can be published in JNSE or not and the second purpose is to contribute to the improvement of the weaknesses of the related article before the publication.
- The peer review process for an article to the JNSE consists of a double-blind review, which means that both the reviewer and author identities are concealed from the reviewers, and vice versa, throughout the review process. Reviewed articles are treated confidentially in JNSE.
- Reviewers must respect the confidentiality of peer review process.
- Reviewers must refrain from using the knowledge that they have obtained during the peer review process for their own or others' interests.
- Reviewers should definitely be in contact with the JNSE if they suspect about the identity of the author(s) during the review process and if they think that this knowledge may raise potential competition or conflict of interest.
- Reviewers should notify the JNSE in case of any suspicion regarding the potential competition or conflict of interest during the review process.
- Reviewers should accept to review the studies in which they have the required expertise to conduct an appropriate appraisal, they can comply with the confidentiality of the double-blind review system and that they can keep the details about the peer review process in confidential.
- Reviewers should be in contact with the JNSE in order to demand some missing documents, following the examination of the article, supplementary files and ancillary materials.
- Reviewers should act with the awareness that they are the most basic determinants of the academic quality of the articles to be published in the journal and they should review the article with the responsibility to increase academic quality.
- Reviewers should be in contact with the JNSE editors if they detect any irregularities with respect to the Ethical Principles and Publication Policy.
- Reviewers should review the articles within the time that has been allowed. If they can not review the article within a reasonable time-frame, then they should notify the journal as soon as possible.
- Reviewers should report their opinions and suggestions in terms of acceptance / revision / rejection for the manuscript in the peer review process through the Referee Review Form which is provided by JNSE.
- In case of rejection, reviewers should demonstrate the deficient and defective issues about the manuscript in a clear and concrete manner in the provided Referee Review Form.
- Review reports should be prepared and submitted in accordance with the format and content of the Referee Review Form which is provided by JNSE.
- Review reports should be fair, objective, original and prudent manner.
- Review reports should contain constructive criticism and suggestions about the relevant article.

The Responsibilities of the Editors:

-Editors are responsible of enhancing the quality of the journal and supporting the authors in their effort to produce high quality research. Under no conditions do they allow plagiarism or scientific misconduct.

-Editors ensure that all submissions go through a double-blind review and other editorial procedures. All submissions are subject to a double-blind peer-review process and an editorial decision based on objective judgment.

-Each submission is assessed by the editor for suitability in the JNSE and then, sent to the at least two expert reviewers.

-Editors are responsible for seeking reviewers who do not have conflict of interest with the authors. A double-blind review assists the editor in making editorial decisions.

-Editors ensure that all the submitted studies have passed initial screening, plagiarism check, review and editing. In case the editors become aware of alleged or proven scientific misconduct, they can take the necessary steps. The editors have the right to retract an article. The editors are willing to publish errata, retractions or apologies when needed.

Etik İlkeler ve Yayın Politikası

Deniz Bilimleri ve Mühendisliği Dergisi (Bundan sonra DBMD olarak anılacaktır.); uluslararası düzeyde, hakemli, çok disiplinli, Nisan ve Kasım aylarında olmak üzere 2003 yılından bu yana yılda iki kez yayınlanan, bilim ve teknoloji dergisidir. DBMD yayın etiğinde en yüksek standartların, editöryal ve hakemlik süreçlerinin kilit unsuru olarak değerlendirildiği bir platform sunmayı taahhüt etmektedir.

DBMD'ne gönderilen her bir makale için değerlendirme sürecinde çift-kör hakemlik sistemi uygulanmaktadır. Buna göre, değerlendirme süreci boyunca hakem ve yazarlar birbirlerinin bilgilerini görememektedir. Dergiye gönderilen çalışmaların yazar-hakem ve hakem-yazar açısından süreçlerinde gizlilik esastır. DBMD'ne gönderilen makalelerin değerlendirme sürecindeki inceleme aşamasında kabul edilmeleri halinde, ilgili makaleler için düzenleme aşamasına geçilmektedir. Düzenleme aşamasında, ilgili makaleler yazım formatı ve dilbilgisel yönlerden incelenir. Makalelerin sayfalar üzerindeki biçimi ve yerleşimleri kontrol edilip düzenlenir. Ayrıca referans kontrolü yapılır. DBMD'nde kontrol edilen ve düzenlenen makaleler gizli tutulmaktadır.

DBMD'ne gönderilen makaleler, [Yayın Kuralları](#) sayfasında belirtilen kriterlere ilişkin, intihal tespit programı aracılığıyla kontrol edilir. Editörler, kanıtlanmış bir bilimsel kullanımdan ya da usulsüzlükten haberdar olurlarsa bu konuda gerekli adımları atabilirler. Bu anlamda, Editörler gerekli durumlarda DBMD'ne gönderilen ya da DBMD'nde yayınlanmış makaleleri geri çekme hakkına sahiptir.

Düzenleme aşamasının başarılı olarak sonuçlanmasını takiben, ilgili makaleler DBMD'nin bir sayısında yayınlanmak üzere saklı tutulur ve kayıt altına alınır. DBMD'ne yayınlanmak üzere gönderilen makaleler; yazılı materyal gönderme, işleme ve yayınlama süreçlerindeki tüm ücretlerden muaf tutulmaktadır. DBMD'nde yayınlanmak üzere kabul edilen makaleler, derginin internet sitesinden çevrimiçi olarak ücretsiz bir şekilde yayınlanır ve basılır. Dergide yayınlanması kabul edilen çalışmalar, derginin web sitesinden açık erişim ile erişilebilir kılınmıştır. Dergi ayrıca, Milli Savunma Üniversitesi, Deniz Harp Okulu Matbaası tarafından basılmaktadır.

DBMD; editörü ve en az beş değişik üniversitenin öğretim üyelerinden oluşmuş danışman grubu ile açık erişim politikasını benimsemektedir. Buna göre, tüm içerikler ücretsiz olarak kullanıcılar veya kurumlar için ulaşılabilir. Kullanıcıların DBMD bünyesindeki makalelerin tam metinlerini okuma, indirme, kopyalama, dağıtma, yazdırma, arama veya bunlara bağlantı verme ve diğer yasal araştırma amaçları için kullanma hakları saklı tutulmaktadır.

DBMD'nin yayın etiği, temel olarak Yayın Etiği Komitesi (COPE), Dünya Mühendislik Kuruluşları Federasyonu (WFEO), Bilim Kurulu Editörleri (CSE) ve Elsevier'in Editörler için Yayın Etiği açıklamaları kapsamında yayınlanmış yönergelere ve önerilere dayanmaktadır.

Editörler, yazarlar ve diğer taraflar da dâhil edilebilecek şekilde yayın sürecindeki görev ve sorumluluklar aşağıdaki gibi tanımlanmıştır.

Yazarların Sorumlulukları:

-Yazarlar, dergide yayınlanan makalelerinin bilimsel, bağlamsal ve dilsel yönlerinden sorumlu tutulmaktadır. Dergide ifade edilen veya ima edilen görüşler, aksi belirtilmediği sürece, Enstitünün resmi görüşü olarak yorumlanamaz ve yansıtılamaz.

-Yazarlar çalışmalarında, DBMD'nin DergiPark internet sayfasında yer alan "Yazım Kuralları"na dikkate almalıdır.

-Yazarlar araştırmalarını etik ve sorumlu bir şekilde yürütmeli ve ilgili tüm mevzuatları takip etmelidir.

-Yazarlar çalışmalarını ve yayınlarının içeriği için ortak sorumluluk almalıdır.

-Yazarlar, yöntemlerin ve bulguların doğru bir şekilde raporlandığından emin olmak için yayınlarını her aşamada dikkatlice kontrol etmelidir.

-Yazarlar, başkalarına ait çalışmalarını dolaylı alıntı, doğrudan alıntı ve referanslar ile doğru bir şekilde göstermelidir. Yazarlar, makalelerindeki fikirlerin şekillendirilmesinde etkili ya da bilgilendirici olmuş her türlü kaynağa referans vermelidir.

-Yazarlar çalışmalarındaki hesaplamaları, ispatları, veri sunumlarını ve yazı tiplerini dikkatlice kontrol etmelidir.

- Yazarlar çalışmalarının sonuçlarını dürüstçe; uydurma, çarpıtma, tahrifat veya uygunsuz manipülasyona yer vermeden sunmalıdır. Çalışmalardaki görsel kaynaklar yanıltıcı bir şekilde değiştirilmemelidir.
- Yazarlar, çalışmalarındaki bulguları açık ve net bir şekilde sunmak için araştırma yöntemlerini tanımlamalı ve paylaşmalıdır.
- Yazarlar, yayınlanmış makalelerinin telif haklarını DBMD yayıncısına devrettiklerini kabul etmektedir.
- Yazarlar çalışmalarına çeşitli görsel kaynakları, figürleri, şekilleri vb. dahil etmek için gerekli izinleri almakla yükümlüdür. İlgili çalışmada yer alması gereken resim, şekil vb. anlatımı destekleyici materyaller için gerekli kişilerden ya da kurumlardan izin alınması yazarın sorumluluğundadır.
- Çok yazarlı yayınlarda -aksi belirtilmedikçe- yazar sıralamaları sunulan katkılara göre yapılmalıdır.
- Yazarlar gönderdikleri çalışmada herhangi bir hata tespit ederlerse bu konuda derhal editörü uyarmalıdır.
- Yazarlar dergiye gönderdikleri makalelerin başka bir yerde yayımlanmamış ya da yayımlanmak üzere gönderilmemiş olmaları ile ilgili DBMD'nin DergiPark internet sayfasında yer alan "Yayın Kuralları"na dikkate alınmalıdır.
- Yazarlar, ilgili çalışmaları DBMD'nde yayınlandıktan sonra hata tespit ederlerse bu konuda gerekli düzeltmelerin yapılabilmesi amacıyla derhal editör veya yayıncı ile iletişime geçip onlar ile birlikte çalışmalıdır.
- İlgili çalışmada, doğası gereği kullanımlarında olağandışı tehlikeler barındıran çeşitli kimyasallar veya ekipmanlardan yararlanılmış ise yazarların tüm bunları çalışmasında açıkça belirtmesi ve tanımlaması gerekmektedir.
- İnsanlar ve hayvanların katılımını gerektiren çalışmalar için, yazarlar tüm sürecin ilgili yasalara ve kurumsal yönergelere uygun olarak gerçekleştirildiğinden emin olmalıdır ve ilgili komitelerden etik onay alındığını çalışmalarında açık bir şekilde ifade edip belgelendirmelidir.
- İnsanların katılımını gerektiren çalışmalar için, yazarlar kurumsal etik kurul onayı almakla yükümlüdürler. Yazarlar, katılımcıların süreç ile ilgili olarak bilgilendirildiklerini ve bu anlamda, katılımcılardan gerekli izinlerin alındığını bildirmek ve belgelemek zorundadır. Yazarlar, katılımcıların haklarının gözetildiğini açıklayan açık bir bildirim sunmalıdır. Ayrıca bu süreçte, katılımcıların gizlilik hakları her zaman korunmalıdır.
- Yazarlar, hakemlerin değerlendirmelerini, yorumlarını ve eleştirilerini zamanında ve işbirliği içerisinde dikkate almalıdır ve bu konuda, gerekli güncellemeleri yapmalıdır.

Hakemlerin Sorumlulukları:

- Hakem değerlendirme sürecinin iki temel amacı vardır: İlk amaç, ilgili makalenin DBMD'nde yayınlanıp yayınlanamayacağına karar vermektir ve ikinci amaç, yayından önce ilgili makalenin eksik yönlerinin geliştirilmesine katkıda bulunmaktır.
- DBMD'ne gönderilen her bir makale için değerlendirme sürecinde çift-kör hakemlik sistemi uygulanmaktadır. Buna göre, değerlendirme süreci boyunca hakem ve yazarlar birbirlerinin bilgilerini görememektedir. Dergiye gönderilen çalışmaların yazar-hakem ve hakem-yazar açısından süreçlerinde gizlilik esastır.
- Hakemler, değerlendirme sürecinin gizliliğine saygı göstermelidir.
- Hakemler, değerlendirme sürecinde elde ettikleri bilgileri kendilerinin veya başkalarının çıkarları için kullanmaktan kaçınmalıdır.
- Hakemler, değerlendirme sürecinde yazar(lar)ın kimliğinden şüphe etmeleri ve bu bilginin herhangi bir potansiyel rekabet veya çıkar çatışması yaratacağını düşünmeleri halinde mutlaka DBMD ile iletişime geçmelidir.
- Hakemler, değerlendirme sürecinde şüphe ettikleri potansiyel rekabet veya çıkar çatışması durumlarını DBMD'ne bildirmelidir.
- Hakemler, uygun bir değerlendirme yapabilmek için gereken uzmanlığa sahip oldukları, çift-kör hakemlik sisteminin gizliliğine riayet edebilecekleri ve değerlendirme süreci ile ilgili detayları gizli tutabilecekleri çalışmaların hakemliğini kabul etmelidir.
- Hakemler makaleyi, ek dosyaları ve yardımcı materyalleri incelemelerini takiben bazı eksik belgelere ihtiyaç duymaları halinde bunları talep etmek üzere DBMD ile iletişime geçmelidir.
- Hakemler dergide yayınlanacak makalelerin akademik kalitesinin en temel tespit edicisi olduklarının bilinciyle davranmalı ve akademik kaliteyi artırma sorumluluğuyla inceleme yapmalıdır.
- Hakemler, Etik İlkeler ve Yayın Politikası ile ilgili herhangi bir usulsüzlük tespit etmeleri halinde DBMD editörleri ile irtibata geçmelidir.

- Hakemler, kendilerine tanınan süre içerisinde makaleleri değerlendirmelidir. Şayet uygun bir zaman içerisinde değerlendirme yapamayacaklarsa, bu durumu en kısa zamanda DBMD'ne bildirmelidirler.
- Hakemler, değerlendirme sürecindeki çalışma için kabul etme / yeniden gözden geçirme / reddetme şeklindeki önerilerini DBMD tarafından sağlanan Hakem Değerlendirme Formu aracılığıyla bildirmelidir.
- Sonucu reddetme şeklinde olan değerlendirmeler için hakemler, ilgili çalışmaya dair eksik ve kusurlu hususları Hakem Değerlendirme Formu'nda açık ve somut bir şekilde ortaya koymalıdır.
- Hakem değerlendirme raporlarının, DBMD tarafından sağlanan Hakem Değerlendirme Formu'na uygun biçimde ve içerikte hazırlanması ve gönderilmesi gerekmektedir.
- Hakem değerlendirme raporları adil, objektif, özgün ve ölçülü olmalıdır.
- Hakem değerlendirme raporları, ilgili makale ile ilgili yapıcı eleştiriler ve tavsiyeler içermelidir.

Editörlerin Sorumlulukları:

- Editörler, derginin bilimsel kalitesini arttırmak ve yazarları bilimsel kalitesi yüksek araştırmalar üretmek için desteklemek ile sorumludur. Hiçbir koşulda, intihal ya da bilimsel kötüye kullanıma izin verilmemektedir.
- Editörler, dergiye gönderilen her çalışmanın çift-kör hakemlik sürecine ve diğer editoryal süreçlere tabi olmasını sağlamaktadır. DBMD'ne gönderilen her çalışma, çift-kör hakemlik sürecine ve nesnel değerlendirmeye dayalı editör kararına bağlı tutulmaktadır.
- DBMD'ne gönderilen her bir çalışma, uygunlukları açısından editör tarafından değerlendirilir ve daha sonrasında, incelenmesi ve değerlendirilmesi amacıyla en az iki uzman hakeme gönderilir.
- Editörler, yazarlar ile çıkar çatışması olmayan hakemleri, çalışmayı değerlendirmek üzere atamakla sorumludur. Çift-kör hakemlik süreci, editör için değerlendirme ve düzenleme aşamalarında katkı sağlamaktadır.
- Editörler, DBMD'ne gönderilen tüm çalışmaların ön kontrol, tarama, intihal kontrolü, değerlendirme ve düzenleme aşamalarından geçmesini sağlar. Editörler iddia edilen veya kanıtlanmış bilimsel kötü kullanımdan haberdar olurlarsa makaleyi geri çekebilirler. Editörler, gerekli durumlarda gönderilen çalışmayı düzeltme, geri çekme veya çalışma hakkında özür yayınlama hakkına sahiptir.

NATIONAL DEFENCE UNIVERSITY
TURKISH NAVAL ACADEMY
JOURNAL OF NAVAL SCIENCES AND ENGINEERING

VOLUME: 19

NUMBER: 1

APRIL 2023

ISSN: 1304-2025

CONTENTS / İÇİNDEKİLER

EDITORIAL

Foreword from the Editor-In-Chief (Önsöz)

1-2

Fatih ERDEN

Materials Engineering / Malzeme Mühendisliği

RESEARCH ARTICLE

Production of Translucent Alumina Ceramics by Tape Casting

3-17

(Yarı Saydam Alümina Seramiklerin Şerit Döküm Yöntemi İle Üretimi)

Yasemin TABAK, Şeyda POLAT, Ayşen KILIÇ, Bayise KAVAKLI VATANSEVER

Physics / Fizik

RESEARCH ARTICLE

Spectroscopic Investigation of Argon DC Glow Discharge In Plasma Medium

19-33

(Plazma Ortamında Argon DC Glow Deşarjının Spektroskopik İncelenmesi)

Esra OKUMUŞ

Electrical-Electronics Engineering / Elektrik-Elektronik Mühendisliği

RESEARCH ARTICLE

**Thermal Analysis of XLPE Insulated Submarine Cables for
Different Loading Conditions**

35-51

(Farklı Yükleme Şartları İçin XLPE İzoleli Denizaltı Kablolarının Isıl Analizi)

Ahmet Yiğit ARABUL, Celal Fadıl KUMRU

Shipbuilding and Ocean Engineering / Gemi ve Deniz Teknolojisi Mühendisliği

RESEARCH ARTICLE

Scale Effects On The Linear Hydrodynamic Coefficients Of DARPA SUBOFF

53-76

(Lineer Hidrodinamik Katsayıların Hesabında Ölçek Etkisi)

Furkan KIYÇAK, Ömer Kemal KINACI

Naval Architecture Engineering / Gemi İnşaatı Mühendisliği

RESEARCH ARTICLE

**Numerical Investigation Of HVAC Systems of a Naval Ship Compartment:
Free Cooling And Air-Conditioning**

77-100

(Bir Savaş Gemisi Kompartımanında HVAC Sistemlerinin Sayısal İncelenmesi:
Doğal Havalandırma ve İklimlendirme)

Alpay ACAR, Murat URYAN, Ali DOĞRUL, Asım Sinan KARAKURT, Cenk ÇELİK

MİLLİ SAVUNMA ÜNİVERSİTESİ
DENİZ HARP OKULU DEKANLIĞI
DENİZ BİLİMLERİ VE MÜHENDİSLİĞİ DERGİSİ

CİLT: 19

SAYI: 1

NİSAN 2023

ISSN: 1304-2025